RATES OF MOLECULAR EVOLUTION AND THEIR APPLICATION TO NEOTROPICAL AVIAN BIOGEOGRAPHY

A Dissertation

Submitted to the Graduate Faculty of the
Louisiana State University and
Agricultural and Mechanical College
in partial fulfillment of the
requirements for the degree of
Doctor of Philosophy

in

The Department of Biological Sciences

by
Christopher C. Witt
B. A., College of the Atlantic, 1997
December 2004

ACKNOWLEGEMENTS

I owe a great debt of gratitude to my advisors, J. V. Remsen, Jr. and Frederick H. Sheldon, for their patient support and guidance during my years in graduate school. I would also like to thank the other members of my graduate committee, Mark S. Hafner, Michael E. Hellberg, and Robb T. Brumfield, for their time and efforts.

This project would not have been possible without the efforts of many dedicated collectors, museum curators, and collection managers over several decades. Museums that contributed specimens to this project include (in descending order according to the number of specimens): Louisiana State University Museum of Natural Science; Field Museum of Natural History; National Museum of Natural History; University of Kansas Museum of Natural History; Academy of Natural Sciences of Philadelphia; American Museum of Natural History; Museo de Zoología, Facultad de Ciencias, Universidad Nacional Autónoma de México; Museum of Vertebrate Zoology, University of California at Berkeley; Barrick Museum of Natural History, University of Nevada-Las Vegas; Zoological Museum of Copenhagen.

For funding, I thank the National Science Foundation, the LSU Board of Regents, the Chapman Memorial Fund of the American Museum of Natural History, Sigma Xi, the American Ornithologists' Union, Charles Fugler, T. Vinton Holmes, the Biological Sciences Graduate Students Organization (BioGrads), the LSU Birdathon and all its supporters.

Numerous individuals among the students and staff at the LSU Museum of Natural Science facilitated my efforts over the years of this project. The following people went out of their way to help me at one or more times: Nanette Crochet, Jason Weckstein, Rob Moyle, Ben Marks, Jessica Light, Kazuya Naoki, Alex Aleixo, Gwen Mahon, Peggy Sims, Donna Dittmann,

Steve Cardiff, Dan Lane, Rob Faucett, Dan Christian, John O'Neill, Bret Whitney, and Mario Cohn-Haft.

Other individuals collected specific specimens or responded to requests for information that were invaluable to my progress and the completion of this dissertation: Mike Sanderson, Tim Barraclough, Gary Langham.

I received spirited assistance from several undergraduate workers including Brian Tetreau, Lily Wei, Julia Raddatz, and Kelly Scott. I enjoyed working together with then high-school student Claire A. Hebert on the motmot project. I later teamed up with Gabriela Ibañez of UNAM to complete the molecular work for the motmots.

I have appreciated friendship and moral support of many other people that have been invaluable for helping me through the process of graduate school. These include, but are not limited to: Matt Carling, Zac Cheviron, Santiago Claramunt, Adam Leaché, Mark McRae, Lori Benson, Jim McGuire, Tom Devitt, Brian O'Shea, David Reed, Frank Burbrink, and Kevin McCracken.

Finally, I would not have been able to make it through this process without the unconditional support of my loving wife, Satya.

TABLE OF CONTENTS

ABSTRACT

The tempo of evolution and the causes of rate variation among lineages are central foci of evolutionary biology. I evaluated two hypothesized sources of variation in molecular evolutionary rate, and I applied a variable molecular clock to estimate the timescale of diversification in three families of Neotropical birds.

First, I examined the phylogenetic evidence for molecular punctuated equilibrium, the hypothesis that speciation drives accelerated molecular evolution. Recent findings that rates of DNA evolution and speciation are linked implicate molecular punctuated equilibrium as an important cause of rate variation among lineages. I used phylogenetic simulations to test this reported link, and I found that it was entirely attributable to a methodological artifact. In a review of the topic, I found no unequivocal empirical evidence for molecular punctuated equilibrium and I concluded that its predicted phylogenetic consequences are theoretically implausible.

Second, I tested the metabolic rate hypothesis, which holds that mutation rate in mtDNA is correlated with mass-specific metabolic rate. This hypothesis predicts that small-bodied lineages should evolve rapidly. Previous studies verified this prediction, but none utilized adequately large samples of independent contrasts among appropriate taxa. The use of many such contrasts from bird mtDNA sequences conspicuously failed to corroborate the link between metabolic and mtDNA rates. On the contrary, high rates of nonsynonymous substitution were associated with large body mass, implicating population size as a pervasive cause of evolutionary rate variation.

Third, I developed molecular phylogenies for puffbirds, jacamars, and motmots to test hypothesized area relationships in the Neotropics. I used penalized likelihood to estimate node times while accommodating significant rate variation under a set of biologically realistic

assumptions. Phylogenetic patterns in each family were consistent with expansion following the formation of the Central American Landbridge and subsequent vicariance across the Andes. I applied a calibration based on the final uplift of the Isthmus of Panama, 3.1 Ma. Average estimated rates were close to the commonly cited 2% sequence divergence/Myr. Concordant area relationships were found among co-distributed species complexes; however, the timescale of divergence was variable, suggesting that common dispersal corridors rather than common vicariant events may be driving co-phylogenetic patterns.

CHAPTER 1: INTRODUCTION

Evolutionary biology seeks to explain how, when, and why organismal change occurs. Understanding the timescale of evolution and rates of character change over time are essential to all three questions. In my dissertation, I examine putative sources of rate variation in the evolution of DNA sequences, and I estimate the timescale of evolution and diversification in three avian families using a method that accounts for rate variation among lineages.

The study of evolutionary rates has flourished as a result of the growth of molecular systematics since the 1970's. Molecular markers provide an abundance of characters that can be quantified objectively. Early workers noted a general clock-like accumulation of nucleotide substitutions that they attributed to a steady underlying rate of mutation across organisms and a penchant for selective neutrality at the vast majority of nucleotide sites. Since the early formulation of the molecular clock hypothesis, patterns of rate variation greater than that expected by chance have been described at a range of hierarchical levels — among nucleotide sites, genes, chromosomes, genomes, and lineages. Understanding the mechanisms driving rate variation at each hierarchical level has been a major, albeit elusive, goal of molecular systematics.

Rate variation among lineages can directly affect macroevolutionary patterns and can cause problems for phylogenetic reconstruction and estimation of divergence dates. Some of the proposed causes of rate variation among lineages include variation in generation time, mass-specific metabolic rate, body temperature, speciation rate, population size, exposure to environmental mutagens, functional constraints, or intrinsic differences in DNA repair efficiency. Above all, the effects of generation time on nuclear DNA rate is well established and solidly grounded in theory. Generation time effects have been especially well documented in

plants, where many closely related species differ in annual versus perennial life history strategies. However, organismal generation time effects are not relevant to mitochondrial DNA because the mitochondrial and organismal generation times are decoupled.

Population size effects on molecular evolutionary rate are predicted by nearly neutral theory. Smaller populations are more susceptible to rapid genetic drift and, as a result, they incur more slightly deleterious DNA substitutions than large populations. Patterns consistent with accelerated nearly neutral drift in small populations have been documented, although the general importance of population size effects on molecular rates over evolutionary timescales are not yet fully known. Population size effects are predicted to be more pronounced in mitochondrial DNA due to the range of functional constraints among sites and the lower effective population size of this maternally inherited, non-recombining genome.

Mitochondrial DNA is highly prone to rate variation among lineages, and the most frequently cited cause is variation in mass-specific metabolic rate. High metabolic rates produce higher concentrations of mutagenic oxygen free-radicals, which are believed to cause higher mutation rates. A series of papers have presented empirical confirmation of this pattern by demonstrating that mitochondrial DNA rate is (1) negatively correlated with body mass in vertebrates, (2) linked to thermal habit in higher level comparisons, and (3) correlated to rates of nuclear DNA evolution. Problems with these studies are that higher-level comparisons use average rates over long periods of evolutionary time, and traits such as body mass may be highly labile. Furthermore, ecological scaling rules predict that mass-specific metabolic rate and population size will have opposite effects on inter-lineage rate variation.

Speciation rate has been reported to be linked to rate of molecular evolution, in accordance with the predictions of the theory of punctuated equilibrium. However, the

theoretical plausibility of this finding is questionable. Could a series of speciation events distributed across geological time have such profound effects on population genetic processes that the average relative rates of lineages can be linked to the number of inferred branching events? In the first part of my dissertation, I use phylogenetic simulations to examine the finding of punctuated molecular equilibrium in phylogenies and to re-evaluate the empirical evidence for this pattern.

In the second part of my dissertation, I explore the effects of mass-specific metabolic rate and population size on mitochondrial DNA evolution. Specifically, what is the relationship between body mass and evolutionary rate? I review the empirical evidence supporting the metabolic rate hypothesis, and I compile a large dataset of mitochondrial DNA sequences from birds that will be ideal for approaching this question.

Given the ubiquity of rate variation among lineages and the difficulties of identifying its causes, methods of estimating divergence time must allow rates to vary across phylogenies without making *a priori* assumptions about relative rates among the component taxa. The penalized likelihood method is one such method. It facilitates date estimation in the absence of a molecular clock by allowing rates to vary across the tree while minimizing the amount of variation between adjacent branches. This method assumes that rates vary across the tree incrementally, as might any continuous character. Different rates can be assigned to each branch, but a roughness penalty is imposed when rates vary too drastically between adjacent branches.

In the third part of my dissertation, I apply the penalized likelihood method to mitochondrial DNA datasets for three families of Neotropical birds in order to estimate the timescale for diversification in the Neotropical avifauna. I use the time-calibrated phylogenies to explore patterns of diversification with respect to the timing of geological events. Furthermore, I

use estimates of divergence dates within co-distributed species complexes to test whether concordant area relationships predict concordant timing of speciation.

CHAPTER 2. A RE-EXAMINATION OF THE PHYLOGENETIC EVIDENCE FOR MOLECULAR PUNCTUATED EQUILIBRIUM

The theory of punctuated equilibrium holds that most evolutionary change is associated with speciation events, whereas lineages that do not speciate are characterized by stasis (Eldredge and Gould 1972, Gould and Eldredge 1977). Speciation by peripheral isolation of small populations, or peripatric speciation (Mayr 1963), has been proposed as the mechanism underlying the punctuated phenotypic evolution observed in the fossil record. Peripheral isolates can experience population bottlenecks or new environments that can cause geologically sudden shifts in morphological traits, as are commonly observed in island populations (e.g. Pergams and Ashley 2001). Bottlenecks and altered selection regimes can also affect rate of evolution at the molecular level. For example, small population size can cause accelerated fixation of slightly deleterious mutations (Ohta 1992, 1995), and positive selection can cause rapid fixation of newly beneficial alleles and linked loci (Fay and Wu 2000). Thus, punctuated equilibrium can apply to both phenotypic and molecular evolution (Gould and Eldredge 1993, Gould 2002, p. 812).

Several studies have tested molecular data for evidence of evolution by punctuated equilibrium, but appropriate methods for such a test have been subject to debate. Early attempts by Avise and Ayala (1975, 1976) and Avise (1977) used phenetic comparisons of mean allozyme divergence within speciose and depauperate clades of fishes. Mayden (1986) argued that the tests used in those studies were invalid because, among other reasons, the age and monophyly of clades under comparison could not be controlled or verified. A survey by Mindell *et al.* (1990) of allozyme divergence in 111 vertebrate genera reported a link between species diversity and mean divergence, but was similarly flawed. Although Mindell *et al.* (1990) reported that

speciation appeared to have caused accelerated molecular evolution, an equally likely explanation is that genera with more species diversity tended to be older.

In a study of *Sceloporus* lizards, Mindell *et al.* (1989) pioneered a phylogenetic approach, rather than a phenetic one, to testing for molecular punctuated equilibrium. In phylogenies with branch lengths proportional to the inferred amount of evolution, clades of equal age that contain different numbers of species can be compared with respect to the path lengths of their component lineages. Mindell *et al.* (1989) found evidence for more evolutionary change along lineages that were more branched. Sanderson (1990) suggested that this inference could be a phylogenetic artifact of differences in taxon sampling, whereby homoplasious changes are more likely to be detected in heavily sampled lineages. Sanderson selectively pruned taxa from the tree in order that each of the sister clade comparisons of Mindell *et al.* (1989) became comparisons between terminal sister lineages. The significant differences observed by Mindell *et al.* were generally not supported in this more conservative but unbiased reanalysis. Subsequently, Murphy and Lovejoy (1998) showed that the allozyme character coding method of Mindell *et al.* (1989) was flawed, and that the phylogenetic topology used in the analysis was one of approximately 10^7 equally parsimonious trees. Nonetheless, the study of Mindell *et al.* (1989) has been repeatedly cited as evidence of molecular punctuated equilibrium (Gould and Eldredge 1993, Gould 2002).

It has long been recognized that parsimony underestimates the amount of change along a phylogenetic branch to the extent that it can neither detect nor account for multiple changes of the same character along the same lineage (Goodman *et al.* 1974, Moore *et al.* 1976, Moore 1977). This underestimation is expected to be most severe in long, unbroken lineages. When such lineages are subdivided through the sampling of additional taxa, previously undetected changes become revealed, and the total number of changes from the root to the tip of the lineage

increases, approaching the true number. This node density effect causes large clades in a parsimony phylogeny to appear to have evolved faster than small clades of equal age. Two proposed methods to overcome the node density effect are the populous path algorithm (Goodman *et al.* 1974, Moore *et al.* 1976, Moore 1977) and the Fitch-Bruschi method (Fitch and Bruschi 1987). Both of these methods compare lengths of unbranched and branched lineages and apply a correction to account for the excess of undetected homoplasious substitutions in unbranched lineages. However, neither method facilitates testing of molecular punctuated equilibrium, because any potential effect of speciation on rate of evolution would be erased by the correction itself.

Maximum likelihood (ML) methods can account for multiple changes at a single site along an evolutionary branch (Felsenstein 1978). As a result, ML is more robust to the node density effect than is parsimony (Bromham *et al.* 2003). However, ML is also known to chronically underestimate genetic distances, especially when sequences are short, evolutionary distances are large, and the ML model employed is simpler than the true model (Zharkikh 1994). Therefore, molecular phylogenies with branch-lengths estimated by ML are still expected to be somewhat prone to the node density effect.

A new method for testing the relationship between speciation and molecular evolution was introduced by Webster *et al.* (2003), who reported evidence of punctuated equilibrium in 56 molecular phylogenies. For each of the 56 phylogenies, they used generalized linear regression to measure the relationship between number of nodes and root-to-tip path length. A covariance matrix was used to account for the degree of non-independence among root-to-tip paths that overlap in the phylogeny to varying degrees. Number of nodes was used as an estimate of the number of speciation events that have occurred along each contiguous lineage from the common

ancestor to the present. The number of substitutions inferred along each root-to-tip path was used as a measure of the rate of evolution relative to other such paths. A likelihood ratio test was used to measure the significance of the regression coefficient (Pagel 1997, 1999). Webster *et al.* (2003) reported that the cumulative frequency distribution of likelihood ratio statistics for the set of 56 phylogenies departed significantly from the Chi-square expected distribution and, thus, that increased rate of speciation was associated with increased rate of molecular evolution.

This potentially powerful approach was facilitated by a creative method, the delta test, developed by Webster *et al.* (2003) to circumvent potential bias introduced by the node density effect. The node density effect is expected to cause paths with more nodes to appear longer than paths with few nodes, and this alone could cause a significant regression between path length and number of nodes. Webster *et al.* (2003) reasoned that as each additional node is added along a path, successively fewer additional substitutions will be revealed along that path. Therefore the relationship between path length and number of nodes will take the form of an exponential curve in any phylogeny that contains saturated or undetected substitutions. This curve can be described by the equation $n = x^{\delta}$, in which n equals the number of nodes along path, and x equals the length of that path measured in units of evolutionary change. Webster *et al.* (2003) assumed that the node density effect would cause delta to be greater than one. They estimated the exponential parameter, delta, by maximum likelihood, and they devised two tests for the node density effect with different levels of stringency. The weak test required that delta be significantly greater than one. The strong test required that the maximum likelihood estimate of delta be greater than one, regardless of the confidence limits. Phylogenies that showed evidence of the node density effect by the weak or strong tests were eliminated from the remainder of the analysis. The weak test

and strong test revealed evidence of the node density effect in 2 and 13 of the 56 phylogenies, respectively.

A subsequent debate raised several potential shortcomings of the Webster *et al.* analysis (Witt and Brumfield 2004, Brower 2004), all of which were disputed by Webster *et al.* (2004). The most significant concern was that the delta test may be insufficient for detecting the node density effect. If the node density effect were not always detected, then it would introduce bias toward finding a link between molecular evolution and speciation. Witt and Brumfield (2004) argued that the node density effect could affect any molecular dataset that contains saturated changes and that the value of delta is dependent on the vagaries of taxon sampling. As evidence they cited Figure 1A from Fitch and Bruschi (1987), which shows a linear relationship between path length and number of nodes. Webster *et al.* (2004) countered that "values of delta [less than or] equal to one are not compatible with the artifact," and that this point is "easily proven mathematically". It is indeed possible that the linear pattern presented by Fitch and Bruschi (1987) was a result of a true relationship between speciation and molecular evolution, rather than the node density effect as surmised by the authors. Webster *et al.* (2004) cited Figure 2 of Fitch and Beintema (1990) as a clear example of the curvilinear relationship between path length and number of nodes expected under the node density effect. However, that figure also seems to illustrate the dependence of the relationship on variation in taxon sampling — if a single terminal clade were removed from the Fitch and Beintema (1987) analysis, the curvilinearity would shift directions, causing delta to be less than one.

Only in simulated molecular phylogenies is it possible to be certain that speciation events exert no effect on molecular evolutionary rate. In this study, I used simulated molecular phylogenies to test whether values of delta less than or equal to one are compatible with the node

density effect. Specifically, I sought to discover whether the test designed by Webster *et al.* (2003) can be applied as an unbiased test of molecular punctuated equilibrium. Furthermore, I explored the effects of parsimony and maximum likelihood methods of branch length estimation on the strength of the node density effect and the application of the delta method.

METHODS

I simulated 20 random tree topologies of 25 taxa each, using the program Phyl-o-Gen (Rambaut 2002), with the birth and death parameters set to 0.2 and 0.1, respectively. I used the program Seq-Gen (Rambaut and Grassly 1997) to simulate 1000 basepair DNA sequence datasets onto each of the topologies using a general time reversible model of molecular evolution, with parameters garnered from a recently published mitochondrial DNA analysis (Jennings *et al.* 2003). The model accounted for six substitution rates, unequal base frequencies, gamma-distributed rate heterogeneity, and a proportion of invariable sites. The model parameters, in PAUP* (Swofford 2001) format, were as follows: Lset Base=(0.3833 0.3188 0.1041) Nst=6 Rmat=(2.4839 11.0727 3.1451 0.7003 19.7931) Rates=gamma NCat=8 Shape=8.665 Pinvar=0.4556;). Ten datasets were simulated onto each of the 20 topologies with a total root to tip distance of 0.8 substitutions per site. This produced sets of distantly related taxa, analogous to different families or orders. Ten additional datasets were simulated onto each of the 20 topologies with a total root to tip distance of 0.2 substitutions per site. This produced sets of closely related taxa, analogous to species or genera.

For each of the 400 simulated datasets, branch lengths were estimated using three different methods as implemented in PAUP* b4.10 (Swofford): (1) parsimony with equal character weighting and ACCTRAN character optimization; (2) maximum likelihood using a simple Kimura 2-parameter model assuming equal base frequencies (K2P; Ts:Tv = 4.21); and (3)

maximum likelihood using the precise general time-reversible model under which the data were simulated, including gamma-distributed rate heterogeneity among sites, a proportion of invariant sites, and unequal base frequencies (GTR + Γ + I, parameters as above). In each case, the branch lengths were estimated onto the correct topology.

Each of the 1200 resulting tree topologies with branch length estimates were input into the program Continuous (Pagel 1997, 1999). For each topology, the number of internal nodes along each root-to-tip path were counted and input as a continuous trait. Continuous was used to perform a likelihood ratio test for positive association between total path length and number of nodes. A significant result would indicate that paths with more nodes have undergone more molecular evolution as inferred by parsimony or maximum likelihood. For these simulated data, I interpret a significant likelihood ratio test as evidence of a node density effect.

I used Continuous to derive a maximum likelihood estimate and confidence intervals for the delta statistic, which describes the curvature in the relationship between path length and number of nodes. Webster *et al.* (2003, 2004) asserted that delta less than one is not consistent with the node density effect. If this assertion is true, then we expect that the maximum likelihood estimate of delta will be greater than one for all or nearly all of the simulated datasets in which a significant node density effect is detected by the likelihood ratio test.

For the subsets of phylogenies that passed the weak and strong delta tests of Webster *et al.* (2003), I compared the distribution of the likelihood ratio statistics with the Chi-square expectation, using a Kolmogorov-Smirnov test. This would determine whether the node density effect causes pervasive bias even in datasets that show no clear evidence of a curvilinear relationship between path length and number of nodes.

To test whether distance-based methods are susceptible to the node density effect, I replicated these analyses for the 200 simulated deep phylogenies using uncorrected p-distances to estimate branch lengths.

RESULTS

All parsimony analyses for the 200 datasets with 0.8 substitutions per site yielded significant LR tests for a positive correlation between total path length and number of nodes (Table 2.1). The ML analyses using the Kimura 2-parameter model and GTR model reduced the number of significant LR tests by 14 and 67 percent, respectively. At the relatively shallow phylogenetic depth of 0.2 substitutions per site, the percentage of datasets with LR significant was substantially reduced for all three methods of analysis; however, 91% of phylogenies still had LR significant when branch lengths were estimated using parsimony.

The removal of all datasets for which delta was significantly greater than one, corresponding to the weak delta test of Webster *et al.* (2003), had a very small effect. Only 5 to 21 % of the phylogenies for each method and depth satisfied the weak criterion, and the percentage of remaining datasets with LR significant was nearly unchanged. Application of the strong delta test by excluding phylogenies in which the ML estimate of delta was greater than one reduced the pool of datasets by 54 to 82 percent, and the percentage with significant LR was reduced slightly.

The distribution of the LR statistic is expected to conform to Chi-square distribution if there is no correlation between total path length and number of nodes. In these datasets simulated under conditions of equal evolutionary rates, such a correlation could only arise as an artifact of the node density effect. In general, the distribution of LR statistics was strongly positively skewed from the Chi-square distribution regardless of analysis method, phylogenetic depth, or

TABLE 2.1. Summary of analyses of 200 simulated sequence datasets at each of two phylogenetic depths and using three methods of analysis. The Kolmogorov-Smirnov D statistic measures the maximum difference between the cumulative distribution frequencies of LR and Chi-square statistics (see Figure 2). The critical P-value after Bonferroni correction is 0.0083.

Phylogenies included	Root-to-tip distance (subs./site)	Method of branch length estimation	Total number of phylogenies	Phylogenies with LR significant	D	P
ML estimate of delta < 1 (strong test)	0.2	Parsimony	36	31	0.8358	2.9×10^{-22}
	0.2	K2P	86	28	0.3840	1.9×10^{-11}
	0.2	GTR+Γ+I	92	17	0.1393	0.0563
	0.8	Parsimony	61	61	0.9953	6.5×10^{-53}
	0.8	K2P	72	54	0.7553	4.2×10^{-36}
	0.8	GTR+Γ+I	92	21	0.2815	9.3×10^{-7}
Delta not significantly > 1 (weak test)	0.2	Parsimony	168	153	0.8704	5.6×10^{-111}
	0.2	K2P	170	74	0.4435	1.8×10^{-29}
	0.2	GTR+Γ+I	189	43	0.2068	1.6×10^{-7}
	0.8	Parsimony	181	181	0.9953	3.6×10^{-156}
	0.8	K2P	158	130	0.7859	3.9×10^{-91}
	0.8	GTR+Γ+I	190	60	0.3509	9.5×10^{-21}
All	0.2	Parsimony	200	181	0.8647	2.6×10^{-130}
	0.2	K2P	200	94	0.4541	3.0×10^{-36}
	0.2	GTR+Γ+I	200	46	0.2041	1.2×10^{-7}
	0.8	Parsimony	200	200	0.9918	2.6×10^{-171}
	0.8	K2P	200	171	0.8067	1.8×10^{-113}
	0.8	GTR+Γ+I	200	66	0.3591	7.9×10^{-23}

value of delta (Figure 2.1). The only exception was the case of shallow phylogenetic depth and the perfectly fitted GTR model in which the strong test yielded a positive, but non-significant departure from the Chi-square expectation (p=0.056). Deeper phylogenies and simpler methods of branch length estimation yielded the highest departures from Chi-square. In this way, variation according to method and phylogenetic depth corresponded to the predicted degree of susceptibility to saturation and the node density effect.

When branch lengths were estimated using uncorrected p-distances, the LR statistics conformed to the Chi-square expected distribution. The non-significant deviation was in the opposite of the expected direction (D = 0.07, P = 0.80).

CONCLUSIONS

The Delta Test

The high frequency of significant LR statistics suggests that the node density effect is pervasive regardless of whether parsimony, a simple Kimura 2-parameter ML model (K2P), or the true ML model (GTR+Γ+I) are used to estimate branch lengths. However, the effect is clearly most severe under parsimony, and least severe under the true ML model. This reinforces the fact that model accuracy is critically important for estimating branch lengths, but it calls into question whether node density bias can be overcome even in the idealized case of a highly accurate model. Distance-based methods appear to be relatively immune to the node density effect, despite that they cannot estimate amounts of evolution with the same degree of accuracy as phylogenetic methods. This is not surprising, considering that pairwise distances are unaffected by the number of intervening taxa.

The marked improvement of LR statistics at the shallower phylogenetic depth suggests that branch length comparisons among closely related taxa are likely to be less affected by node density bias. Surprisingly, delta was no less likely to be greater than one in shallower phylogenies. The delta correction, even under the conservative "strong test" of Webster *et al.* (2003) had little impact on the percentage of phylogenies that showed evidence of the node density effect by the LR test. This suggests that the delta statistic is not an effective tool for identifying the node density effect. The generally poor performance and the broad confidence

Figure 2.1. Cumulative distribution frequencies of LR statistics for simulated datasets, using three methods of estimating branch lengths. The left column (A, C, E) contains the results from 200 datasets simulated with a total root-to-tip distance of 0.2 substitutions per site. The right column (B, D, F) contains the results from the 200 datasets simulated with a phylogenetic depth of 0.8 substitutions per site. The LR statistics are consistently skewed to the right of the Chi-square distribution (Kolmogorov-Smirnov test statistics in Table 1), indicating that there is a positive correlation between number of nodes and root-to-tip path length regardless of whether delta is greater than or less than one.

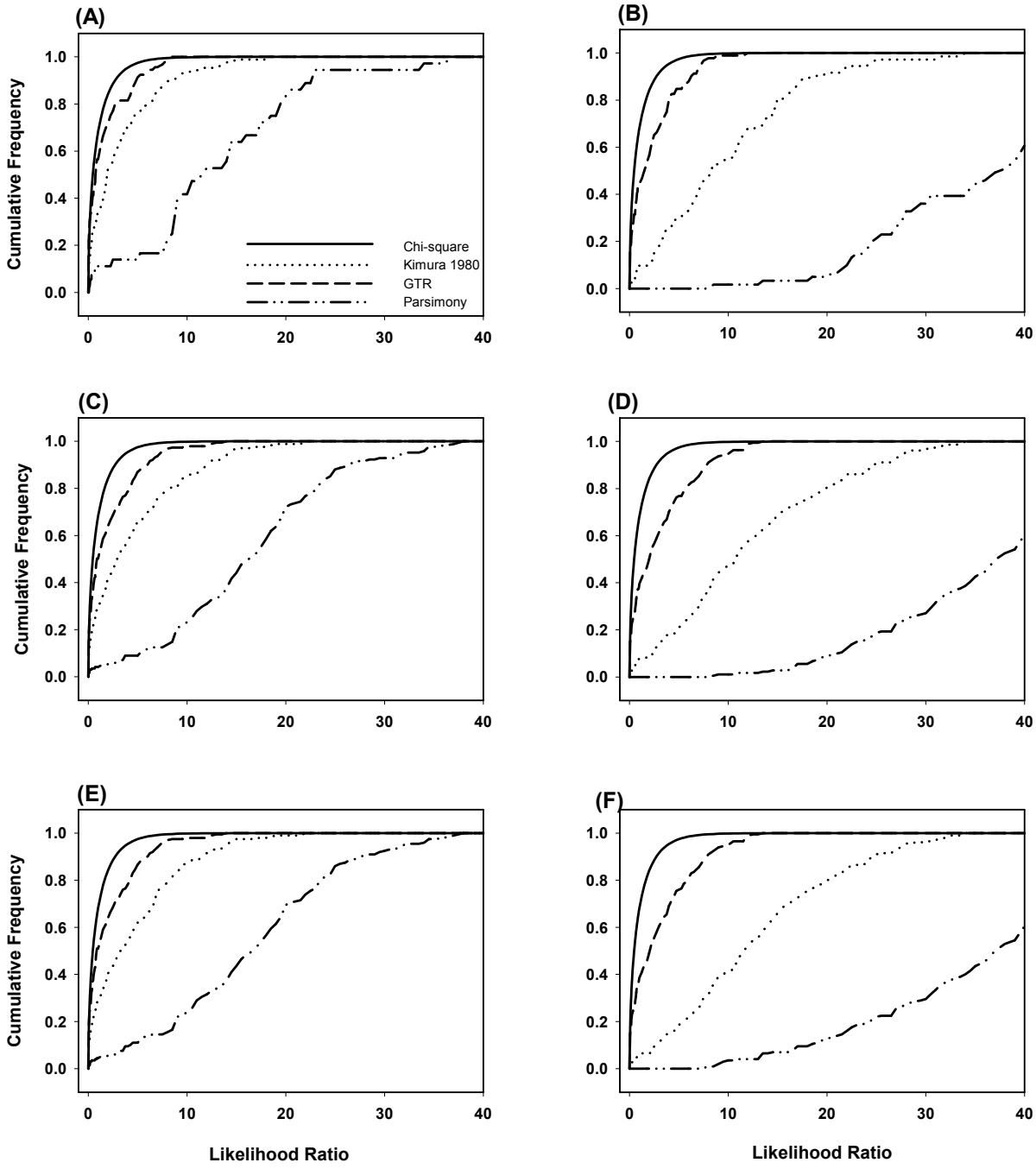
(A)
(B)
(C)
(D)
(E)
(F)
Cumulative Frequency
Likelihood Ratio
Chi-square
Kimura 1980
GTR
Parsimony
0.0
0.2
0.4
0.6
0.8
1.0
0
10
20
30
40

intervals around maximum likelihood estimates of delta indicate that the problem is unlikely to be solved by making the critical levels of delta more conservative.

Only in the idealized scenario of the true ML model at the shallow phylogenetic depth did the distribution of LR statistics approach the Chi-square expected distribution. Even in that case, 18 percent of the simulated phylogenies possessed significant LR statistics, and the lack of overall significance was probably a byproduct of small sample size.

The percentage of simulated phylogenies in which apparent punctuated evolution would be inferred was comparable to the 30% (strong test) and 50% (weak test) reported by Webster *et al.* (2003) for empirical data (Table 2.2), especially considering that the empirical datasets varied extensively in phylogenetic depth and method of branch length estimation. I suggest that the high LR statistics reported by Webster *et al.* (2003) are mostly or entirely attributable to the node density effect.

The delta test assumes that the number of previously undetected substitutions revealed by each additional node diminishes as more nodes are added to a given path. This is expected to be true on average. However, nodes that evenly subdivide internal branches are likely to uncover more additional substitutions than those that occur in rapid succession. Thus, the actual contribution of each node depends on its proximity to other nodes. Instances of known rapid radiations are numerous (Levinton 2001), indicating that nodes will often be clustered in nature. When the temporal distribution of nodes is uneven, the assumption that the node density effect causes paths with higher node density to have fewer substitutions per node than paths with lower node density is frequently violated. For example, when nodes are clustered towards the base of the tree, but widely spaced toward the tips, the node density effect is expected to cause basal

lineages to contain fewer inferred substitutions per node than derived lineages. This scenario would cause delta to be less than one despite the presence of a node density effect.

Node density and distribution effects are ignored in most phylogenetic studies, although they can potentially affect any analysis that depends on branch-length estimates, including inferences of divergence times, ancestral character states, and the correlates of trait evolution or evolutionary rate variation.

TABLE 2.2. The percentage of phylogenies in which a correlation between path length and number of nodes would be inferred using the delta method of Webster *et al.* (2003).

Source	Branch length estimation method	Strong test	Weak test
Webster *et al.*	Mixed	30%	50%
Simulated, 0.2 sub./site	Parsimony	86	91
Simulated, 0.2 sub./site	ML: K2P	33	44
Simulated, 0.2 sub./site	ML: GTR + I + g	18	23
Simulated, 0.8 sub./site	Parsimony	100	100
Simulated, 0.8 sub./site	ML: K2P	75	82
Simulated, 0.8 sub./site	ML: GTR + I + g	23	32

Evidence for Molecular Punctuated Equilibrium

The best evidence to date of a link between rates of speciation and molecular evolution is from Barraclough and Savolainen (2001), who analyzed the relationship between number of species and relative rate of molecular evolution in 89 sister pairs of plant families. For most families, a single representative taxon was used, and terminal phylogenetic branches were used as estimates of relative rate of molecular evolution. Among 89 independent contrasts, family diversity and molecular evolutionary rate were significantly correlated. Most of the 89 comparisons used by Barraclough and Savolainen (2001) were robust to the node density effect because each family was represented by a single taxon on an undivided terminal branch. However, in the 28 comparisons in which families were represented by more than one species, phylogenetically estimated branch lengths were averaged at each node to derive an estimate of the average rate of

molecular evolution for the family, relative to its sister family. Those comparisons were prone to the node density effect and could cause bias, particularly if diverse families tended to be sampled more thoroughly than depauperate families. Barraclough and Savolainen were aware of this problem, and so they replicated their analysis using only families represented by equal numbers of terminal taxa. The result was essentially unchanged. However, the node density effect could still potentially bias the anlaysis if the distribution of nodes between speciose and depauperate families differed consistently. I re-analyzed the Barraclough and Savolainen (2001) dataset using a single representative taxon for each family. I found that node density effects induced by branch-length averaging were minimal and had almost no effect on the overall result. The correlation between rate and diversity was much stronger for synonymous than nonsynonymous substitutions, suggesting that speciose clades have a higher underlying mutation rate than depauperate clades. The authors suggested that the weak positive correlation with nonsynonymous substitution rate may be a secondary result of the difference in mutation rate rather than an effect of speciation. Faster mutation rate itself could cause faster speciation or, alternatively, rates of mutation and speciation could be linked due to some unrelated factor such as climate (Wright *et al.* 2003) or life history (Gaut *et al.* 1996). A complimentary finding was made in a study of speciose and depauperate sister clades of carnivorous plants by Jobson and Albert (2002), who found a significant relationship between species diversity and rate of evolution in seven genes. This relationship was confirmed by distance-based relative rate tests, and is therefore not a mere artifact of node density. The causal mechanism and the generality of these associations remain to be tested in additional studies that include dense taxon-sampling schemes and non-plant taxa.

Omland (1997) reported a correlation between rates of morphological and molecular evolution in an analysis of eight molecular phylogenies. Such a correlation would be expected under molecular punctuated equilibrium. However, in a broader survey of datasets, Bromham *et al.* (2003) found no link between rates of morphological and molecular evolution. Furthermore, Bromham *et al.* (2003) showed that Omland's (1997) method may have violated the assumption of phylogenetic non-independence.

The hypothesis that rates of molecular evolution and speciation are linked is premised on the assumption that population bottlenecks and selective sweeps occur more frequently in association with speciation events. However, population genetic studies have revealed that phyletic population expansions and bottlenecks are common, and such events could erase any signal of rate acceleration caused by a lineage splitting event. Furthermore, it must be remembered that the number of extant nodes depends on the total diversification rate (speciation plus extinction); thus, variation in both extinction rate and speciation rate affect the number of nodes along a path. Clades with high mean extinction rates may appear similar to those with low mean speciation rates (Kubo and Iwasa 1995). Extinction rate in a given clade may be positively correlated with demographic stochasticity (Legendre *et al.* 1999), and therefore frequency of population bottlenecks. Thus, the expected direction of differences in rate of evolution between two lineages could depend on whether the difference in number of inferred bifurcations is attributable to speciation rate or extinction rate, parameters that are usually unknowable.

A correlation between path length and number of nodes could indicate that speciation events cause accelerated molecular evolution, perhaps by a mechanism such as proposed by Mayr (1954). Alternatively, it could suggest that lineages that undergo relatively rapid DNA substitution for some unrelated reason tend to speciate faster (Orr 1995). The extent to which

speciation rate is generally linked to inter-lineage variation in rate of molecular evolution is yet to be determined. Future attempts to test the association between speciation rate and molecular evolutionary rate will need to estimate branch lengths in a way that completely overcomes the bias caused by variation in node density and node distribution. Pruning taxa to allow comparisons of unbranched sister-lineages is one such unbiased method (Sanderson 1990, Bromham *et al.* 2003). Statements by Webster *et al.* (2004) that "rates of evolution are linked to rates of speciation in a statistically significant way" and that this result applies "generally across a range of taxa" are not yet justified.

CHAPTER 3. BODY MASS AND RATE OF MOLECULAR EVOLUTION IN BIRDS: A TEST OF THE METABOLIC RATE HYPOTHESIS

The metabolic rate hypothesis holds that variation in rate of mitochondrial DNA (mtDNA) evolution among lineages reflects variation in rate of metabolism (Martin and Palumbi 1993). Its premise is the expectation that mtDNA will be exposed to higher concentrations of mutagenic oxygen free-radicals in organisms with higher mass-specific metabolic rates (Shigenaga *et al.* 1989). Two lines of evidence suggest the influence of metabolism on evolutionary rate: (1) faster mtDNA evolution in homeothermic than in poikilothermic animals (Avise *et al.* 1992, Martin, Naylor, and Palumbi 1992); and (2) faster evolution in lineages of smaller bodied animals (Martin and Palumbi 1993), which have higher mass-specific metabolic rates according to the laws of allometric scaling (Calder 1984). However, the apparent link between small body size and fast evolutionary rate may be an artifact of inadequate comparative methods. Here I show that a large number of independent phylogenetic contrasts among closely related bird lineages conspicuously fails to corroborate the association between small body size and elevated rate of mtDNA evolution. On the contrary, lineages consisting of larger animals tend to exhibit faster rates of nonsynonymous substitution, implicating population size as a pervasive cause of evolutionary rate variation.

Causes of evolutionary rate variation can be identified by considering molecular and life history data together in a phylogenetic context. Numerous such empirical studies have reported patterns consistent with a metabolic rate effect, including studies of birds (Nunn and Stanley 1998) mammals (Martin 1995, Bromham *et al.* 1996), reptiles (Bromham 2002), sharks (Martin Naylor, and Palumbi 1992, Martin 1999), and a broad sampling of vertebrates (Martin and Palumbi 1993). As a result, the apparent inverse relationship between body mass and

evolutionary rate has gained wide acceptance, and the metabolic rate hypothesis has been considered a leading explanation for mtDNA rate variation in reviews and syntheses (e.g. Rand 1994, Page and Holmes 1998). Patterns inconsistent with the metabolic rate hypothesis have been considered anomalies. These include the findings that mtDNA rates are slower in birds than mammals (Adachi, Cao, and Hasegawa 1993, Mindell *et al.* 1996) faster in elephants than other orders of mammals (Hauf *et al.* 1999), and faster in giant tortoises than other ectotherms (Caccone *et al.* 2002).

Previous studies that have addressed the causes of rate heterogeneity have been hindered by methodological obstacles (Bromham 2002, Slowinski and Arbogast 1999), including limited numbers of phylogenetically independent contrasts or use of non-independent contrasts (Avise *et al.* 1992, Martin, Naylor, and Palumbi 1992, Martin 1995, Adachi, Cao, and Hawegawa 1993, Mindell *et al.* 1996, Mooers and Harvey 1994, Cantatore 1994, Gissi *et al.* 2000, Rowe and Honeycutt 2002), failure to adjust rate estimates for the effects of saturation (Martin and Palumbi 1993, Nunn and Stanley 1998), use of inaccurate or misleading body mass data (Nunn and Stanley 1998, Mooers and Harvey 1994), and over-reliance on higher level comparisons (Avise *et al.* 1992, Martin, Naylor, and Palumbi 1992, Martin 1995, Adachi, Cao, and Hawegawa 1993, Mindell *et al.* 1996, Mooers and Harvey 1994, Cantatore 1994, Gissi *et al.* 2000, Rowe and Honeycutt 2002). Ideally, testing the correlation between mtDNA rate and body mass would require a large number of phylogenetically independent contrasts to control for confounding effects of phylogeny on evolutionary rate or body mass. In addition, analyses should be restricted to closely related pairs of taxa that differ in body mass. Estimates of rate become less accurate at deeper phylogenetic levels due to saturation, base composition bias, and resulting incorrect topology. Considering the high frequency of body mass shifts over evolutionary time, the

avoidance of deep phylogenetic nodes is critical to insure that body mass data are representative of the entire lineages being compared. Furthermore, limiting the set of comparisons to close relatives that differ in body mass minimizes the possibility that detected rate heterogeneity could be the result of other, unidentified life history character differences that are not linked to body mass.

I used phylogenetic relationships inferred by maximum likelihood to identify a large sample of independent contrasts between terminal sister taxa of birds that are definitively different in body mass. This study was designed to maximize the possibility of finding an inverse relationship between body mass and evolutionary rate. If no inverse relationship exists, then these comparisons would refute the role of metabolic rate variation in causing evolutionary rate variation among lineages. Birds present an excellent opportunity to test the relationship between body mass and mtDNA rate because body mass variation is common among closely related lineages. In addition, basal metabolic rates of neognathous birds are higher and vary more radically with changes in body mass than in any other group of organisms (Calder 1984). The relationship between body mass and evolutionary rate in birds is likely to have general implications as indicated by the universality of the relationship between metabolic rate (B) and body mass (M) for all organisms such that $B \propto M^{3/4}$.

METHODS

Over 4000 mitochondrial cytochrome b sequences from Genbank were combined with 36 original sequences from the families Bucconidae and Galbulidae to form a dataset representing approximately 1750 out of 9700 avian species (18%) and 149 out of 182 avian families (82%) (Table 3.1, Appendix). The longest available sequences for each species were sorted into 48 computationally manageable alignments based on taxonomy or established monophyly, using

published higher-level molecular phylogenies as a guide (Barker, Barrowclough, and Groth 2001, Burns and Hackett 2002, Groth and Barrowclough 1999, Cooper *et al.* 2001, Irestedt *et al.* 2001, Paton, Haddrath, and Baker 2002, Sibley and Ahlquist 1990, Sibley and Monroe 1990, Sorenson and Payne 2001, Van Tuinen *et al.* 2001, Van Tuinen, Sibley, and Hedges 2000). Each alignment was intended to be monophyletic with respect to every other alignment. However, because many sequence fragments were partially overlapping or non-overlapping, some nested sets of taxa were analyzed separately; thus, some alignments were paraphyletic with respect to others. Care was taken to insure that all pair-wise rate comparisons were phylogenetically independent. Alignment was performed using SEQUENCHER (Version 4.1, Genecodes, Ann Arbor, MI).

For each of the 48 alignments, PAUP* 4.0 b10 (Swofford 2000) was used in combination with MODELTEST (Posada and Crandall 1998) to estimate the simplest appropriate model of evolution using hierarchical log-likelihood ratio tests. Correcting for multiple substitutions is critical when estimates of lineage-specific substitution rates are the primary purpose of the analysis (Slowinski and Arbogast 1999). PAUP* 4.0 b10 was used to build neighbor-joining trees based on maximum-likelihood distances and to estimate branch lengths for those trees under the likelihood optimality criterion.

Rate comparisons were limited to terminal sister taxa. After phylogenetic analysis, sequences of sister taxa were trimmed to the same length and position, and ambiguous bases in one sister were made ambiguous in the other sister. Iterative phylogenetic analysis and sequence trimming were carried out until all sister-taxon pairs were represented by completely overlapping sequences of identical length.

Body mass data were gathered from literature and museum specimens. When available, mean female body mass was used because of its relevance to the evolution of the matrilineal mtDNA genome. To overcome daily, seasonal, and individual body mass variation, pairs of sister taxa were only used in rate comparisons if their reported mean female body masses differ by at least 10%, and if they satisfied at least one of the following criteria: (1) non-overlapping ranges or standard deviations; (2) mass differences consistent with other morphological measurements; or (3) mass differences consistent with an explicit statement in the literature. Comparisons between species in different genera or families were only included if body mass differences were consistent across all members of both higher-level taxa. If female data were unavailable, data for males or individuals of unknown sex were used provided that the direction of sexual size dimorphism for the relevant group of birds would have conservatively biased the degree of inferred body mass difference. The midrange of a range of values was substituted for the mean body mass if the mean was not available.

For terminal sister pairs of taxa that satisfied the body mass criteria, the relationship between relative mass and relative branch length was tested using a binomial sign test. If both members of the taxon pair possessed equal zero-length branches, the comparison was dropped from the analysis.

Correlation analysis was carried out to test for a relationship between difference in mass (mass of the rapidly evolving bird minus mass of the slowly evolving bird) and the difference in branch length. These variables were log-transformed to approach normality, and to allow for graphical visualization of patterns; however, the difference in branch lengths violated normality in all analyses, so only the non-parametric Spearman's rank correlation statistic was used. A few taxa that possessed zero-length or near zero-length branches created a severe bimodal

distribution for the variable representing difference in branch length. Although this skew should not create a problem for non-parametric statistical methods, it may reflect the fact that near-zero branch lengths can result from incorrect phylogenetic estimation, or can otherwise be artifacts of the phylogenetic methods. Therefore these outlying comparisons were excluded from the analyses. The inclusion of the outlying comparisons did not have a profound impact on the results of the correlation analyses (after zero-length branches were converted to 1×10^{-5} for the purposes of computational tractability).

All analyses were repeated using synonymous and nonsynonymous distances calculated using the Kumar method as implemented in MEGA, version 2.1 (Kumar *et al.* 2001). Relative synonymous and nonsynonymous branch lengths were derived by a relative rate calculation using the nearest possible outgroup as identified by the PAUP* topology.

Because passerine birds (order Passeriformes) possess a unique scaling relationship between body mass and metabolic rate (Calder 1984), passerine and non-passerine birds were analyzed separately. Those taxon pairs that differ by greater than 50% in body mass were analyzed in separate sign tests to allow the most powerful possible test for a metabolic rate effect. To test for an effect of phylogenetic depth on the detectability of a body mass effect, the sign test was performed separately for intra-generic and inter-generic rate comparisons.

RESULTS AND CONCLUSIONS

From among cytochrome b sequences for 1750 species of birds, 504 pairs of terminal sister taxa were identified, of which 191 were at least 10% different in body mass (Table 3.1). Among these 191 sister-taxon pairs, smaller body mass was not associated with faster overall rate of evolution in a sign test (Fig. 3.1a). No association between relative body mass and rate of evolution was evident when the analyses were limited to each of two taxonomic subsets of comparisons

TABLE 3.1. Branch length and body mass data for 191 terminal sister taxon pairs used in rate comparisons. Each row in the table represents one pair of taxa that comprised a single data point in analyses. Lines between rows demarcate sets of taxon pairs that were analyzed in the same phylogenetic dataset. Taxon pairs are listed in taxonomic order following Dickinson (2003) when possible. Taxon 1 always has a longer branch length than Taxon 2 when all substitutions are considered.

bp	Taxon 1	Mass (g)	Branch length (substitutions per site)			Taxon 2	Mass (g)	Branch length (substitutions per site)		
			All	ns	s			All	ns	s
1143	*Casuarius bennetti*[b]	17600	0.03590	0.00530	0.07168	*Casuarius casuarius*[a]	44000	0.00901	0.00106	0.03277
654	*Apteryx owenii*[a]	1351	0.01454	0.00491	0.03027	*Apteryx haastii*[b]	2400	0.01211	0.00245	0.03060
1139	*Crypturellus strigulosus*[b]	390	0.27172	0.02681	0.41354	*Crypturellus tataupa*[a,b]	264	0.16855	0.02580	0.31137
253	*Crax alector*[a,b]	3400	0.00416	0.00000	0.01166	*Crax globulosa*[b]	2500	0.00000	0.00000	0.00001
325	*Megapodius eremita*[b]	607.5	0.16140	0.01678	0.24737	*Alectura lathami*[a]	2330	0.11589	0.02404	0.20036
1143	*Alectoris magna*[a,b]	524.5	0.03377	0.00388	0.08030	*Alectoris philbyi*[a,b]	441	0.01385	0.00272	0.03522
660	*Francolinus capensis*[a]	547	0.01581	0.00486	0.03514	*Francolinus adspersus*[a]	394	0.01495	0.00272	0.02846
656	*Francolinus gularis*[a,b]	510	0.03910	0.00596	0.09754	*Francolinus pondicerianus*[a,b]	228	0.03897	0.00593	0.04621
660	*Francolinus africanus*[a]	359	0.03094	0.00001	0.07871	*Francolinus levaillantoides*[a]	414.5	0.01978	0.00189	0.04328
547	*Tetrao mlokosiewiczi*[b]	767	0.02914	0.00001	0.06634	*Tetrao tetrix*[a]	910	0.01647	0.00228	0.06838
1143	*Chrysolophus pictus*[a]	607.5	0.06543	0.00328	0.12452	*Catreus wallichi*[a]	1305	0.05245	0.00669	0.12272
1143	*Lophura nycthemera*[a]	1230	0.01895	0.00000	0.04840	*Lophura leucomelana*[a]	794	0.01050	0.00000	0.02903
1143	*Lophura diardi*[a]	835	0.03446	0.00277	0.07223	*Lophura ignita*[a]	1600	0.02179	0.00495	0.05403
1143	*Polyplectron bicalcaratum*[a]	480	0.00871	0.00415	0.02304	*Polyplectron chalcurum*[a]	251	0.00664	0.00001	0.01204
1143	*Pavo cristatus*[a]	3375	0.02313	0.00136	0.04838	*Pavo muticus*[a]	1110	0.01342	0.00278	0.03472
608	*Dendragapus obscurus*[a]	891	0.05754	0.00834	0.12290	*Lagopus mutus*[a]	422	0.04872	0.00178	0.10730
306	*Anser albifrons*[a,b]	2456	0.00348	0.00000	0.00900	*Anser erythropus*[a,b]	1964	0.00000	0.00000	0.00001
306	*Cereopsis novaehollandiae*[a]	3560	0.09965	0.01741	0.10755	*Dendrocygna guttata*[a]	800	0.06845	0.01202	0.14359
306	*Malacorhynchus membranaceus*[a]	344	0.13512	0.01934	0.18679	*Biziura lobata*[a]	1551	0.05111	0.01170	0.12593
306	*Chloephaga melanoptera*[a]	2900	0.01128	0.00530	0.00001	*Neochen jubatus*[a]	1250	0.00000	0.00001	0.02459
1045	*Tachyeres pteneres*[a]	4228	0.04769	0.01206	0.08787	*Speculanas specularis*[a]	975	0.03075	0.00429	0.06617
1045	*Pteronetta hartlaubi*[a]	790	0.07450	0.00929	0.16000	*Cyanochen cyanopterus*[a]	1520	0.05952	0.00619	0.10127
306	*Cairina moschata*[a]	2022	0.10250	0.01461	0.21650	*Aix galericulata*[a]	512	0.06475	0.00514	0.14352
1045	*Anas strepera*[a]	849	0.01400	0.00459	0.02608	*Anas falcata*[a]	585	0.00522	0.00001	0.01746
1045	*Anas versicolor*[b]	407.5	0.00492	0.00153	0.01471	*Anas puna*[a,b]	550	0.00356	0.00306	0.00101
1045	*Anas hottentota*[a,b]	240	0.06531	0.00153	0.14195	*Anas querquedula*[a,b]	326	0.04551	0.00392	0.10050
771	*Spheniscus mendiculus*[a,b]	2500	0.00440	0.00001	0.01382	*Spheniscus humboldti*[a]	5000	0.00431	0.00206	0.00703
1143	*Pygoscelis antarctica*[a]	4150	0.06075	0.01332	0.09497	*Pygoscelis papua*[a]	5500	0.03496	0.00723	0.08083
1143	*Gavia stellata*[a]	1551	0.09048	0.00876	0.17573	*Gavia immer*[a]	4134	0.05699	0.00831	0.09890
1143	*Fulmarus glacialoides*[a]	1000	0.02569	0.00001	0.06249	*Fulmarus glacialis*[a]	479	0.02077	0.00248	0.04966
297	*Puffinus griseus*[a]	787	0.02737	0.00422	0.06523	*Puffinus tenuirostris*[a]	543	0.02485	0.00000	0.06497
1143	*Garrodia nereis*[a]	38.2	0.11205	0.01290	0.13332	*Pelagodroma marina*[a]	47.2	0.08264	0.01266	0.17019
1041	*Oceanodroma tethys*[a,b]	23.5	0.06030	0.00339	0.12876	*Halocyptena microsoma*[a,b]	20.5	0.03605	0.00121	0.09334
1040	*Oceanodroma castro*[a]	41.8	0.18533	0.02107	0.32098	*Oceanodroma tristrami*[a]	84	0.08246	0.01210	0.11546
1143	*Hydrobates pelagicus*[a]	25.2	0.07363	0.00801	0.15866	*Oceanodroma furcata*[a]	55.3	0.06623	0.00168	0.13649
298	*Phalacrocorax brasilianus*[a]	1070	0.02035	0.00000	0.04653	*Phalocrocorax auritus*[a]	1540	0.00525	0.00000	0.02089
804	*Sula variegata*[a,b]	1300	0.00417	0.00394	0.00332	*Sula nebouxii*[a,b]	1801	0.00382	0.00195	0.01307
1041	*Botaurus lentiginosus*[a]	706	0.08583	0.01634	0.15653	*Ixobrychus exilis*[a]	86.3	0.06941	0.00923	0.13906
336	*Egretta rufescens*[a]	450	0.07723	0.00471	0.13180	*Egretta caerulea*[a]	315	0.04128	0.01538	0.06153
1041	*Ardea herodias*[a]	2204	0.06009	0.00418	0.15782	*Ardea alba*[a]	812	0.05868	0.00635	0.11679
1018	*Ciconia ciconia*[a]	3473	0.02716	0.00142	0.06411	*Ciconia boyciana*[a]	4687	0.01529	0.00804	0.03095
1042	*Ciconia nigra*[a]	3000	0.11258	0.01682	0.16830	*Leptoptilos crumeniferus*[a]	5400	0.06515	0.01516	0.13220
1014	*Ephippiorhynchus asiaticus*[a]	4100	0.06409	0.01545	0.12770	*Ephippiorhynchus senegalensis*[a]	5947	0.05777	0.00718	0.14107
1003	*Cathartes burrovianus*[a]	953	0.04759	0.01760	0.09560	*Cathartes aura*[a]	1467	0.03363	0.00502	0.07923
1005	*Coragyps atratus*[a]	1989	0.06321	0.01527	0.16140	*Gymnogyps californianus*[a]	10104	0.05268	0.01076	0.09867
997	*Sarcoramphus papa*[a]	3400	0.05358	0.00164	0.13347	*Vultur gryphus*[a]	10100	0.03936	0.00001	0.12617

(TABLE 3.1, cont.)

1026	*Haliaeetus leucoryphus*[a]	3088	0.05698	0.00475	0.09325	*Haliaeetus pelagicus*[a]	7757	0.04497	0.00001	0.10899
1026	*Haliaeetus leucogaster*[a,b]	2638	0.00327	0.00159	0.00265	*Haliaeetus sanfordi*[a,b]	2400	0.00000	0.00001	0.00253
300	*Circus aeruginosus*[a]	763	0.09771	0.00539	0.13681	*Circus cyaneus*[a]	513	0.00001	0.00001	0.07713
1022	*Accipiter striatus*[a]	174	0.14726	0.01381	0.23400	*Accipiter gentilis*[a]	1137	0.13717	0.00824	0.17451
1024	*Aquila pomarina*[a]	1540	0.01139	0.00121	0.03281	*Aquila clanga*[a]	2678	0.00953	0.00157	0.01393
1005	*Gypaetus barbatus*[a]	5680	0.22817	0.02802	0.26636	*Neophron percnopterus*[a]	2120	0.18552	0.01830	0.26128
1143	*Herpetotheres cachinans*[a]	715	0.19508	0.01298	0.25068	*Micrastur gilvicollis*[a]	204	0.08750	0.01680	0.09788
1143	*Polihierax semitorquatus*[a,b]	57	0.23282	0.01579	0.28164	*Microhierax erythrogenys*[a,b]	43.5	0.22943	0.02370	0.35041
272	*Falco sparverius*[a]	120	0.11983	0.00000	0.24589	*Falco tinnunculus*[a]	217	0.07055	0.00000	0.16362
246	*Gallirallus sylvestris*[b]	456	0.00952	0.00000	0.00878	*Gallirallus philippensis*[a,b]	180	0.00597	0.00000	0.02584
246	*Porzana tabuensi*[a]	45.5	0.12859	0.00273	0.21628	*Porzana pusilla*[a]	32.5	0.05989	0.00474	0.13481
1143	*Grus nigricollis*[a]	6000	0.01364	0.00421	0.03501	*Grus monacha*[a]	3540	0.00384	0.00281	0.00383
1143	*Grus vipio*[a]	4663	0.02438	0.00509	0.02299	*Grus rubicunda*[a]	5663	0.01719	0.00454	0.05582
444	*Elseyornis melanops*[a]	31.5	0.14472	0.00530	0.26892	*Thinornis rubricollis*[a]	47.5	0.05144	0.00811	0.12820
456	*Oreopholus ruficollis*[a]	133	0.23749	0.01458	0.25820	*Charadrius alexandrinus*[a]	41.4	0.05125	0.00255	0.16115
1143	*Tringa glareola*[a]	73	0.06812	0.00142	0.12035	*Tringa totanus*[a]	129	0.05223	0.00139	0.11689
1045	*Calidris alpina*[a]	54.7	0.16260	0.01075	0.17388	*Calidris tenuirostris*[a]	167	0.11866	0.01146	0.18370
1143	*Recurvirostra avosetta*[a]	306	0.12496	0.00651	0.15169	*Haematopus ostralegus*[a]	526	0.11405	0.00367	0.16717
345	*Jacana spinosa*[a]	112	0.01127	0.00001	0.04181	*Jacana jacana*[a]	143	0.01032	0.00488	0.02863
343	*Irediparra gallinacea*[a]	130	0.07986	0.01625	0.18119	*Microparra capensis*[a]	41.3	0.07503	0.01814	0.13225
975	*Catharacta skua*[e]	1485	0.00331	0.00000	0.00841	*Stercorarius pomarinus*[a]	740	0.00317	0.00000	0.00853
974	*Stercorarius parasiticus*[a]	508	0.08365	0.01166	0.15990	*Stercorarius longicaudus*[a]	313	0.03666	0.00123	0.09131
258	*Larus michahelli*[b]	1150	0.00383	0.00000	0.01099	*Larus marinus*[a,b]	1488	0.00000	0.00000	0.00001
290	*Larus heermanni*[a]	500	0.01409	0.00000	0.03885	*Larus occidentalis*[a]	1011	0.00000	0.00000	0.00001
282	*Larus philadelphia*[a]	212	0.04819	0.00015	0.06171	*Larus genei*[a]	281	0.00000	0.00001	0.05598
290	*Larus serranus*[b]	478	0.01114	0.00001	0.02987	*Larus novae-hollandiae*[a,b]	323	0.00736	0.00432	0.00954
284	*Larus modestus*[a]	360	0.03419	0.00000	0.08517	*Larus pipixcan*[a]	280	0.00209	0.00000	0.00887
290	*Larus ichthyaetus*[a]	1215	0.03563	0.00000	0.11022	*Larus melanocephalus*[a]	256	0.01288	0.00000	0.03378
290	*Pagophila eburnea*[a]	616	0.02597	0.00427	0.05067	*Xema sabini*[a]	177	0.02567	0.00561	0.06456
273	*Sterna sandvicensis*[a]	208	0.02806	0.01061	0.00675	*Sterna maxima*[a]	367	0.01105	0.00001	0.07975
1044	*Synthliboramphus hypoleucus*[a,b]	167	0.01136	0.00000	0.02029	*Synthliboramphus craveri*[a,b]	151	0.00188	0.00000	0.01174
1044	*Aethia cristatella*[a]	264	0.05541	0.00308	0.11265	*Aethia pygmaea*[a]	121	0.03392	0.00464	0.07767
1044	*Fratercula cirrhata*[a]	779	0.04191	0.00154	0.08124	*Fratercula arctica*[a]	381	0.01408	0.00154	0.04770
1045	*Columba plumbea*[a]	207	0.04377	0.00349	0.08412	*Columba subvinacea*[a]	164	0.04249	0.00076	0.10995
1042	*Streptopelia senegalensis*[a]	101	0.07946	0.00203	0.14918	*Streptopelia chinensis*[a]	159	0.06935	0.00497	0.13525
1045	*Oena capensis*[a]	40.6	0.22792	0.00569	0.35030	*Ducula bicolor*[a]	483	0.12504	0.00870	0.20313
881	*Phaps chalcoptera*[a]	310	0.16156	0.00193	0.25009	*Geopelia cuneata*[a]	35.5	0.12492	0.01496	0.16848
1045	*Zenaida asiatica*[a,c]	153	0.03507	0.00154	0.05201	*Zenaida meloda*[b]	216	0.02867	0.00154	0.07499
1042	*Zenaida graysoni*[a]	192	0.00590	0.00311	0.00711	*Zenaida macroura*[a]	115	0.00429	0.00001	0.01428
1045	*Ptilinopus leclancheri*[a]	162	0.08870	0.00298	0.18944	*Ptilinopus occipitalis*[a]	238	0.03498	0.00586	0.06408
655	*Aegotheles albertisi*[a,b]	38	0.12631	0.01219	0.21203	*Aegotheles cristatus*[a,b]	50	0.02826	0.00001	0.05168
656	*Podargus papuensis*[a]	350	0.10154	0.01258	0.18292	*Podargus ocellatus*[a]	140	0.04568	0.00103	0.10291
656	*Nyctibius maculosus*[b,c]	170	0.12414	0.01737	0.18102	*Nyctibius leucopterus*[b]	80	0.10478	0.00740	0.20385
406	*Chaetura pelagica*[a]	23.6	0.03210	0.00000	0.07498	*Chaetura vauxi*[a]	17.1	0.02501	0.00000	0.05674
406	*Aerodramus elaphrus*[b]	10.5	0.00894	0.00000	0.02159	*Aerodramus francicus*[a,b]	9.25	0.00889	0.00000	0.02159
406	*Cypsiurus balasiensis*[a]	8.1	0.08125	0.01176	0.12728	*Apus nipalensis*[a]	24.3	0.06891	0.01888	0.13534
248	*Lafresnaya lafresnaya*[a]	5.3	0.11231	0.00001	0.12390	*Agleactis cupripennis*[a]	7.6	0.04919	0.00028	0.25314
249	*Sephanoides fernandensis*[a]	7	0.04909	0.00931	0.06292	*Sephanoides sephanoides*[a]	4.7	0.00000	0.00264	0.02826
249	*Eriocnemis nigrivestis*[b]	4.45	0.30896	0.01563	0.26587	*Chlorostilbon aureoventris*[a,b]	3.2	0.22758	0.01563	0.21715
248	*Heliangelus viola*[a]	5.3	0.19641	0.01910	0.07766	*Metallura tyrianthina*[a]	3.8	0.04787	0.00001	0.22465
1080	*Todus multicolor*[a]	5.8	0.12948	0.01615	0.12926	*Todus angustirostris*[a]	8.3	0.11387	0.01750	0.16755
1020	*Momotus momota*[a]	102	0.07690	0.00490	0.11923	*Momotus mexicanus*[a]	75.7	0.02549	0.00589	0.07817
1018	*Ceryle torquata*[a]	317	0.30738	0.04833	0.23017	*Chloroceryle americana*[a]	37.5	0.23525	0.01902	0.27558

(TABLE 3.1, cont.)

1047	*Bucco tamatia*[a]	33.9	0.07403	0.00661	0.15280	*Hypnelus bicinctus*[a]	49.8	0.06850	0.01015	0.09403
1047	*Notharchus macrorhynchos*[a]	95.9	0.10337	0.01478	0.16072	*Notharchus ordii*[b]	51.5	0.09444	0.01067	0.14133
1047	*Malacoptila fulvogularis*[a,c]	65	0.13764	0.01395	0.20385	*Malacoptila panamensis*[a]	42.6	0.11364	0.01051	0.18167
1047	*Monasa nigrifrons*[a]	80.7	0.06006	0.00761	0.10689	*Monasa flavirostris*[b]	39	0.04541	0.00146	0.10456
1047	*Galbula dea*[a]	27.4	0.21079	0.00977	0.33656	*Galbula albirostris*[a]	22.1	0.07380	0.00801	0.14131
1047	*Galbula leucogastra*[b]	16.5	0.01171	0.00001	0.03191	*Galbula chalcothorax*[b]	25.5	0.00611	0.00153	0.01223
881	*Lybius bidentatus*[a]	77.9	0.35393	0.00494	0.39733	*Pogoniulus bilineatus*[a]	13.6	0.22603	0.01888	0.32752
924	*Semnornis ramphastinus*[a]	97.5	0.15263	0.01365	0.19531	*Semnornis frantzii*[a]	57.3	0.03422	0.00261	0.10160
992	*Picoides major*[a]	81.6	0.04491	0.00676	0.08141	*Picoides leucotos*[a]	108	0.01369	0.00001	0.04365
962	*Picoides maculatus*[a]	27.1	0.07777	0.00530	0.15858	*Picoides canicapillus*[a]	23.3	0.04988	0.01026	0.09851
1009	*Veniliornis callonotus*[a,c,d]	25	0.03490	0.00413	0.07555	*Veniliornis nigriceps*[a,d]	39	0.02228	0.00394	0.04869
1023	*Piculus rubiginosus*[a]	55.4	0.05825	0.00444	0.10710	*Colaptes rupicola*[a]	180	0.04719	0.00937	0.10226
985	*Dendropicos fuscescens*[a]	26	0.09842	0.01514	0.12180	*Dendropicos griseocephalus*[a]	38	0.09068	0.00459	0.18006
835	*Tyrannus melancholicus*[a]	38.6	0.17218	0.01427	0.30046	*Sublegatus modestus*[a]	12.3	0.10128	0.00739	0.27264
321	*Laniisoma elegans*[a]	47.1	0.47618	0.03446	0.67779	*Piprites chloris*[a]	20	0.23646	0.01631	0.27117
321	*Xipholena punicea*[a]	68.1	0.07033	0.00798	0.16113	*Carpodectes hopkei*[a]	89	0.05320	0.01276	0.09882
321	*Haematoderus militaris*[c]	239	0.17089	0.02047	0.24909	*Querula purpurata*[a]	106	0.06471	0.01434	0.10987
320	*Lipaugus unirufus*[a]	82.1	0.21863	0.05175	0.24208	*Lipaugus fuscocinereus*[a]	138	0.05151	0.00603	0.10714
320	*Gymnoderus foetidus*[a]	275	0.14646	0.04457	0.17250	*Conioptilon mcilhennyi*[a]	90	0.14418	0.00856	0.25598
321	*Pipreola chlorolepidota*[a]	29.5	0.12849	0.02110	0.52772	*Pipreola arcuata*[a]	120	0.01379	0.02183	0.24537
322	*Pipra pipra*[a]	12	0.09005	0.00470	0.25252	*Pipra fasciicauda*[a]	15.9	0.07362	0.01046	0.16658
322	*Rupicola peruviana*[a]	221	0.12785	0.05164	0.08594	*Rupicola rupicola*[a]	140	0.06664	0.03100	0.46540
321	*Tityra cayana*[a]	73.9	0.18378	0.03030	0.27460	*Tityra inquisitor*[a]	43.3	0.13950	0.02169	0.20706
238	*Lepidocolaptes souleyetii*[a]	25.7	0.03178	0.00000	0.11153	*Lepidocolaptes lacrymiger*[a]	34.6	0.02777	0.00000	0.05497
238	*Xiphorhynchus obsoletus*[a]	39	0.12897	0.01171	0.19544	*Dendrocolaptes fuscus*[a]	21.8	0.10988	0.00000	0.19222
378	*Grallaria ridgelyi*[f]	167	0.15821	0.01757	0.19914	*Grallaria nuchalis*[a]	117	0.01929	0.00229	0.10776
307	*Corvus corax*[a]	1158	0.03891	0.01068	0.09210	*Corvus cryptoleucus*[a]	512	0.03134	0.00001	0.05769
440	*Menura novaehollandiae*[a]	746	0.44967	0.02786	0.36687	*Pitohui dichrous*[a]	72	0.01369	0.00936	0.13813
1143	*Manorina melanocephala*[a]	68	0.17704	0.01061	0.25263	*Meliphaga lewini*[a]	33.3	0.09074	0.00276	0.14095
925	*Pyrrhocorax pyrrhocorax*[a]	324	0.17001	0.00473	0.42835	*Pyrrhocorax graculus*[a]	223.5	0.10511	0.00479	0.32103
636	*Smicrornis brevirostris*[a]	5.1	0.21656	0.01494	0.21051	*Acanthiza ewingii*[a]	10	0.08407	0.01380	0.16494
298	*Orthonyx spaldingii*[a]	169.5	0.17060	0.02058	0.17240	*Orthonyx temminkii*[a]	57.5	0.17015	0.02072	0.26075
282	*Pomatostomus isidori*[a]	70	0.31320	0.04250	0.22418	*Pomatostomus superciliosus*[a]	35	0.11889	0.00330	0.18218
1113	*Lanius ludovicianus*[a]	47.4	0.02159	0.00387	0.02877	*Lanius excubitor*[a]	65.6	0.01252	0.00195	0.04576
1143	*Cyanocitta cristata*[a]	86.8	0.11363	0.00397	0.20796	*Cyanocitta stelleri*[a]	128	0.08464	0.00834	0.14070
924	*Cissa chinensis*[a]	122	0.20639	0.01740	0.23050	*Urocissa erythrorhyncha*[a]	214	0.16274	0.01492	0.21771
1143	*Manucodia keraudrenii*[a]	152	0.14514	0.00676	0.24189	*Manucodia comrii*[a]	192	0.11899	0.01637	0.14061
1143	*Epimachus fastuosus*[a]	218	0.05576	0.00392	0.11220	*Epimachus meyeri*[a]	145	0.04932	0.00282	0.05868
835	*Hypothymis helenae*[a]	9.9	0.10390	0.01103	0.10508	*Terpsiphone viridis*[a]	14.4	0.06839	0.00253	0.12090
836	*Myiagra cyanoleuca*[a]	17.5	0.07396	0.01052	0.05696	*Myiagra caledonica*[a]	10.8	0.03910	0.00371	0.10099
273	*Vireo latimeri*[a]	11.2	0.03718	0.00593	0.10509	*Vireo bellii bellii*[a]	8.5	0.03000	0.01189	0.05800
1050	*Bombycilla cedrorum*[a]	33.1	0.20163	0.00236	0.21859	*Bombycilla garrulus*[a]	56.4	0.05273	0.00609	0.08395
1143	*Myadestes obscurus*[a]	50	0.09480	0.00705	0.14440	*Myadestes genibarbis*[a]	27.1	0.05059	0.00111	0.12502
292	*Cinclus cinclus*[a]	55.4	0.25545	0.01874	0.31360	*Cyornis banyumas*[a]	14.3	0.14124	0.01278	0.31360
433	*Toxostoma longirostre*[a]	69.9	0.05415	0.01419	0.10255	*Toxostoma guttatum*[a]	52.8	0.01593	0.01130	0.00761
306	*Parus ater*[a]	9.1	0.01691	0.01594	0.00001	*Parus major*[a]	19	0.00130	0.00001	0.03094
210	*Baeolophus inornatus*[a]	16.3	0.06160	0.00000	0.19187	*Baeolophus bicolor*[a]	21.6	0.04453	0.00000	0.10608
906	*Tachycineta bicolor*[a]	20.1	0.24559	0.00953	0.19961	*Progne chalybea*[a]	42.9	0.15911	0.00497	0.24929
901	*Neochelidon tibialis*[a,c]	9.1	0.12556	0.00542	0.13062	*Atticora fasciata*[a,c]	14	0.11593	0.00501	0.13033
905	*Riparia riparia*[a]	14.6	0.18475	0.00362	0.26857	*Riparia cincta*[a]	21.5	0.16383	0.00272	0.18076
906	*Hirundo rustica*[a]	15.8	0.28400	0.01638	0.28147	*Notiochelidon cyanoleuca*[a]	9.7	0.22673	0.00586	0.17956
850	*Hippolais icterina*[a]	14.6	0.13398	0.00150	0.17518	*Hippolais polyglotta*[a]	11	0.08089	0.00150	0.10129
1038	*Hippolais olivetorum*[a]	18.1	0.12941	0.01163	0.16446	*Hippolais languida*[a]	10	0.11825	0.00569	0.11539
1037	*Phylloscopus bonelli*[a]	7.2	0.13603	0.00446	0.15338	*Phylloscopus sibilatrix*[a]	8.2	0.10653	0.00105	0.16103

(TABLE 3.1, cont.)

1024	*Phylloscopus schwarzi*[a]	9.9	0.17817	0.00367	0.24054	*Phylloscopus affinis*[a]	7	0.15436	0.00749	0.15303
1034	*Phylloscopus pulcher*[a]	6.8	0.16110	0.01013	0.16204	*Phylloscopus maculipennis*[a]	5.1	0.14746	0.00065	0.18360
902	*Sylvia melanocephala*[a]	11.3	0.34820	0.01399	0.26107	*Sylvia atricapilla*[a]	15.5	0.22563	0.01054	0.31392
1041	*Anthus campestris*[a]	23	0.02179	0.00038	0.06476	*Anthus berthelotii*[a]	16.5	0.01862	0.00081	0.04284
307	*Vidua paradisaea*[a]	22.2	0.04580	0.00977	0.09499	*Vidua chalybeata*[a]	12.5	0.02403	0.00001	0.08667
894	*Serinus canaria*[a]	8.4	0.06900	0.00679	0.04654	*Serinus mozambicus*[a]	10.6	0.02885	0.00001	0.00001
894	*Carduelis magellanica*[a]	11	0.04193	0.00179	0.07820	*Carduelis pinus*[a]	14.6	0.02132	0.00001	0.06243
924	*Haematospiza sipahi*[a]	39.5	0.08756	0.00657	0.16295	*Carpodacus erythrinus*[a]	24.1	0.05421	0.00173	0.13953
924	*Mycerobas carniceps*[a]	56.95	0.10221	0.01429	0.14479	*Mycerobas affinis*[a]	83	0.07603	0.00756	0.12755
790	*Pseudonestor xanthophrys*[a]	20	0.04545	0.00001	0.10331	*Loxops coccineus*[a]	11	0.00980	0.00158	0.02175
894	*Euphonia musica*[a]	13	0.14610	0.00824	0.27878	*Euphonia laniirostris*[a]	15	0.06714	0.00896	0.13254
924	*Emberiza rustica*[a]	23.2	0.05667	0.00174	0.12097	*Emberiza pusilla*[a]	13	0.05474	0.00172	0.08974
849	*Oreomanes fraseri*[a]	25	0.15429	0.01124	0.17610	*Lamprospiza melanoleuca*[a]	34	0.11131	0.01145	0.12930
1045	*Delothraupis castaneoventris*[a]	28	0.08166	0.00389	0.11271	*Dubusia taeniata*[a]	37	0.05618	0.00612	0.09513
890	*Tangara gyrola*[a]	21	0.11430	0.00514	0.16180	*Thraupis episcopis*[a]	35	0.11419	0.00687	0.15320
845	*Hemithraupis flavicollis*[a]	13	0.16370	0.00746	0.16340	*Heterospingus xanthopygius*[a]	38	0.11990	0.01076	0.17803
920	*Creurgops dentata*[a]	19	0.12498	0.00647	0.14066	*Schistochlamys melanopis*[a]	33	0.09302	0.00562	0.12982
884	*Saltator striatipectus*[a]	36.9	0.06006	0.00647	0.10661	*Saltator coerulescens*[a]	54.9	0.04400	0.00645	0.04124
849	*Poospiza torquata*[a]	10.3	0.05637	0.00534	0.09586	*Poospiza alticola*[c]	19	0.05037	0.00190	0.09394
921	*Loxigilla noctis*[a]	18.4	0.08579	0.01194	0.09360	*Tiaris bicolor*[a]	9.7	0.04601	0.00524	0.07790
920	*Geospiza difficilis*[a]	12.3	0.00842	0.00620	0.00871	*Geospiza scandens*[a]	22.6	0.00404	0.00136	0.00605
921	*Sporophila castaneiventris*[a]	7.7	0.06595	0.00338	0.10828	*Oryzoborus angolensis*[a]	12.3	0.04847	0.00419	0.09524
1143	*Cyanocompsa parellina*[a]	15	0.09234	0.00390	0.15025	*Cyanocompsa brissonii*[a]	20.6	0.06812	0.00422	0.09050
891	*Spiza americana*[a]	24.6	0.15652	0.00142	0.23886	*Cyanocompsa cyanoides*[a]	32.5	0.05617	0.00299	0.08861
921	*Pheucticus aureoventris*[a]	65.5	0.07046	0.00494	0.09754	*Pheucticus ludovicianus*[a]	45.6	0.04796	0.00168	0.11298
1143	*Passerina caerulea*[a]	27.5	0.04336	0.00250	0.08548	*Passerina amoena*[a]	15	0.03286	0.00390	0.07993
1143	*Passerina leclancherii*[a]	14	0.06451	0.00563	0.11703	*Passerina rositae*[a]	20	0.05189	0.00248	0.10322
1143	*Passerina ciris*[a]	15	0.03212	0.00001	0.04912	*Passerina versicolor*[a]	11.8	0.01316	0.00141	0.04117
1039	*Piranga ludoviciana*[a]	28.1	0.05413	0.00476	0.08556	*Piranga bidentata*[a]	34.7	0.03109	0.00237	0.06434
1029	*Piranga leucoptera*[a]	16	0.07577	0.00647	0.14072	*Piranga rubriceps*[a]	35	0.07108	0.00528	0.12904
430	*Pipilo aberti*[a]	44.8	0.01570	0.00747	0.01757	*Pipilo crissalis*[a]	51.8	0.01098	0.00001	0.03868
891	*Geothlypis aequinoctialis*[a]	13.1	0.06121	0.00179	0.09852	*Geothlypis trichas*[a]	9.9	0.06008	0.00181	0.17502
871	*Cacicus uropygialis*[a]	54	0.06513	0.00617	0.13411	*Cacicus cela*[a]	77.9	0.03652	0.00224	0.09405
857	*Chrysomus ruficapillus*[a]	32	0.02536	0.00601	0.06946	*Agelaioides badius*[a]	44.5	0.02176	0.00002	0.06320
839	*Xanthopsar flavus*[a]	43	0.02549	0.00150	0.06519	*Pseudoleistes virescens*[a]	64	0.01862	0.00389	0.03905
878	*Gnorimopsar chopi*[a]	79.5	0.06607	0.00804	0.11013	*Chrysomus thilius*[a]	30	0.04742	0.00251	0.11592
885	*Molothrus oryzivorus*[a]	162	0.02896	0.00376	0.05897	*Molothrus aeneus*[a]	57.4	0.00171	0.00001	0.01178
880	*Dolichonyx oryzivorus*[a]	37.1	0.10644	0.00001	0.20685	*Xanthocephalus xanthocephalus*[a]	49.3	0.04824	0.00518	0.13259

Sources of body mass data: [a] Dunning 1993; [b] del Hoyo *et al.*1992; [c] Louisiana State University Museum of Natural Science, specimen label data; [d] Winker *et al.* 1995; [e] Furness 1987; [f] Krabbe *et al.* 1999.

TABLE 3.2. Results of sign tests for the association between relative rate and relative body mass among 191 terminal sister taxon pairs. Asterisks mark the significant results linking large body mass and nonsynonymous substitution rate.

Substitutions	Pairwise comparison set	Larger mass – faster rate	Smaller mass – faster rate	p-value
All	All comparisons	96	95	0.500
	Passerines only	37	42	0.326
	Non-passerines only	59	53	0.318
	> 50% Mass difference	61	45	0.072
	Inter-generic comparisons only	33	32	0.500
	Intra-generic comparisons only	63	63	0.535
Nonsynonymous	All comparisons	97	76	0.064
	Passerines only	43	33	0.151
	Non-passerines only	54	43	0.155
	> 50% Mass difference	61	38	0.013*
	Inter-generic comparisons only	41	22	0.011*
	Intra-generic comparisons only	56	54	0.462
Synonymous	All comparisons	99	91	0.306
	Passerines only	36	42	0.286
	Non-passerines only	63	49	0.110
	> 50% Mass difference	56	49	0.279
	Inter-generic comparisons only	30	34	0.354
	Intra-generic comparisons only	69	57	0.164

(passerines and non-passerines), each of two hierarchical taxonomic levels (intra-generic and inter-generic comparisons), or to synonymous substitutions alone (Table 3.2, Figs. 3.1e, 3.1f). However, when the sign test was limited to the subset of all birds that possessed radical body mass variation (>50% difference), faster overall substitution rate was weakly associated with larger body mass (Fig. 3.1b). When all comparisons were considered, faster nonsynonymous substitution rate was weakly associated with larger body mass (Fig. 3.1c). When nonsynonymous rates were considered for taxon pairs that are radically different in body mass, a significant association between large body size and fast rate emerged (Fig. 3.1d). Inter-generic comparisons contributed disproportionately to this significant result (Table 3.2), probably due to the greater body mass disparity present at this slightly deeper taxonomic level.

Overall, mtDNA rate was not significantly correlated with body mass, as evidenced by Spearman's correlation coefficients (Fig. 3.2a). However, a positive correlation was found

FIGURE 3.1. The association between relative body mass and relative evolutionary rate for all mtDNA substitutions (a, b), nonsynonymous substitutions (c, d), and synonymous substitutions (e, f). The three graphs in the right hand column (b, d, f) represent only the subset of independent contrasts that compared lineages that are at least 50% different in body mass. Binomial sign tests measure the probability that relative size and relative rate are associated no more often than expected by chance: a, p=0.500; b, p=0.072; c, p=0.064; d, p=0.013; e, p=0.306; f, p=0.279.

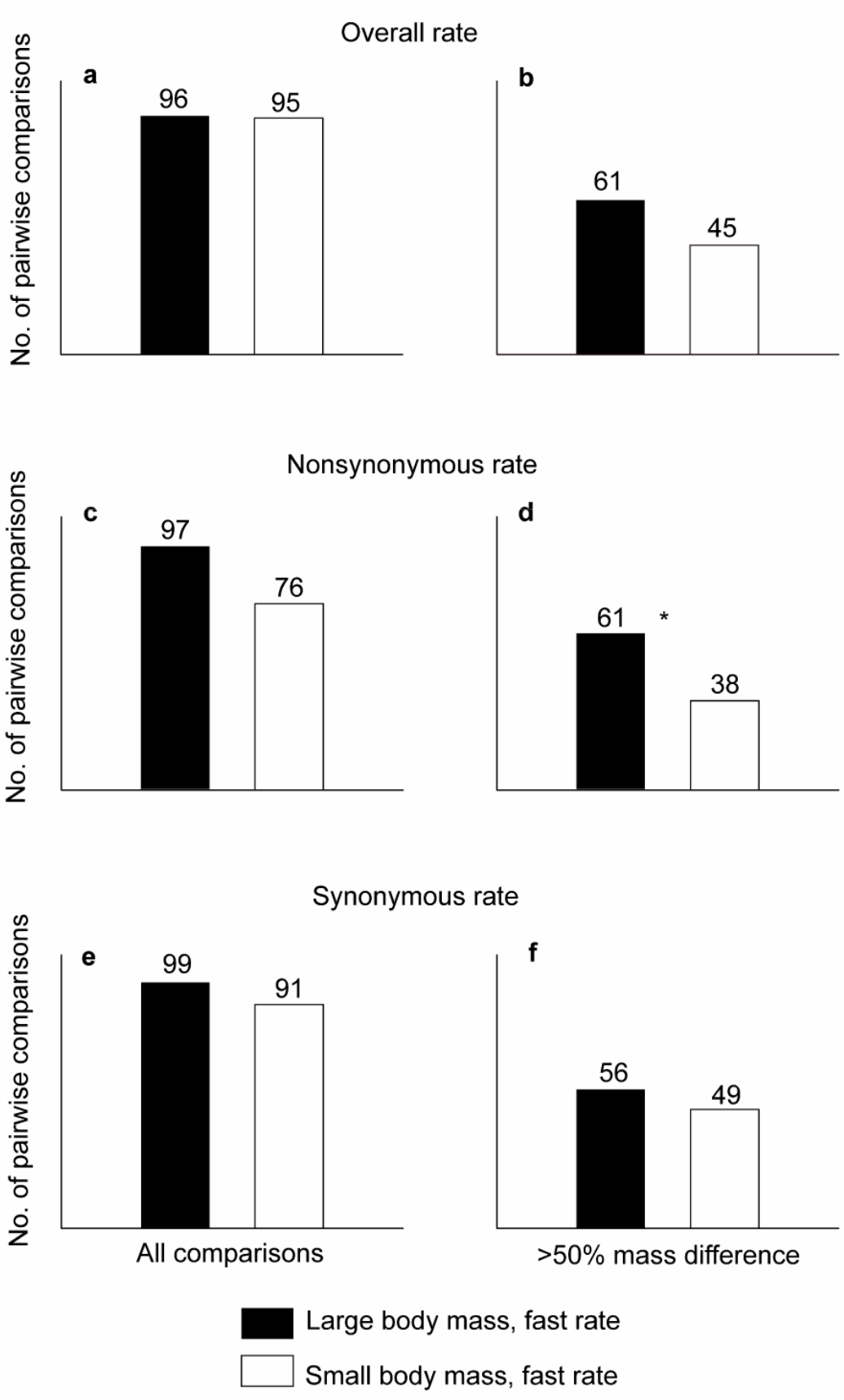
Overall rate
a
96
95
b
61
45
No. of pairwise comparisons
Nonsynonymous rate
c
97
76
d
61
*
38
No. of pairwise comparisons
Synonymous rate
e
99
91
f
56
49
No. of pairwise comparisons
All comparisons
>50% mass difference
Large body mass, fast rate
Small body mass, fast rate

FIGURE 3.2. The relationship between relative body mass and relative mtDNA rate. The Y-axis represents the difference in log-transformed branch lengths, when branch lengths are calculated for: a, all substitutions, r=0.0497, p=0.5043; b, nonsynonymous substitutions, r=0.1704, p=0.0419; or c, synonymous substitutions, r=0.0015, p=.9837. The X-axis represents the difference in log-transformed mass (mass of faster taxon minus mass of slower taxon). Open circles represent comparisons among passerine birds; solid circles represent comparisons among non-passerines. Comparisons with zero or near-zero length branches are excluded (see Methods).

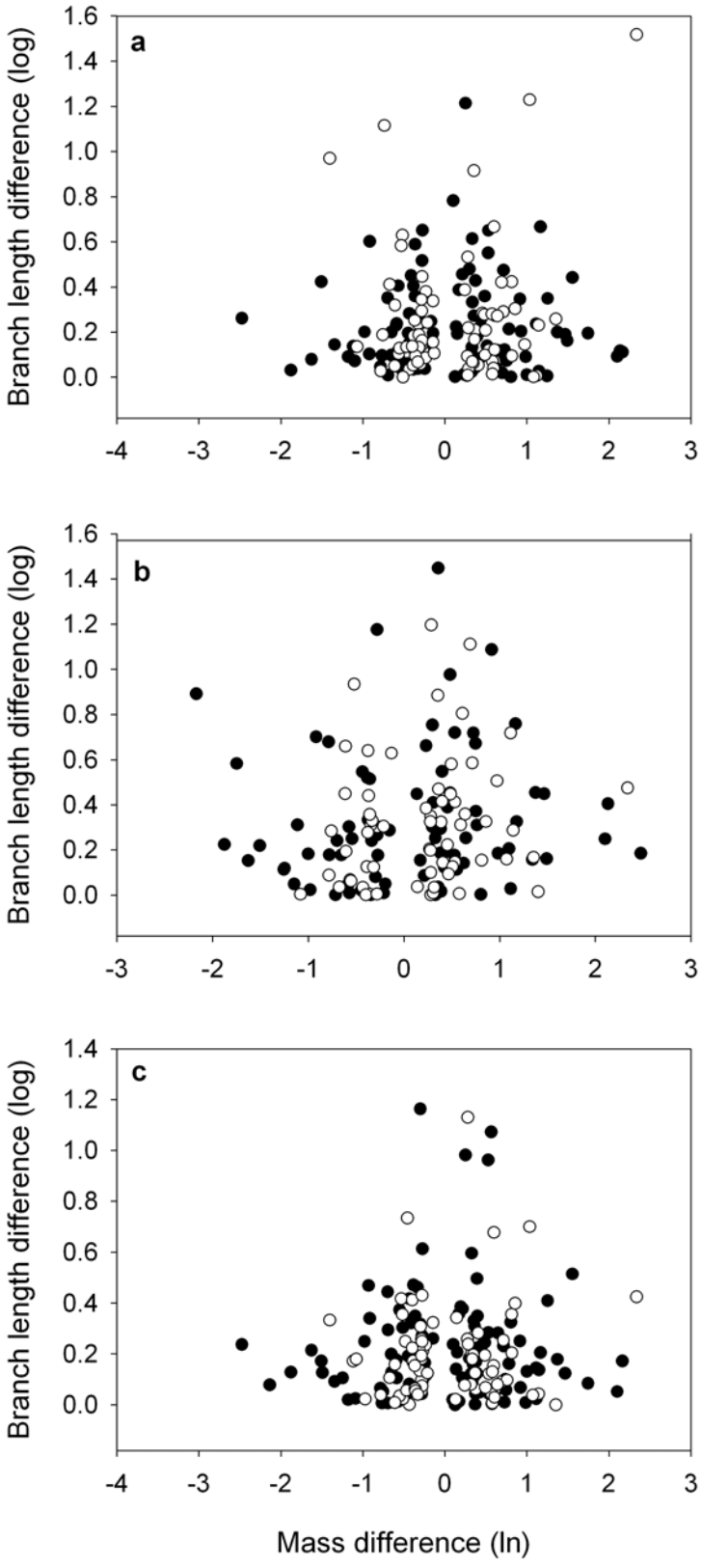
a
b
c
Branch length difference (log)
Mass difference (ln)

between body mass and rate of evolution at nonsynonymous sites (Fig. 2b). It is important to note that the metabolic rate hypothesis predicts a negative correlation, not a positive one. The metabolic rate hypothesis specifically predicts an effect of metabolic rate only on mutation rate. Evolutionary rate for neutral changes should be directly proportional to mutation rate (Kimura 1983). However, the effects of selection or drift on non-neutral mutations could obscure an overall correlation between metabolic rate and mutation rate. When the analyses were restricted to synonymous, and presumably neutral, substitutions a conspicuous lack of association remained between small body size (high mass-specific metabolic rate) and fast rate (Figs. 3.1e, 3.1f, 3.2c). Thus, although nonsynonymous substitution rate is positively correlated with body size, no evidence is found for a negative correlation between body mass and overall mtDNA rate or neutral, synonymous rate.

The apparent relationship between large body size and fast nonsynonymous rate, particularly demonstrated by comparing birds differing in body mass by greater than 50%, suggests a population size effect. Because population density is negatively correlated with body mass (Calder 1984), a population size effect would be expected to cause larger-bodied taxa to evolve more rapidly. When population size is small, slightly deleterious mutations will have a higher probability of drifting to fixation (Ohta 1992). However, rapid evolution in small populations will only manifest itself at nonsynonymous, non-neutral sites. Elevated nonsynonymous rate is exactly the pattern observed in this study. These findings may help to explain why some exceptionally large-bodied taxa, including elephants (Hauf *et al.* 1999) and giant tortoises (Caccone *et al.* 2002), do not have slow rates of mtDNA evolution.

Correlations between rates of evolution in nuclear and organelle genomes have been reported in multiple studies (e.g. Martin 1999, Sheldon *et al.* 2000). This suggests that lineage-

specific factors similarly affect rates of all genes and genomes evolving within the same lineage. Although generation time (see Rand 1994) and metabolic rate effects (this study) fail to explain mtDNA rate variation, population size effects could apply to both the mitochondrial and nuclear genome, thus reconciling the correlation of mitochondrial and nuclear rates with the potential for common causation.

The link between large body size and fast nonsynonymous rate within the class Aves should be considered in light of previous findings that birds evolve more slowly than expected given their high metabolic rates. The slow rate of molecular evolution in birds relative to mammals has been explained by increased constraints on avian proteins as a result of high body temperatures (Mindell *et al.* 1996). If the intensity of functional constraints varies with body mass among closely related taxa within the class Aves, then it could provide another potential explanation for the observed pattern. However, recent evidence indicates that both resting temperature and the amplitude of daily temperature fluctuations are size independent (Refinetti 1999). In fact, daily temperature fluctuations are heavily dependent on ecological factors such as climate and foraging behavior. Alternatively, the hypothesis of nearly neutral evolution in small populations is not only theoretically plausible, but also consistent with population size variation observed in nature, and it is supported by other recent empirical studies (see Rand 2001).

This study suggests that mass-specific metabolic rate is not a significant factor underlying evolutionary rate variation among closely related lineages; however, it does not exclude the possibility that more extreme differences in metabolic rate, such as those among homeothermic and poikilothermic taxa, are sufficient to cause meaningful differences in mutation rate. It would be difficult to use the independent contrasts approach for multiple homeothermic and poikilothermic taxa, and it would be impossible to account for the myriad other factors that could

lead to the appearance of disparate evolutionary rates among such distantly related taxa. Furthermore, accumulating examples of rapid mtDNA evolution in poikilotherms, such as chewing lice (Hafner *et al.* 1994) and land snails (Chiba 1999), cast doubt on the role of metabolic rate in causing evolutionary rate variation even among deep lineages.

CHAPTER 4: MOLECULAR PHYLOGENY, BIOGEOGRAPHY, AND TIMING OF DIVERSIFICATION IN THREE FAMILIES OF NEOTROPICAL BIRDS

Current patterns of species diversity provide a snapshot of a complex process of diversification over geological time. Molecular phylogenetic data provide a window into the history of speciation, extinction, dispersal, and vicariance that led to current patterns. Recently methodological advances in tree-building and divergence time estimation have greatly improved our ability to resolve the order and absolute timing of speciation events. The application of these methods to phylogenetic patterns among co-distributed clades can illustrate the extent to which species histories reflect regional geological and climatic histories. In this study, I set out to describe the phylogenetic histories of three co-distributed families of Neotropical birds. I estimate the temporal profile of diversification for each family. Specifically, I consider the similarities and differences among the three groups, the potential interplay of speciation with regional geological and climatic history, and the effects of ancestral distribution on subsequent diversification patterns. The patterns that emerge from this analysis will shed light on the evolutionary origins of the remarkably diverse Neotropical avifauna.

Evolutionary biologists and biogeographers have long sought an historical explanation for the exceptionally high species diversity in the Neotropics relative to other regions (Haffer 1969, Prance 1982). This diversity is attributable in part to deep events, such as the break up of Gondawana, that are difficult to resolve with precision because their historical signal has been obscured by subsequent evolution. However, the understanding of recent diversification among closely related species and genera is tractable, and has been the focus of study and debate about competing mechanisms. One widely used approach has been to attribute speciation to specific geological or climatic events. Haffer (1969, 1974) linked analyses of species distributions to geological evidence of extensive Pleistocene climatic fluctuations, suggesting that speciation in

the Neotropics had been driven by cool, dry episodes during the Pleistocene that caused forests to repeatedly contract into isolated refugia. Under this 'refugia hypothesis,' bird populations isolated in forest remnants would diverge over time. In light of genetic evidence, the refugia hypothesis was later broadened to apply to climatic fluctuations in the Pleistocene, Pliocene, or Miocene (Haffer 1997). The role of historical vicariance in Neotropical populations also has been ascribed to other geophysical causes, including river barriers (Capparella 1988), inland seas (Nores 1999), and geological arcs (Patton *et al.* 2000, Silva and Patton 1998).

Another approach has involved the analysis of distribution data using cladistic methods to define areas of endemism and area relationships (Silva and Oren 1996, Bates *et al.* 1998). The distribution data provide strong signal for discrete biogeographic regions comprising the lowland Neotropical humid forests, and studies of birds and monkeys generally agree on area definitions (Cracraft 1985, Silva and Oren 1996, Bates *et al.* 1998; but see Beven 1986). Estimates of the relationships among areas as measured by shared distributions (Bates *et al.* 1998) or by phylogenetic relationships (Cracraft and Prum 1988) share some similar and some unique aspects. Molecular phylogenetic patterns in single taxa of birds (Marks *et al.* 2002), bats (Hoffman and Baker 2003), snakes (Zamudio and Green 1997), butterflies (Hall and Harvey 2002), monkeys (Cortes-Ortiz *et al.* 2003), and trees (Dick *et al.* 2003, Cavers *et al.* 2003) each reveal some unique area relationships, although most agree on the fundamental importance of the Andes as a primary barrier to gene flow. Hall and Harvey (2002) showed that estimated area relationships among amphibians, primates, rodents, marsupials, reptiles, birds, and butterflies contained concordant elements. The standard interpretation for phylogeographic concordance is allopatric speciation and a common history of vicariant events. Assuming that the underlying phylogenies and distributions are correctly known, conflicting patterns for co-distributed species

suggests one of two possible explanations: (1) species respond uniquely to geological and climatic shifts, depending on their ecology and life history; or (2) ancestral species have undergone multiple cycles of vicariance, dispersal, and extinction in the Neotropics, and phylogenies reflect events at different time scales. Under the first explanation, topological discordance provides evidence that speciation has a unique cause in each clade. Under the second explanation, however, topological discordance is expected, and it is equivocal with respect to underlying cause. Thus, phylogenetic relationships alone are insufficient for assessing similarities and differences in the evolutionary histories of co-distributed species. Such an assessment requires information about the timing of speciation, such as that derived from calibrated DNA sequence data. Large molecular datasets, particularly those that incorporate exhaustive taxon sampling schemes, are only recently becoming available to perform such tests (e.g. Barraclough and Vogler 2000). Methods that allow for the dating of nodes while taking into account patterns of rate heterogeneity among lineages are another important recent advance (Sanderson 1997, 2002). The incorporation of node-timing has fostered improvement in the power of biogeographic analyses over purely cladistic, pattern-based approaches (Donaghue and Moore 2003).

A second area for improvement over traditional cladistic biogeography is in the incorporation of direction of movement. Independent evidence of the ancestral range, such as that derived from higher level phylogenies, geological data, and the fossil record, can facilitate inference of biogeographic events by allowing the incorporation of direction of dispersal or expansion. For example, biogeographic inferences for Neotropical taxa might be influenced by evidence for the restriction to either North America or South America before the formation of the landbridge, approximately 3 million years ago, that proceded the great biotic interchange.

Taxa of Interest

In this study, I examine three families of birds that have nearly identical overall distributions in forest habitats throughout the Neotropical region. These are the puffbirds (Bucconidae, 35 species), the jacamars (Galbulidae, 18 species), and the motmots (Momotidae, 10 species). The puffbirds and jacamars are sister families that are distantly related to, but usually included within the order Piciformes (Johansson *et al.* 2003). The motmots are in the order Coraciiformes and their closest relatives are thought to be the todies (Todidae), a relictual family that is restricted to a few Caribbean islands. There are several similarities among the three families that make them excellent potential subjects for biogeographical analysis and comparison. First, nearly all species seem to have low vagility, as evidenced by the absence of any members from oceanic islands and the near total lack of known seasonal movements in any species. Second, most species occur in lowland forested habitats. There are only three species of puffbirds, one species of jacamar, and three species of motmots that occur exclusively in montane forests. Third, all three families are ecologically similar in that they nest exclusively in burrows, and they are sit-and-wait predators that have oversized bills for capturing and subduing large insect and small vertebrate prey.

Objectives

1. Use mitochondrial and nuclear DNA sequences to reconstruct phylogenetic relationships among genera and species within each of the three study clades.

2. Estimate the absolute dates of phylogenetic nodes using independent fossil and biogeographic calibrations, in such a way that accounts for rate heterogeneity among lineages.

3. Test whether clades originating in different ancestral areas have similar or different patterns of species diversification. For example, what are the relative effects of the formation of the Central

American Landbridge on diversification in groups that were previously restricted to South America versus those that were restricted to Central America?

4. Use the phylogeny along with distribution data to delimit superspecies groups, or paralogy-free subtrees (Nelson and Ladiges 1996) which provide units for biogeographic analysis.

5. Use extensive geographic sampling within each subtree to test whether superspecies groups have similar and contemporaneous histories of vicariance and dispersal. Specifically, do allospecies from Neotropical endemic areas such as the trans-Andean region, the Guyanan shield, and southeastern Brazil share a common historical origin?

METHODS

Specimens and Genes Sampled

I sampled genes and taxa in an attempt to reconstruct the phylogeny and estimate the timing of divergence among genera, species, and geographically separated populations within each of three bird families. To do this, I attempted to strike an appropriate balance between the number and type of genes sequenced and the number of taxa. More bases sampled provide increased accuracy of divergence date estimation (Swofford *et al.* 1996). However, additional taxa have been shown to increase phylogenetic resolution (Graybeal 1998, Hillis *et al.* 2003), even when the taxa added are near the tips of the tree (Omland *et al.* 1999). I chose to sequence three mitochondrial genes totaling approximately 1.8 kilobases for as many species and geographical representative populations as possible. Mitochondrial DNA (mtDNA) evolves rapidly and sorts rapidly, making it the best single marker for resolving phylogenies among closely related species and populations. Rates of mtDNA evolution have been shown to be relatively similar among widely divergent bird lineages (Lovette 2004), and clock-like evolution has frequently been observed within clades. Furthermore, mtDNA retains reasonable utility as a phylogenetic marker

at deeper levels, especially if models of evolution are used in phylogenetic reconstruction to account for the marked rate heterogeneity among sites (Yang 1996). I sampled 34 of the 35 described species of puffbirds, 18 of 18 species of jacamars, and 10 of 10 species of motmots. Additionally, I sampled a total of 71 puffbirds, 64 jacamars, and 105 motmots in an attempt to maximize geographic representation within species and insure near exhaustive sampling of unique and divergent evolutionary units (Table 4.1). In order to improve phylogenetic resolution at basal nodes and to provide an independent check on the mtDNA topology, I sequenced parts of two nuclear introns for a subset of 31 puffbirds, 17 jacamars, and 12 motmots representing most of the major lineages identified from the mitochondrial data.

DNA Extraction, Amplification, and Sequencing

For most individuals, total genomic DNA was extracted from frozen muscle or liver tissue using a DNEasy tissue kit (Qiagen, Valencia, California), following the manufacturer's protocol. In cases where no preserved tissue samples were available in U.S. museum tissue collections, DNA was extracted from the shafts of contour feathers or from small fragments of the toepads of dried skins that were collected between 1899 and 1982 (see Table 4.1). For these 'ancient DNA' samples, negative control extractions were performed, and great care was taken to insure against cross-contamination, including the use of aerosol-barrier pipette tips, a work space that was isolated from tissue material or PCR products, and incubation in a dry oven rather than a common water bath. For the feather extractions, 30 µl of dithrietol (DTT) solution (10 mg/ml) was added to the initial digest, and incubation was extended to 24 hours. Amplification and sequencing primers were gathered from the literature or designed specifically for the taxa in this study (Table 4.2). For all individuals, the last 1047 bp of cytochrome b was amplified. For the puffbirds and jacamars, the first 441 bp of the NADH dehydrogenase subunit II (ND2) and the

entire 346 bp NADH dehydrogenase subunit III gene (ND3) were amplified. For the motmots, the first 362 bp of ND2 and a 489 bp fragment comprised of the end of cytochrome oxidase subunit III, the entire tRNA gly, and all of ND3 was amplified. Intron 5 of the nuclear adenylate kinase I gene (AK1; Shapiro and Dumbacher 2001) was amplified for a subset of puffbirds, jacamars, and motmots. I amplified a small fragment (approximately 300 bp) of the β-fibrinogen intron 7 (βF7, Prychytko and Moore 1997) for the same subset of puffbirds and jacamars. For the subset of motmot taxa, I also amplified introns 4 and 5 of the eukaryotic elongation factor II (EEF2). Larger fragments were generally amplified in multiple shorter pieces for degraded samples, including those from feathers and toepads of museum specimens. Negative controls were included with every PCR reaction to verify that reagents were free of DNA and that methods were robust to cross-contamination of samples. PCR products were visualized on an agarose gel with ethidium bromide staining. Most successful amplifications were cleaned directly with a Qiaquick kit (Qiagen). Reactions that produced multiple bands and PCR products that led to failed DNA sequences were gel-extracted using a Qiagen Gel Extraction kit. Cycle-sequencing reactions were carried out in both directions using the external primers in quarter-volume reactions with Big Dye Terminator Cycle Sequencing Kit (versions 2 and 3.1, Applied Biosystems [ABI], Foster, California). Internal sequencing primers were used for cytochrome b and EEF2 only (Table 4.2). Cycle-sequencing products were purified using Sephadex columns or Dye-Ex 96-well plates (Qiagen) and were sequenced on an automated DNA sequencer (ABI 377 or ABI 3100, Applied Biosystems). Chromatograms for contiguous fragments were assembled, inspected, and manually corrected using Sequencher 4.1 (GeneCodes, Ann Arbor, MI). Measures taken to avoid misidentification of nuclear paralogues of mitochondrial genes included confirmation of the correct reading frame, inspection for indels or conspicuous double peaks,

TABLE 4.1. List of specimens sequenced in this study.

Taxon	Locality	Area of endemism	Specimen number	Source
GALBULIDAE (JACAMARS)				
Brachygalba albogularis	Peru: Ucayali; Rio Shesha	Inambari	B10617	LSUMZ
Brachygalba goeringi [a]	Venezuela: Carabobo, N Valencia		68522	LSUMZ
Brachygalba l. lugubris	Guyana	Guyana	B05268	USNM
Brachygalba lugubris caquetae [a,b]	Ecuador: Napo; Limoncocha	Napo	50310	LSUMZ
Brachygalba lugubris melanosterna	Brazil: Rondonia	Rondonia	389737	FMNH
Brachygalba lugubris melanosterna	Bolivia: Santa Cruz: Velasco	Rondonia	B12676	LSUMZ
Brachygalba salmoni	Panama: Darien: Cana: Cerro Pirre	Chocó/C. Amer.	B2318	LSUMZ
Galbalcyrhynchus leucotis	Ecuador: Sucumbios	Napo	2730	ANSP
Galbalcyrhynchus leucotis	Ecuador: Sucumbios	Napo	3274	ANSP
Galbalcyrhynchus purusianus	Peru: Ucayali; W bank Rio Shesha	Inambari	B10819	LSUMZ
Galbula albirostris	Guyana: 4 20'N, 58 51'W	Guyana	1218	KU
Galbula albirostris	Guyana: 4 17'N, 58 31'W	Guyana	1382	KU
Galbula albirostris	Venezuela: Bolivar, Tumeremo	Guyana	CJW213	AMNH
Galbula albirostris [a,b]	Ecuador: Napo; Limoncocha	Napo	82911	LSUMZ
Galbula albirostris albirostris	Brazil: Amazonas; 80km N Manaus	Guyana	B20253	LSUMZ
Galbula albirostris chalcocephala	Peru: Loreto; N bank, Rio Napo	Napo	B2737	LSUMZ
Galbula cyanescens	Peru: Ucayali; W bank Rio Shesha	Inambari	B10508	LSUMZ
Galbula cyanescens	Peru: Ucayali; W bank Rio Shesha	Inambari	B10838	LSUMZ
Galbula cyanicollis	Peru: Loreto; S Rio Amazonas; Quebrada Vainilla	Inambari	B4816	LSUMZ
Galbula cyanicollis	Brazil: Pará; Caixuana	Pará	391278	FMNH
Galbula cyanicollis	Brazil: Pará; 52 km SSW Altamira	Pará	B06863	USNM
Galbula d. dea	Guyana	Guyana	B04401	USNM
Galbula d. dea	Brazil: Roraima; Rio Quitanau	Guyana	389202	FMNH
Galbula d. dea	Brazil: Amapa; Amapa, Fazenda Itapoa	Guyana	391282	FMNH
Galbula d. dea	Brazil: Amazonas; 80km N Manaus	Guyana	B20351	LSUMZ
Galbula dea amazonum	Brazil: Pará; 52 km SSW Altamira	Pará	B06926	USNM
Galbula dea brunneiceps	Peru: Ucayali: Cerro Tahuayo	Inambari	B11034	LSUMZ
Galbula galbula	Brazil: Roraima; E bank Rio Branco, across from Boa Vista	Guyana	389203	FMNH
Galbula galbula	Brazil: Amapa	Guyana	391280	FMNH
Galbula galbula	Brazil: Pará; Monte Alegre, Colonia do Erere	Guyana	392536	FMNH
Galbula galbula	Guyana	Guyana	B12373	USNM

(TABLE 4.1, cont.)

Galbula l. leucogastra	Guyana	Guyana	B12436	USNM
Galbula l. leucogastra	Bolivia: Pando	Inambari	B9608	LSUMZ
Galbula l. leucogastra	Brazil: Pará; 113 km SSW Santerem	Rondonia	B35619	LSUMZ
Galbula l. leucogastra	Brazil: Rondonia; Cachoeira Nazare, W bank Rio Jiparána	Rondonia	389741	FMNH
Galbula leucogastra chalcothorax	Peru: Loreto: 1km N Rio Napo	Napo	B2803	LSUMZ
Galbula pastazae	Ecuador: Morona-Santiago, Cordillera Cutucu	Napo	B6098	LSUMZ
Galbula r. ruficauda	Colombia: Santander; San Alberto	Nechi	44195	LSUMZ
Galbula r. ruficauda	Venezuela: Carabobo dist.		881	LSUMZ
Galbula r. ruficauda	Trinidad: St. Andrews Co.		B35921	LSUMZ
Galbula r. ruficauda	Trinidad: St. Andrews Co.		B35935	LSUMZ
Galbula r. ruficauda	Trinidad: St. Andrews Co.		B35972	LSUMZ
Galbula ruficauda heterogyna	Bolivia: El Beni; Laguna Suarez, 5 km sw Trinidad		334410	FMNH
Galbula ruficauda heterogyna	Bolivia: Santa Cruz; Mina Don Mario		B37713	LSUMZ
Galbula ruficauda melanogenia [a,b]	Mexico: Chiapas; ca 8km S Solosuckiapa	Central America	40672	LSUMZ
Galbula ruficauda melanogenia	Costa Rica: Cartago	Central America	B35766	LSUMZ
Galbula ruficauda melanogenia [a,b]	Colombia: Narino; La Guayacana	Chocó	38600	LSUMZ
Galbula ruficauda melanogenia	Ecuador: Esmeraldas: 30 km S Chontaduro, W bank Rio Verde	Chocó	185298	ANSP
Galbula ruficauda melanogenia	Panama: Bocas del Toro		B41628	LSUMZ
Galbula ruficauda rufoviridis	Brazil: Pará; 52 km SSW Altamira	Pará	B06883	USNM
Galbula ruficauda rufoviridis [a,b]	Brazil: Minas Gerais; Pompea		65143	LSUMZ
Galbula ruficauda rufoviridis	Brazil: Pernambuco; Timbauba		392427	FMNH
Galbula ruficauda rufoviridis	Bolivia: Santa Cruz; Santa Rosa		B38198	LSUMZ
Galbula t. tombacea	Ecuador: Sucumbios	Napo	3214	ANSP
Galbula t. tombacea	Ecuador: Sucumbios	Napo	3237	ANSP
Galbula t. tombacea	Ecuador: Sucumbios	Napo	4779	ANSP
Jacamaralcyon tridactyla [a,b]	Brazil: Sao Paulo; Victoria	SE Brazil	113483	LSUMZ
Jacamerops a. aureus	Guyana: 4 17'N, 58 31'W	Guyana	1401	KU
Jacamerops a. aureus	Venezuela: Bolivar; Tumeremo	Guyana	CJW203	AMNH
Jacamerops a. aureus	Guyana: Potaro-Siparuni	Guyana	7543	ANSP
Jacamerops a. aureus	Guyana: Potaro-Siparuni	Guyana	8633	ANSP
Jacamerops a. aureus	Brazil: Roraima; Rio Cachorro, 4 mi N on Canta-Confianca Rd.	Guyana	389204	FMNH
Jacamerops aureus isidori	Peru: Loreto: San Jacinto; 2 18'S, 76 07'W	Napo	971	KU
Jacamerops aureus isidori	Peru: Loreto; Rio Cushabatay	Inambari	B27424	LSUMZ
Jacamerops aureus penardi	Panama: Colon	Central America	B26500	LSUMZ
Jacamerops aureus ridgwayi	Brazil: Pará; 52 km SSW Altamira	Pará	B07045	USNM

(TABLE 4.1, cont.)

Jacamerops aureus ridgwayi	Brazil: Rondonia; Cachoeira Nazare, W bank Rio Jiparána	Rondonia	389744	FMNH
BUCCONIDAE (PUFFBIRDS)				
Argicus macrodactylus	Peru: Ucayali; W bank Rio Shesha	Inambari	B10820	LSUMZ
Argicus macrodactylus	Bolivia: Pando; Nicolas Suarez	Inambari	B9740	LSUMZ
Argicus macrodactylus	Peru: Loreto; 90km N Iquitos	Napo	B4504	LSUMZ
Argicus macrodactylus [b]	Venezuela: Amazonas; Neblina	Imerí	RWD17180	AMNH
Bucco capensis	Guyana	Guyana	B04213	USNM
Bucco capensis	Venezuela: Amazonas; Neblina	Imerí	B7526	LSUMZ
Bucco capensis	Peru: Loreto; S Rio Amazonas	Inambari	B5096	LSUMZ
Chelidoptera t. tenebrosa	Guyana: 4 20'N, 58 51'W	Guyana	1254	KU
Chelidoptera t. tenebrosa	Guyana, Potaro-Siparuni	Guyana	7707	ANSP
Chelidoptera t. tenebrosa	Guyana, Potaro-Siparuni	Guyana	7782	ANSP
Chelidoptera t. tenebrosa	Peru: Loreto; San Jacinto; 2 18'S, 76 07'W	Napo	1028	KU
Chelidoptera t. tenebrosa	Brazil: Pará; 52 km SSW Altamira	Pará	B07013	USNM
Chelidoptera t. tenebrosa	Bolivia: Santa Cruz; Velasco	Rondonia	B12787	LSUMZ
Hapaloptila castanea	Ecuador: Pichincha; Mindo		B12059	LSUMZ
Hypnelus ruficollis bicinctus	Venezuela: Sucre; Guaraunos, 14 km SSE		339641	FMNH
Malacoptila f. fulvogularis	Bolivia: La Paz; B. Saavedra Prov.		B22620	LSUMZ
Malacoptila f. fulvogularis	Peru: Cajamarca; Nuevo Peru		B33626	LSUMZ
Malacoptila fusca	Brazil: Amazonas; 80km N Manaus	Guyana	B20439	LSUMZ
Malacoptila fusca [a,b]	Ecuador: Napo; Limoncocha	Napo	82915	LSUMZ
Malacoptila fusca	Peru: Pasco	Napo/Inambari	B2007	LSUMZ
Malacoptila mystacalis [a,b]	Venezuela: Tachira		68525	LSUMZ
Malacoptila p. panamensis	Panama	Central America	B00441	USNM
Malacoptila p. panamensis	Panama	Central America	B01381	USNM
Malacoptila p. panamensis	Panama: Darien; Cana, Cerro Pirre	Chocó/C. Amer.	B2293	LSUMZ
Malacoptila panamensis poliopis	Ecuador: Esmeraldas	Chocó	B29998	LSUMZ
Malacoptila r. rufa	Peru: Loreto: S Rio Amazonas; Quebrada Vainilla	Inambari	B4586	LSUMZ
Malacoptila r. rufa	Bolivia: Santa Cruz; Velasco	Rondonia	B18325	LSUMZ
Malacoptila r. rufa	Brazil: Rondonia; 10° 50' S 64° 45' W	Rondonia	B36718	LSUMZ
Malacoptila r. rufa	Brazil: Rondonia; 10° 50' S 64° 45' W	Rondonia	B36722	LSUMZ
Malacoptila r. rufa	Brazil: Rondonia; 10° 50' S 64° 45' W	Rondonia	B36733	LSUMZ
Malacoptila rufa brunnescens	Brazil: Pará; 52 km SSW Altamira	Pará	B06987	USNM
Malacoptila rufa brunnescens	Brazil: Pará; Serra dos Carajas	Pará	391288	FMNH

(TABLE 4.1, cont.)

Malacoptila rufa brunnescens	Brazil		391289	FMNH
Malacoptila s. striata [a]	Brazil: Sao Paulo	SE Brazil	65147	LSUMZ
Malacoptila semicincta	Bolivia: La Paz; Rio Beni	Inambari	B1053	LSUMZ
Malacoptila semicincta	Peru: Ucayali; Cerro Tahuayo	Inambari	B11091	LSUMZ
Micromonacha lanceolata	Peru: Ucayali; Cerro Tahuayo	Inambari	B11211	LSUMZ
Monasa atra	Guyana: 4 20'N, 58 51'W	Guyana	1232	KU
Monasa atra	Venezuela: Amazonas: Neblina	Imerí	B7522	LSUMZ
Monasa flavirostris	Peru: Loreto; 79km WNW Contamana	Inambari	B27879	LSUMZ
Monasa morphoeus grandior [a,b]	Costa Rica: Limón	Central America	35385	LSUMZ
Monasa morphoeus peruana	Ecuador: Napo, 0 32 S, 75 30 W, Zancudo Cocha	Napo	3292	ANSP
Monasa morphoeus peruana	Bolivia: Santa Cruz; Velasco	Rondonia	B12608	LSUMZ
Monasa morphoeus peruana	Brazil: Pará; 113 km SSW Santerem	Rondonia	B35587	LSUMZ
Monasa morphoeus rikeri	Brazil: Pará; 52 km SSW Altamira	Pará	B06986	USNM
Monasa n. nigrifrons	Peru: Loreto; S Rio Amazonas; E bank Quebrada Vainilla	Inambari	B5042	LSUMZ
Monasa n. nigrifrons	Brazil: Pará	Pará	B07074	USNM
Monasa n. nigrifrons	Brazil: Pará; Serra dos Carajas	Pará	391290	FMNH
Monasa nigrifrons canescens	Bolivia: Santa Cruz		B37765	LSUMZ
Nonnula brunnea	Peru: Loreto 02 35'S, 76 07'W	Napo	1118	KU
Nonnula brunnea	Ecuador: Napo; Rio Pacuyacu	Napo	4791	ANSP
Nonnula f. frontalis	Panama: Darien; Cana, Cerro Pirre	Chocó/C. Amer.	B2227	LSUMZ
Nonnula r. ruficapilla	Peru: Loreto; S Bank Maranon	Inambari	B103532	LSUMZ
Nonnula rubecula	Guyana	Guyana	B10388	USNM
Nonnula rubecula	Argentina: Misiones; Parque Prov.		RTC309	AMNH
Nonnula rubecula cineracea	Peru: Loreto; 90km N Iquitos	Napo	B4253	LSUMZ
Nonnula ruficapilla nattereri	Bolivia: Santa Cruz; Velasco; P.N. Noel Kempf	Rondonia	B18570	LSUMZ
Nonnula sclateri	Peru: Ucayali; Cerro Tahuayo	Inambari	B11192	LSUMZ
Notharchus m. macrorhynchos	Guyana	Guyana	B13147	USNM
Notharchus macrorhynchus hyperrynchus	Mexico: Quintana Roo; 20 50'N, 86 54'W	Central America	544	KU
Notharchus macrorhynchus hyperrynchus	Peru: Ucayali; Rio Shesha	Inambari	B10680	LSUMZ
Notharchus macrorhynchus swainsoni [a,b]	Brazil: Sao Paulo	SE Brazil	65145	LSUMZ
Notharchus ordii	Venezuela: Amazonas; Neblina	Imerí	B7559	LSUMZ
Notharchus ordii	Bolivia: Pando	Inambari	B9073	LSUMZ
Notharchus pectoralis	Panama: Colon	Central America	B28507	LSUMZ
Notharchus t. tectus	Guyana: 4° 17' N, 58° 31' W	Guyana	1361	KU

(TABLE 4.1, cont.)

Notharchus t. tectus	Brazil: Pará; Monte Alegre; Colonia do Erere	Guyana	392532	FMNH
Notharchus t. tectus	Brazil: Amazonas; 80km N Manaus	Guyana	B20262	LSUMZ
Notharchus tectus picatus	Peru: Loreto	Napo	42326	LSUMZ
Notharchus tectus picatus	Bolivia: Santa Cruz; Velasco	Rondonia	B12270	LSUMZ
Notharchus tectus picatus (?)	Brazil: Pará; 113 km SSW Santerem	Rondonia	B35618	LSUMZ
Notharchus tectus subtectus	Panama: Colon Province; 17 km by road NW Gamboa	Central America	B26514	LSUMZ
Notharchus tectus subtectus	Ecuador: Esmeraldas; 20 km ENE Muisne, Cabeceras de Bilsa	Chocó	4648	ANSP
Nystactes noanamae [a,b]	Colombia: Chocó	Chocó	786999	AMNH
Nystactes t. tamatia	Brazil: Amapa	Guyana	391283	FMNH
Nystactes t. tamatia	Brazil: Pará; Monte Alegre, Colonia do Erere	Guyana	392535	FMNH
Nystactes t. tamatia	Brazil: Amazonas; 80km N Manaus	Guyana	B20222	LSUMZ
Nystactes t. tamatia [b]	Venezuela: Bolivar, Guaiquinima	Guyana	CJW20	AMNH
Nystactes tamatia (inexpectatus)	Brazil: N bank Rio Solimóes	Napo	B35697	LSUMZ
Nystactes tamatia (interior)	Bolivia: Santa Cruz; S Huanchaca	Rondonia	B14727	LSUMZ
Nystactes tamatia (interior)	Bolivia: Santa Cruz; Velasco, P. N. Noel Kempf	Rondonia	B15320	LSUMZ
Nystactes tamatia pulmentum	Peru: Loreto: S Rio Amazonas; E bank Quebrada Vainilla	Inambari	B5064	LSUMZ
Nystalus chacuru uncirostris	Bolivia: Santa Cruz; Ea. Cambaras		B38159	LSUMZ
Nystalus chacuru uncirostris	Bolivia: Beni; Pampas de San Lorenzo, 35 km from Ribaralta		391062	FMNH
Nystalus m. maculatus	Brazil: Pernambuco; Caatinga		392469	FMNH
Nystalus m. maculatus	Brazil: Sergipe; Caninde do Sao Francisco, Curituba		392814	FMNH
Nystalus maculatus (pallidigula)	Bolivia: Santa Cruz; Santa Fe		B37827	LSUMZ
Nystalus maculatus (pallidigula)	Bolivia: Santa Cruz; Rio Tucuvaca		B6683	LSUMZ
Nystalus maculatus striatipectus	Paráguay: 22 59'N, 59 57'W		2856	KU
Nystalus maculatus striatipectus	Bolivia: Santa Cruz; Ea. Perforacion		B18721	LSUMZ
Nystalus radiatus	Panama: Darien: Cana; Cerro Pirre	Chocó/C. Amer.	B2280	LSUMZ
Nystalus s. striolatus	Peru: Ucayali: W bank Rio Shesha	Inambari	B10628	LSUMZ
MOMOTIDAE (MOTMOTS)				
Aspatha gularis	Guatemala		DHB4453	BMNH
Aspatha gularis [a]	Mexico: Chiapas		167029	LSUMZ
Aspatha gularis	México: Chiapas; Volcán Tacaná		BMM833	MZFC
Baryphthengus martii martii	Bolivia: La Paz	Inambari	B22906	LSUMZ
Baryphthengus martii martii	Bolivia: Pando: Nicolás Suarez	Inambari	B9657	LSUMZ

(TABLE 4.1, cont.)

Baryphthengus martii martii	Peru: Loreto; 79 km WNW Contanama	Inambari	B27572	LSUMZ
Baryphthengus martii martii	Peru: Madre de Dios	Inambari	433233	FMNH
Baryphthengus martii martii	Peru: Ucayali; Cerro Tahuayo	Inambari	B11256	LSUMZ
Baryphthengus martii martii	Ecuador: Morona-Santiago; 5 km SW of Taisha	Napo	2680	ANSP
Baryphthengus martii martii	Ecuador: Napo; ca 14km N Tigre Playa, 0° 20' N, 76° 40' W	Napo	5675	ANSP
Baryphthengus martii martii	Ecuador: Pastaza; N Canelos	Napo	115424	ZMUC
Baryphthengus martii martii	Peru: Loreto; San Jacinto; 2 18'S, 76 07'W	Napo	1041	KU
Baryphthengus martii martii	Bolivia: Santa Cruz; Velasco	Rondonia	B15241	LSUMZ
Baryphthengus martii martii	Brazil: Rondonia; Cachoeira Nazare, W bank, Rio Jiparana	Rondonia	389736	FMNH
Baryphthengus martii semirufus	Panama	Central America	B41651	LSUMZ
Baryphthengus martii semirufus	Panama: Bocas del Toro; Isla San Cristobal, Bocatorito	Central America	B00363	USNM
Baryphthengus martii semirufus	Panama: Bocas del Toro; Valiente Peninsula, Punta Alegre	Central America	B01306	USNM
Baryphthengus martii semirufus	Ecuador: El Oro; 9 km W Pinas	Chocó	113890	ZMUC
Baryphthengus martii semirufus	Ecuador: Esmeraldas	Chocó	B11893	LSUMZ
Baryphthengus martii semirufus	Panama: Darién	Chocó/C. Amer.	B2297	LSUMZ
Baryphthengus ruficapillus [a]	Brazil: Sao Paulo	SE Brazil	63322	LSUMZ
Baryphthengus ruficapillus	Paraguay: Itapua; 26 43'S, 55 48'W	SE Brazil	3633	KU
Baryphthengus ruficapillus	Paraguay: Itapua; 26 43'S, 55 48'W	SE Brazil	3677	KU
Electron carinatum	Honduras	Central America	GMS116	BMNH
Electron carinatum [a]	Honduras: Santa Barbara	Central America	29261	LSUMZ
Electron p. platyrhynchum	Ecuador: Esmeraldas; 20 km NNW of Alto Tambo	Chocó	2287	ANSP
Electron platyrhynchum minor	Panama: Chiriqui, Gualaca-Chiriqui Grande Rd.	Central America	B05481	USNM
Electron platyrhynchum minor	Panama: Colon	Central America	B26501	LSUMZ
Electron platyrhynchum pyrrholaemum	Bolivia: La Paz; Rio Beni	Inambari	B1170	LSUMZ
Electron platyrhynchum pyrrholaemum	Bolivia: Pando: Nicolás Suarez	Inambari	B9638	LSUMZ
Electron platyrhynchum pyrrholaemum	Peru: Loreto; 84 km WNW Contamana	Inambari	B27393	LSUMZ
Electron platyrhynchum pyrrholaemum	Peru: Madre de Dios; Hacienda Amazonia	Inambari	320985	FMNH
Electron platyrhynchum pyrrholaemum	Peru: Ucayali; Cerro Tahuayo	Inambari	B11274	LSUMZ
Electron platyrhynchum pyrrholaemum	Ecuador: Morona-Santiago; 5 km SW of Taisha	Napo	2681	ANSP
Electron platyrhynchum pyrrholaemum	Peru: Loreto; Rio Corrientes, Tiente Lopez, 02 35'S, 76 07'W	Napo	1100	KU
Eumomota s. superciliosa	Mexico: Campeche; Nayarit de Castellot, Mpio. Champotón		GES472	MZFC
Eumomota superciliosa apiaster	El Salvador		434021	FMNH
Eumomota superciliosa apiaster	Nicaragua		DAB1514	BMNH
Eumomota superciliosa bipartite [a]	Mexico: Chiapas		167030	LSUMZ

(TABLE 4.1, cont.)

Eumomota superciliosa bipartite	Mexico: Chiapas, Road to La Victoria, Valdivia		FC22524	MVZ
Hylomanes momotula	Mexico: Campeche; 18 14'N, 90 12'W	Central America	2161	KU
Hylomanes momotula	Mexico: Campeche; 18 14'N, 90 12'W	Central America	2182	KU
Hylomanes momotula	Panama: Darién	Chocó/C. Amer.	B2117	LSUMZ
Momotus a. aequatorialis [a]	Colombia: Cauca; Cerro Munchique		38599	LSUMZ
Momotus a. aequatorialis	Ecuador: Napo; 3 km S Cosanga; Hacienda San Isidro		5120	ANSP
Momotus a. aequatorialis	Peru: Cajamarca		B32766	LSUMZ
Momotus aequatorialis chlorolaemus	Bolivia: La Paz; Prov. B. Saavedra		B22739	LSUMZ
Momotus aequatorialis chlorolaemus	Bolivia: La Paz; Prov. Yungas, near Rio Elena		MV22	AMNH
Momotus aequatorialis chlorolaemus	Peru: Pasco		B8156	LSUMZ
Momotus mexicanus [a]	Mexico: Oaxaca		40640	LSUMZ
Momotus momota argenticinctus	Ecuador: Loja: SE Celica, along Rio Catamayo	Chocó/Tumbes	1715	ANSP
Momotus momota argenticinctus	Ecuador: Loja: SE Celica, along Rio Catamayo	Chocó/Tumbes	1731	ANSP
Momotus momota argenticinctus	Ecuador: Loja; 1 km NE of Cruzpamba	Chocó/Tumbes	1820	ANSP
Momotus momota argenticinctus [a]	Peru: Tumbes; 24km SE Pampa de Hospital	Chocó/Tumbes	91995	LSUMZ
Momotus momota bahamensis [a]	Tobago: 4 mi. N Mt. St. George		140424	LSUMZ
Momotus momota bahamensis [a,b]	Trinidad: St. George County; Arima Ward		140426	LSUMZ
Momotus momota coeruliceps	México: San Luis Potosí; Tanlacut	Central America	HGO131	MZFC
Momotus momota coeruliceps [a]	Mexico: Tamaulipas	Central America	40661	LSUMZ
Momotus momota conexus	Panama: Panama	Central America	B28724	LSUMZ
Momotus momota conexus	Panama: Panama	Central America	B37141	LSUMZ
Momotus momota goldmani	Mexico: Oaxaca	Central America	B19274	LSUMZ
Momotus momota goldmani	Mexico: Veracruz; El Bastonal, 3 km E Sierra de Santa Marta	Central America	343221	FMNH
Momotus momota goldmani	Mexico: Veracruz; El Bastonal, 3 km E Sierra de Santa Marta	Central America	393905	FMNH
Momotus momota ignobilis	Bolivia: La Paz; Rio Beni, ca. 20 km N Puerto Linares	Inambari	B927	LSUMZ
Momotus momota ignobilis	Bolivia: Pando	Inambari	B9762	LSUMZ
Momotus momota ignobilis	Peru: Madre de Dios; 15 km NE Puerto Maldonado	Inambari	443	KU
Momotus momota ignobilis	Peru: Madre de Dios; 13.4 km NNW Atalaya	Inambari	433236	FMNH
Momotus momota ignobilis	Peru: Madre de Dios; 3 km E Shintuya, Alto Madre de Dios	Inambari	397895	FMNH
Momotus momota ignobilis	Peru: Ucayali	Inambari	B10835	LSUMZ
Momotus momota ignobilis	Bolivia: La Paz; Palmasola, Rio Manupari		391058	FMNH
Momotus momota ignobilis	Bolivia: La Paz; Palmasola, Rio Manupari		391059	FMNH
Momotus momota lessonii	Costa Rica: San Jose	Central America	B27300	LSUMZ
Momotus momota lessonii	El Salvador: Municipio Izalco	Central America	434018	FMNH
Momotus momota lessonii	El Salvador: Municipio Izalco	Central America	434020	FMNH

(TABLE 4.1, cont.)

Momotus momota lessonii	Mexico: Chiapas; Road to La Victoria, Valdivia	Central America	FC22525	MVZ
Momotus momota lessonii	Mexico: Veracruz	Central America	393905	FMNH
Momotus momota lessonii	Mexico: Campeche: 18 14'N, 90 12'W	Central America	2015	KU
Momotus momota microstephanus	Ecuador: Rio Pacuyacu; 6 km from Rio Aguarico	Napo	4785	ANSP
Momotus momota microstephanus	Peru: Loreto; ca. 90 km N Iquitos	Napo	B4451	LSUMZ
Momotus momota momota	Brazil: Amapá	Guyana	391276	FMNH
Momotus momota momota	Brazil: Amapá	Guyana	392181	FMNH
Momotus momota momota	Guyana: Berbice, W bank Berbice River, Dubulay Ranch	Guyana	B04186	USNM
Momotus momota momota	Guyana: Essequibo, E bank Waruma River	Guyana	B05213	USNM
Momotus momota momota	Guyana: Iwokrama Reserve	Guyana	8644	ANSP
Momotus momota momota	Guyana: Iwokrama Reserve; S side Siparuni River	Guyana	8575	ANSP
Momotus momota momota	Guyana: N side Acari Mountains	Guyana	B10643	USNM
Momotus momota momota	Guyana: Parabara savanna	Guyana	B12693	USNM
Momotus momota momota	Guyana:Iwokrama Reserve; Burro Burro R.; WNW Kurupukari	Guyana	8010	ANSP
Momotus momota momota [a,b]	Venezuela: Mt. Marahuaca; Camp Jaime Benitez	Guyana	25255	LSUMZ
Momotus momota parensis	Brazil: Pará; Serra dos Carajas	Pará	391277	FMNH
Momotus momota pilcomajensis [a,b]	Brazil: Sao Paulo; Adolfo	SE Brazil	65142	LSUMZ
Momotus momota pilcomajensis (?)	Bolivia: Santa Cruz		B37670	LSUMZ
Momotus momota pilcomajensis (?)	Bolivia: Santa Cruz		B38522	LSUMZ
Momotus momota simplex (?)	Brazil: Mato Grosso	Rondonia	B35502	LSUMZ
Momotus momota simplex (?)	Brazil: Mato Grosso; Rio Cristalino	Rondonia	114499	ZMUC
Momotus momota simplex (?)	Brazil: Rondonia	Rondonia	B36765	LSUMZ
Momotus momota subrufescens [a]	Colombia: Magdalena; Bonda	Nechi	61946	LSUMZ
Momotus momota subrufescens [a]	Colombia: Magdalena; La Tigrera	Nechi	44864	LSUMZ
TODIDAE (TODIES)				
Todus mexicanus	Puerto Rico		B16815	LSUMZ
Todus todus	Jamaica		331068	FMNH

[a] DNA extracted from feather or toepad of dried specimen. [b] Incomplete mtDNA sequence obtained and used in analysis. Museum collections include: Louisiana St. Univ. Museum of Natural Science (LSUMZ); Univ. of Kansas Museum of Natural History (KU); Field Museum of Natural History (FMNH); Academy of Natural Sciences, Phila. (ANSP); National Museum of Natural History, Smithsonian Institution (USNM); Zoological Museum of Copenhagen (ZMUC); Barrick Museum of Natural History, Univ. Nevada, Las Vegas (BMNH); American Museum of Natural History (AMNH); Museum of Vertebrate Zoology, Univ. of California at Berkeley (MVZ); Museo de Zoología, Facultad de Ciencias, Univ. Nacional Autónoma de México (MZFC).

TABLE 4.2. Amplification and sequencing primers. Sources are (1) this study; (2) Kocher *et al.* 1989; (3) Hackett 1996; (4) Chesser 1999; (5) Mindell *et al.* 1998; (6)Shapiro and Dumbacher 2001; (7) R. Kimball and E. Braun.

Name	Sequence	Gene	Taxa	Source
H4b	GTGGTAAGTCTTCAGTCTTTGGTTT	CYTB	all	1
L14841	GCTTCCATCCAACATCTCAGCATGATG	CYTB	all	2
CBaeqF57	GCTCTCTCCTGGGCATCTG	CYTB	*M. aequatorialis*	1
CBaeqR1063	ATTTTCTAGGGCTCCGGCTA	CYTB	*M. aequatorialis*	1
CBMF650	ACGAATCYGGYTCAAACAAC	CYTB	motmots	1
CBMR440	GAAGTGTARGGCRAAGAATCG	CYTB	motmots	1
HMA	TCTTTGGTTTACAAGACCGATGT	CYTB	motmots	1
MCBF826	CTATTCGCCTACGCYATYYTAC	CYTB	motmots	1
MCBR873	CCTCCTAGTTTRTTGGGRATT	CYTB	motmots	1
GCBH-514	GGTTGTTTGAGCCGGATTC	CYTB	puffbirds, jacamars	1
GCBH-563	AAGTAGGGGTGGAATGGGAT	CYTB	puffbirds, jacamars	1
GCBL-425	AACCCCACACTAACCCGATT	CYTB	puffbirds, jacamars	1
H15299	GGAGGAAGTGCAGGGCGAAGAATCG	CYTB	puffbirds, jacamars	3
L15514	CTACACGAATCCGGCTCAAACAACC	CYTB	puffbirds, jacamars	1
L15557	ACTGCGACAAAATCCCATTCCA	CYTB	puffbirds, jacamars	1
L5215	TATCGGGCCCATACCCCGAAAAT	ND2	all	3
ND2J-R548	KTTTTCGRATYTGTGTTTGG	ND2	jacamars	1
H5578	CCTTGAAGCACTTCTGGGAATCAGA	ND2	motmots	3
ND2P-R528	GTTTGGTTRAGRCCYATT	ND2	puffbirds	1
H11151	GATTTGTTGAGCCGAAATCAAC	ND3	all	4
L10647	TTYGAAGCMGCMGCMTGATACTG	ND3	motmots	5
ND3MF220	CRTAYGARTGYGGCTTYGAYC	ND3	motmots	1
ND3MR446	AGRCCBCCYTGTRTYCAYTC	ND3	motmots	1
L10755	TTCCAATCTTTAAAATCTGG	ND3	puffbirds, jacamars	4
AK5b+	ATTGACGGCTACCCTCGCGAGGTG	AK1	motmots	6
AK5c-	CACCCGCCCGCTGGTCTCTCC	AK1	motmots	6
AK1GF20	AGAAGAAGGTGAGGACTCATGC	AK1	puffbirds, jacamars	1
AK1GR563	CATYGTYTCCTTCCCWGCAT	AK1	puffbirds, jacamars	1
BF7J-R357	GCATCCAGWTTTGYTATTTGTCTAYGG	βF7	jacamars	1
BF7P-R354	TGCRYCTRGATTTGCTGATTTTTC	βF7	puffbirds	1
BF7-F3	TGGCATGTTCTTCAGTACYTATG	βF7	puffbirds, jacamars	1
EEF2-4Fnew	GAAACAGTTTGCTGAGATGTATGTTGC	EEF2	motmots	7
EEF2-5F	CCTTGAYCCCATCTTYAAGGT	EEF2	motmots	7
EEF2-5R	CACCTTRAAGATGGGRTCAAG	EEF2	motmots	7
EEF2-6R	GGTTTGCCCTCCTTGTCCTTATC	EEF2	motmots	7
EEF2-7F	ACCTGCCTTCTCCTGTCACAG	EEF2	motmots	7
EEF2-7R	TATGGCRGCCTCATCATCAGG	EEF2	motmots	7
EEF2-8Rb	CCATGATYCTGACTTTCARGCCAGT	EEF2	motmots	7

analysis of transition-transversion ratios, and exploration of rate variation among codon positions. Alignment was performed by eye for the intron sequences, and indels that were shared by more than one taxon were coded as presence/absence characters.

Phylogenetic Analyses

Nucleotide frequency homogeneity across taxa was tested in PAUP* version 4.0b10 (Swofford 2002) for each family for the combined mitochondrial datasets and for each nuclear dataset separately. Phylogenetic analyses were performed separately for each of nine datasets, as follows: (1) concatenated mtDNA for puffbirds; (2) concatenated mtDNA for jacamars; (3) concatenated mtDNA for motmots; (4) AK1 for puffbirds; (5) AK1 for jacamars; (6) AK1 for motmots; (7) βF7 for puffbirds; (8) βF7 for jacamars; and (9) EEF2 for motmots. Because the puffbirds and jacamars are sister groups, they formed reciprocal outgroups in phylogenetic analyses. Two tody species were used as outgroups for the motmots. Analyses included maximum parsimony (MP) and maximum likelihood (ML) implemented in PAUP* version 4.0b10 (Swofford 2002), and Bayesian analysis using a Markov-chain Monte Carlo (MCMC) search method, as implemented in Mr. Bayes 3.0b4 (Huelsenbeck and Ronquist 2003). Maximum parsimony utilized equal weighting of characters and a heuristic search search strategy with tree bisection-reconnection (TBR) branch swapping. Nonparametic bootstrapping was performed to estimate statistical support for each node. Using the program Modeltest (version 3.06, Posada and Crandall 1998), the appropriate maximum likelihood model for each dataset was estimated through a series of likelihood ratio tests for nested models of sequence evolution, using model parameters estimated onto a simple neighbor-joining tree. The appropriate model was deemed to be the simplest one under which the increase of an additional parameter did not cause a significant increase in likelihood (Huelsenbeck and Rannala 1997). Models selected by the Akaike Information Criterion were generally similar and are not discussed further here. A heuristic search with TBR branch swapping was performed in PAUP* under the selected model.

The three concatenated mtDNA datasets were each analyzed using Mr. Bayes under a general time reversible model with gamma distributed rate heterogeneity and a proportion of invariant sites (GTR + Γ + I). Additionally, rate parameters were estimated separately for each of the three codon positions and for non-coding positions. Two independent runs of four MCMC chains were run for 2 million generations, using the default chain swapping and heating settings, and random starting trees. The chains were sampled every 50 generations. Both independent runs yielded highly similar results, with topology and model parameters reaching a stable likelihood plateau by 60,000 generations for the puffbirds, 58,000 generations for the jacamars, and 66,000 generations for the motmots. In all cases, the first 100,000 generations were discarded as "burn-in" and the remaining 36,000 sampled trees (from both independent runs combined) were used to calculate posterior probabilities for each node.

Estimation of Divergence Dates

The maximum likelihood phylogeny was tested for clock-like behavior using a likelihood ratio test approach. The likelihood of the tree when branch lengths were constrained to a molecular clock was compared to the likelihood of a tree that was unconstrained. All three concatenated mtDNA datasets rejected the molecular clock constraint. This significant variation in the rate of molecular evolution, commonly encountered in molecular datasets with broad taxon sampling, poses an obstacle for divergence time estimation. Methods devised by Sanderson (1997, 2002) including nonparametric rate-smoothing (NPRS) and penalized likelihood (PL) facilitate date estimation in the absence of a clock by allowing rates to vary across the tree while minimizing the amount of variation between adjacent branches. These methods assume that rates vary across the tree incrementally, as might any continuous character. PL allows different rates to be assigned to each branch, but it imposes a roughness penalty when rates vary too drastically

between adjacent branches. The relative contribution of the roughness penalty to the overall likelihood is determined by a smoothing parameter. At high smoothing values, the roughness penalty becomes more severe, and amount of rate variation among branches is more constrained. The smoothing parameter can be estimated from the data using a cross validation procedure that is incorporated in the program r8s (version 1.5, Sanderson 2002).

I used r8s to analyze the ML tree estimated by PAUP* for each of the three concatenated mtDNA datasets. The optimal smoothing parameters based on the cross validation procedure were 1 for motmots, and 10 for the both puffbirds and jacamars. Dates were calibrated using two independent lines of evidence. First, the fossil record for motmots and their sister family, the todies reveals that both families were extant during the Oligocene. Thus, the minimum age of the common ancestor of the motmots and todies can be constrained at 24 million years. Second, the date of the final uplift of the Isthmus of Panama is known with reasonable precision to have occurred between 3.1 and 3.5 million years ago (Keigwin 1982, Coates and Obando 1996). The closure of the seaway between the eastern Pacific and western Atlantic Oceans has served as an important calibration point for molecular divergence between geminate pairs of marine species (Marko 2002). Geological estimates of the timing of seaway closure correspond well with the fossil record of the first interchange of mammals between North America and South America, which is thought to have occurred 2.5 – 3.0 Ma (Webb and Rancy 1995). Given their low vagility, it is unlikely that puffbirds, jacamars, and motmots crossed a water barrier separating Central America and South America before the final completion of the landbridge. The present day centers of diversity and the molecular phylogenies presented in this study both suggest that motmots were restricted to Central America and that the puffbirds and jacamars were restricted to South America before the formation of the landbridge. It follows that the oldest divergence

between Central American and South American motmot lineages likely corresponds to the formation of this dispersal corridor. The oldest South America/Central America divergence was therefore fixed at 3.1 Ma, and all other such divergences within the motmot tree were constrained to have occurred less than 3.1 Ma. No fossil jacamars exist, and the fossil puffbirds that are known cannot be placed within the stem or crown group of puffbirds with any degree of certainty. Therefore, a biogeographic calibration must be used for the puffbirds and jacamars. However, seven puffbird and three jacamar superspecies share a common distribution pattern with three motmot species that allow us to link divergence between puffbird species with the formation of the Central American Landbridge. In each superspecies, genetically divergent populations occur in lowland forests of the trans-Andean and cis-Andean regions. The Andean barrier to gene flow between these geminate pairs must have formed after the final closure of the trans-Panama seaway, and likely coincided with the final uplift of the northern Andes, which culminated approximately 3 Ma (Helmens and van der Hammen 1994). To calibrate the timescale of evolution for puffbirds and jacamars using this information, the maximum divergence between cis-Andean and trans-Andean populations was fixed at 3.1 Ma. However, trans-Andean and cis-Andean representatives from one superspecies group of puffbirds (*Malacoptila*) and one of jacamars (*Brachygalba*) appeared to originate considerably before 3.1 Ma. Application of the common 0.01 substitutions per site (2 % divergence) per million years rate for avian mtDNA yielded divergence times across the Andes of 12 Myr and 9 Myr for *Malacoptila* and *Brachygalba*, respectively. The next oldest divergences across the Andes for the puffbirds (*Nystalus*) and jacamars (*Jacamerops*) were compatible with previously estimated rates of avian mtDNA evolution, and were fixed at 3.1 Ma.

The overall timing of diversification was characterized using lineage-through-time plots and each family was compared using Kolmogorov-Smirnov tests for cumulative distribution frequencies. Lineage accumulation through time was examined at four different levels of sampling: (1) species based on current taxonomy; (2) superspecies comprised of clades of allotaxa with non-overlapping distributions; (3) phylogroups, defined as all sampled named taxa plus additional clades or lineages that are estimated to have diverged at least 0.5 Ma ; and (4) phylogroups plus unsampled taxa whose positions on the tree were systematically estimated by identifying the maximum recorded divergence within their likely crown group, and randomly assigning the unsampled taxon to a point between zero and the natural log of the maximum recorded divergence.

Biogeographic Inference

Ancestral areas for each family were inferred using dispersal-vicariance analysis as implemented in the program DIVA (version 1.1, Ronquist 1996). This event-based method reconstructs the biogeographic history of a clade by imposing a cost matrix on distribution transitions at each node. Vicariance, in which a broadly distributed ancestor is subdivided into two daughter species, is assumed to be the most likely mode of speciation, and is assigned zero cost. Dispersal and extinction are assumed to happen less frequently, and are each assigned a cost of one. Distributions were coded as either South America or Central America, and only one ancestral area was permitted, corresponding to the assumption that all three low-vagility families were restricted to Central America or South America before the formation of the Central American Landbridge.

The geography of recent diversification within each family was examined separately for each monophyletic set of allopatrically distributed replacement species. These units are the

equivalent of superspecies and are comprised of multiple allospecies or subspecies, depending on the degree of morphological divergence as divined by taxonomists. Nelson and Ladiges (1996) dubbed these units 'paralogy-free subtrees' and recommended that they form the units of analysis for area biogeography because they reveal only the most recent set of vicariant events affecting each subtree. Subtrees were defined by estimating the degree of distribution overlap between sister clades at each node in the tree, starting at the tips. Clades on either side of the node were combined until the clade distributions overlapped by at least 10 percent. Distribution overlap was quantified using ArcView 3.2 (ESRI), with distribution data from Ridgeley *et al.* (2003). Samples were assigned to endemic areas following the framework devised by Cracraft (1985), and followed by Prum (1988) and Bates *et al.* (1998), for Neotropical birds. That framework is generally concordant with distribution limits and subspecies boundaries in puffbirds, jacamars, and motmots. Area cladograms for each superspecies subtree were compared, and compatible nodes were explored for temporal concordance.

RESULTS

DNA Sequences

No evidence was found for significant heterogeneity of base composition in any of the nine data partitions. Nearly all of the mtDNA sequences appeared to be of mitochondrial origin, as evidenced by high transition-transversion ratios, and absence of indels, double peaks on chromatograms, or stop codons. However, a nuclear psuedogene was preferentially amplified using primers for the 1047 bp fragment of cytochrome b in five individuals of *Momotus aequatorialis* and one individual of *M. momota argenticinctus*. The pseudogene was identified due to its unexpectedly high level of divergence from other *Momotus* cytochrome b sequences and presence of several indels and stop codons. Uncorrected sequence divergence between the

pseudogenes from *M. aequatorialis* and *M. m. argenticinctus* was 1.1 %, compared to an average mitochondrial sequence divergence of 6.1 % between the same taxa. New primers were designed specifically for *M. aequatorialis* that preferentially amplified the true mtDNA sequence.

For puffbirds, motmots, and jacamars, mitochondrial gene trees for ND2, ND3, and cytochrome b possessed compatible phylogenetic signal and were combined for the remainder of the analyses. The combined analyses are justified because the mitochondrial genes comprise a single linkage group. Total mtDNA alignment lengths were 1864 bp for motmots and 1846 bp for puffbirds and jacamars. Partial sequences as short as 420 bp were included for some important taxa, as noted in Table 4.1. Most of the partial sequences were samples derived from decomposed frozen tissue or feathers or toe pad scrapings from dried specimens, many of which had to be amplified in smaller overlapping fragments using specific primers designed from closely related taxa.

The nuclear AK1 intron for a subset of 50 puffbirds and jacamars ranged from 515 to 555 bp, with the total alignment length of 604 bp. The entire BF7 intron ranged in size between 950 and 1060 bp, with a total alignment length of 1184 bp for a subset of 24 puffbirds and jacamars. However, no successful amplification was achieved for the entire sequence for several key puffbird and jacamar taxa. In *Nonnula* and in the *Galbula galbula* superspecies, a nuclear paralogue that would not align with other sequences was amplified consistently. Only a small fragment consisting of the first 264 to 294 bp of BF7 was amplified successfully for the full subset of 50 puffbird and jacamar taxa, and these produced a total alignment of 303 bp. For a subset of 14 motmot taxa, the AK1 intron ranged from 495 to 528 bp, forming a total alignment of 564 bp. EEF2 ranged from 846 to 862 bp for motmots, with the total alignment of 1202 bp

due to one 357 indel in the outgroup kingfisher. Alignment was relatively straightforward for all of the nuclear intron data.

There was ample evidence of saturation in the mitochondrial dataset at uncorrected divergence levels above approximately 8 % (Fig. 4.1). Pairwise sequence divergence gradually approached a plateau near 20 %, whereas maximum likelihood distances continued to increase to a maximum divergence levels of approximately 0.6 (within puffbirds), 0.7 (within jacamars), and 0.3 substitutions per site (within motmots). Maximum likelihood distances for mtDNA ranged from 0.6 to 1.0 substitutions per site between puffbirds and jacamars, and from 0.5 to 0.7 substitutions per site between motmots and todies. The very high levels of divergence between ingroup and outgroup taxa in each of the three datasets suggests that the dates of these deep splits cannot be estimated with great precision using these data. Mitochondrial and nuclear (AK1) pairwise divergences for puffbirds and jacamars reveal a more complex relationship that reflects different patterns of rate variation in each independent linkage group (Fig. 4.2A). Relative divergence levels within puffbirds form three distinct clusters. The highest levels of mtDNA divergence relative to nuclear DNA divergence were for comparisons involving members of the genus *Nonnula*, whereas the highest levels of nuclear relative to mtDNA divergence were found among comparisons involving members of the genera *Nystalus* and *Bucco*. This pattern reflects the apparent nuclear DNA rate acceleration in the ancestor of the *Bucco*/*Nystalus* clade, and mtDNA rate acceleration in *Nonnula*. Jacamars differ from puffbirds in that mtDNA appears to have evolved considerably faster relative to the rate of the AK1 intron (Fig. 4.2A). When the comparisons between puffbirds and jacamars are considered, the overall relationship between mtDNA and AK1 divergence is basically linear. For motmots, the relationship between nuclear

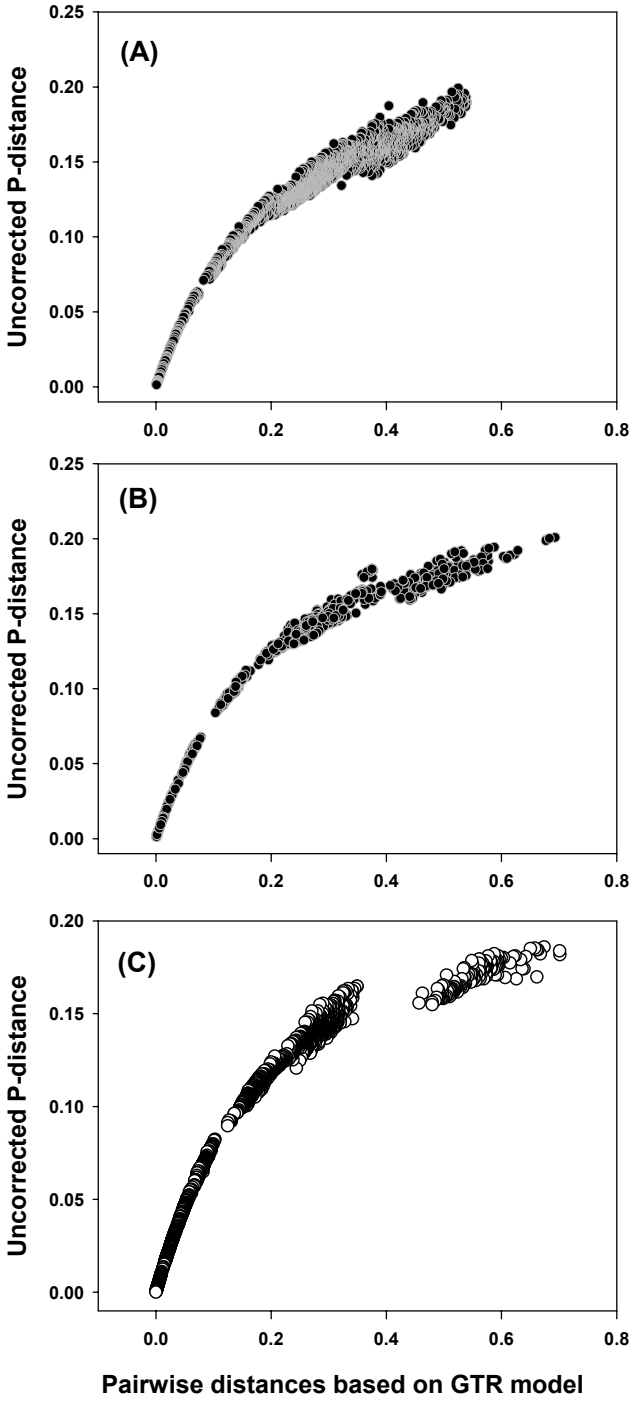

FIGURE 4.1. The relationship between uncorrected percent sequence divergence (p-distance) and maximum likelihood distances based on a general time reversible model incorporating gamma-distributed rate heterogeneity and a proportion of invariant sites (GTR + Γ + I) in combined mtDNA datasets for puffbirds (A), jacamars (B), and motmots (C). Yellow points represent comparisons between motmots and todies.

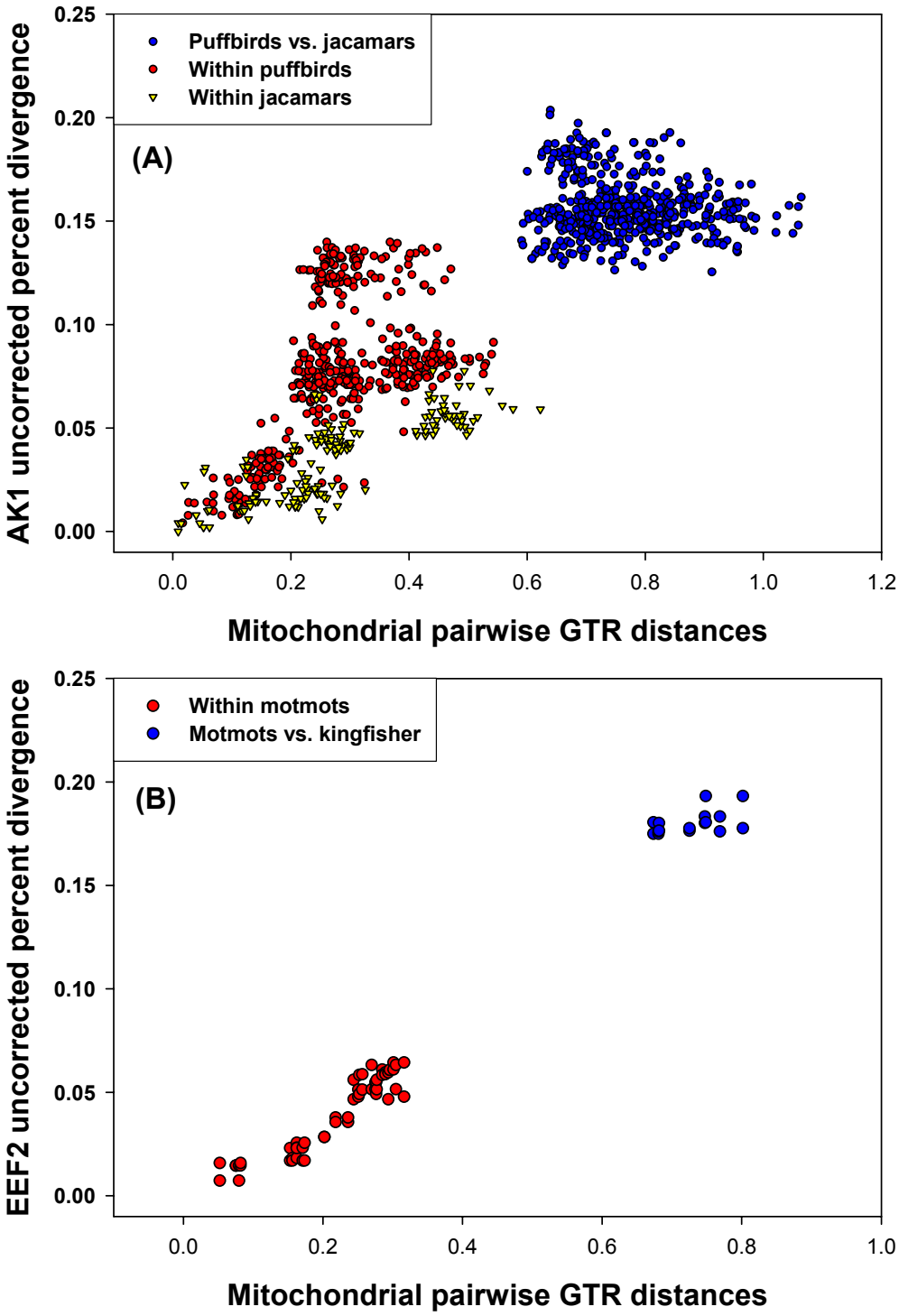

FIGURE 4.2. The relationship between nuclear DNA uncorrected percent sequence divergence (p-distance) and mtDNA maximum likelihood distances (GTR + Γ + I). (A) AK1 intron for puffbirds (red points), jacamars (yellow) and comparisons between jacamars and puffbirds. (B) EEF2 introns for within motmots and between motmots and a kingfisher outgroup (blue).

EEF2 pairwise distance and mtDNA maximum likelihood distance is also basically linear, although there is almost no divergence in EEF2 at levels of mtDNA divergence below approximately 0.2 substitutions/site (Fig. 4.2B). The low rates of divergence in the nuclear introns for all three families caused poor resolution at apical nodes, and limited the utility of the nuclear data for analyses of topology or divergence dates within superspecies groups.

Phylogenetic Analyses

The puffbird maximum likelihood phylogeny based on mtDNA is depicted in Fig. 4.3. All nodes that were strongly supported by Bayesian posterior probabilities (>0.95) were also present in the maximum likelihood topology. The parsimony topology possessed several conflicts, but no conflicting nodes were supported by bootstrap values over 70 percent. Several deep nodes were poorly resolved by all methods, and short internodes suggest that bifurcations occurred in rapid succession. However, the genus *Nonnula* is strongly supported as the basal clade, and several other groupings are strongly supported including *Bucco capensis* as sister to *Nystalus*, and *Monasa* as sister to *Chelidoptera*. The monotypic genera *Hapaloptila* and *Micromonacha* fall on long branches outside of a clade that includes the genera *Argicus*, *Notharchus*, *Nyctastes*, and *Hypnelus*. Both the DIVA analysis and a simple parsimony reconstruction of the ancestral area for puffbirds strongly suggests that the family was limited to the South American continent before the formation of the Central American Landbridge. A total of 23 superspecies, or paralogy-free subtrees were identified from the puffbird topology. Deep phylogenetic structure was present among allotaxa in most superspecies, and was deepest in the genera *Malacoptila* and *Nonnula*. Only the genus *Chelidoptera* possessed no genetic structure across a broad geographic range.

The mtDNA maximum likelihood phylogeny for the jacamars is presented in Fig. 4.4. All the basal nodes of the jacamar tree were well supported by Bayesian posterior probabilities and parsimony bootstrap percentages. The genera *Brachygalba* and *Jacamaralcyon* comprise a very ancient offshoot from the jacamars. Parsimony unambiguously suggests that the ancestral distribution was restricted to South America before the formation of the Central American Landbridge. Seven distinct superspecies complexes were identified.

Like the jacamar phylogeny, the motmot mtDNA maximum likelihood phylogeny was generally well resolved (Fig. 4.5) and there was near perfect agreement between parsimony, maximum likelihood, and Bayesian analyses. The motmots appear to have been restricted to Central America before the connection between the continents. Six superspecies were identified. The EEF2 and AK1 intron phylogeny for the motmots (not shown) is concordant in all respects except that it is ambiguous with respect to the relative positions of the genera *Hylomanes*, *Electron*, and *Eumomota*. All analyses agree that these three genera form a monophyletic group and that *Hylomanes* is sister to either *Electron* or *Eumomota*. The resolution of this conflict will require more data and will not be treated further here.

The nuclear AK1 and BF7 introns for puffbirds and jacamars possessed compatible phylogenetic signal and were combined for phylogenetic analysis. The maximum likelihood and Bayesian topologies were highly concordant, although they were very poorly resolved at most apical nodes due to a paucity of phylogenetically informative sites (Fig. 4.6). Puffbird mitochondrial and nuclear gene trees conflicted on one major node that was well supported in each dataset by both parsimony bootstrap and Bayesian posterior probabilities. The mtDNA data indicate that the genus *Nonnula* is basal to all other puffbirds. This hypothesis is appealing given that *Nonnula* differs from all other puffbirds in its small size, slender shape, and unmarked

FIGURE 4.3. Phylogenetic hypothesis for the puffbirds based on three mitochondrial genes. Branch lengths are proportional to the number of substitutions per site as inferred by maximum likelihood. Values at the nodes represent Bayesian posterior probability percentages (above the slash) and non-parametric bootstrap percentages for equally-weighted parsimony (below the slash). Red triangles represent inferred invasions of Central America. Blue circles denote superspecies groups, below which no taxa overlap in distribution by more than 10%.

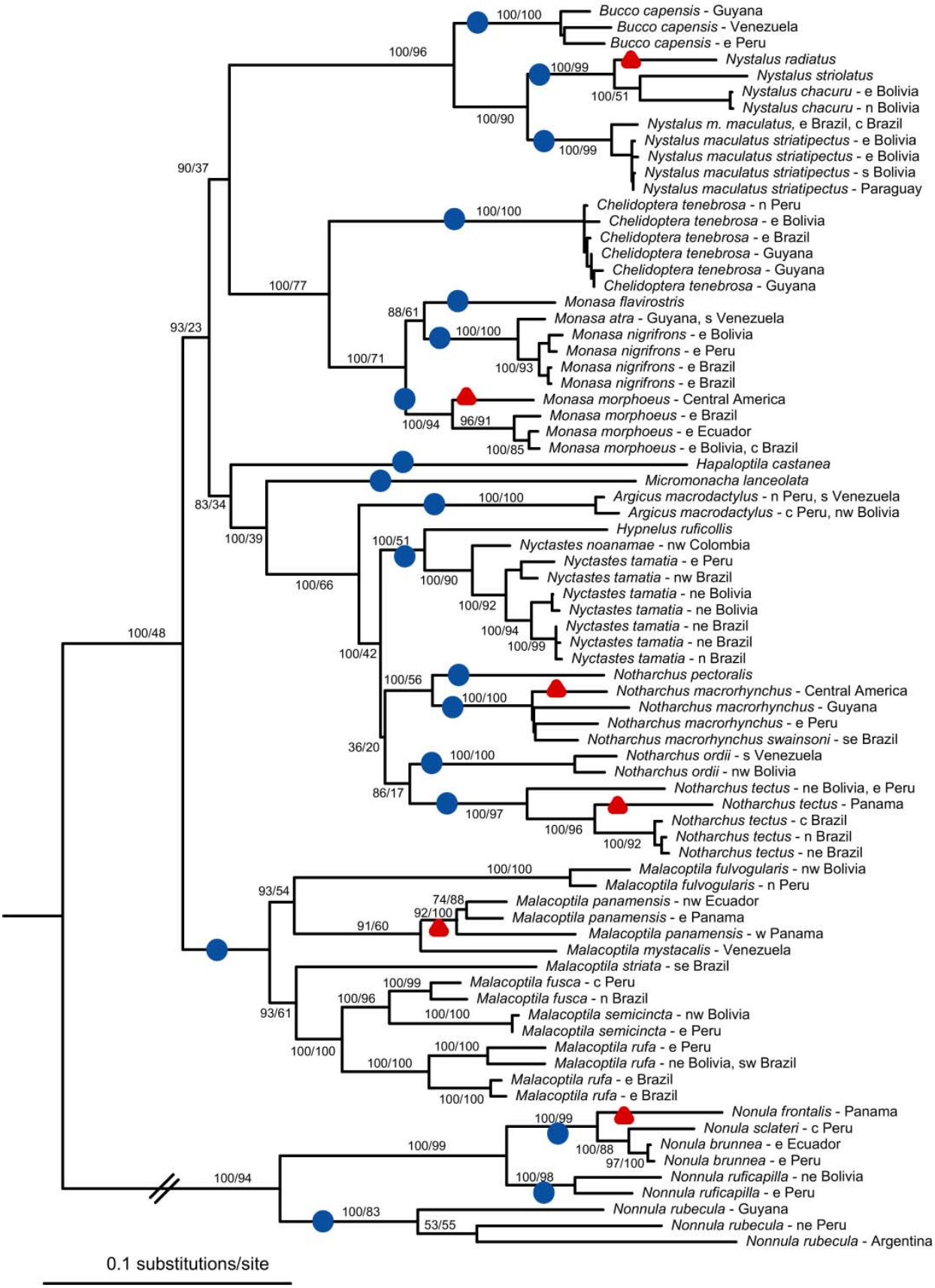
Bucco capensis - Guyana
Bucco capensis - Venezuela
Bucco capensis - e Peru
Nystalus radiatus
Nystalus striolatus
Nystalus chacuru - e Bolivia
Nystalus chacuru - n Bolivia
Nystalus m. maculatus, e Brazil, c Brazil
Nystalus maculatus striatipectus - e Bolivia
Nystalus maculatus striatipectus - e Bolivia
Nystalus maculatus striatipectus - s Bolivia
Nystalus maculatus striatipectus - Paraguay
Chelidoptera tenebrosa - n Peru
Chelidoptera tenebrosa - e Bolivia
Chelidoptera tenebrosa - e Brazil
Chelidoptera tenebrosa - Guyana
Chelidoptera tenebrosa - Guyana
Chelidoptera tenebrosa - Guyana
Monasa flavirostris
Monasa atra - Guyana, s Venezuela
Monasa nigrifrons - e Bolivia
Monasa nigrifrons - e Peru
Monasa nigrifrons - e Brazil
Monasa nigrifrons - e Brazil
Monasa morphoeus - Central America
Monasa morphoeus - e Brazil
Monasa morphoeus - e Ecuador
Monasa morphoeus - e Bolivia, c Brazil
Hapaloptila castanea
Micromonacha lanceolata
Argicus macrodactylus - n Peru, s Venezuela
Argicus macrodactylus - c Peru, nw Bolivia
Hypnelus ruficollis
Nyctastes noanamae - nw Colombia
Nyctastes tamatia - e Peru
Nyctastes tamatia - nw Brazil
Nyctastes tamatia - ne Bolivia
Nyctastes tamatia - ne Bolivia
Nyctastes tamatia - ne Brazil
Nyctastes tamatia - ne Brazil
Nyctastes tamatia - n Brazil
Notharchus pectoralis
Notharchus macrorhynchus - Central America
Notharchus macrorhynchus - Guyana
Notharchus macrorhynchus - e Peru
Notharchus macrorhynchus swainsoni - se Brazil
Notharchus ordii - s Venezuela
Notharchus ordii - nw Bolivia
Notharchus tectus - ne Bolivia, e Peru
Notharchus tectus - Panama
Notharchus tectus - c Brazil
Notharchus tectus - n Brazil
Notharchus tectus - ne Brazil
Malacoptila fulvogularis - nw Bolivia
Malacoptila fulvogularis - n Peru
Malacoptila panamensis - nw Ecuador
Malacoptila panamensis - e Panama
Malacoptila panamensis - w Panama
Malacoptila mystacalis - Venezuela
Malacoptila striata - se Brazil
Malacoptila fusca - c Peru
Malacoptila fusca - n Brazil
Malacoptila semicincta - nw Bolivia
Malacoptila semicincta - e Peru
Malacoptila rufa - e Peru
Malacoptila rufa - ne Bolivia, sw Brazil
Malacoptila rufa - e Brazil
Malacoptila rufa - e Brazil
Nonula frontalis - Panama
Nonula sclateri - c Peru
Nonula brunnea - e Ecuador
Nonula brunnea - e Peru
Nonnula ruficapilla - ne Bolivia
Nonnula ruficapilla - e Peru
Nonnula rubecula - Guyana
Nonnula rubecula - ne Peru
Nonnula rubecula - Argentina
0.1 substitutions/site

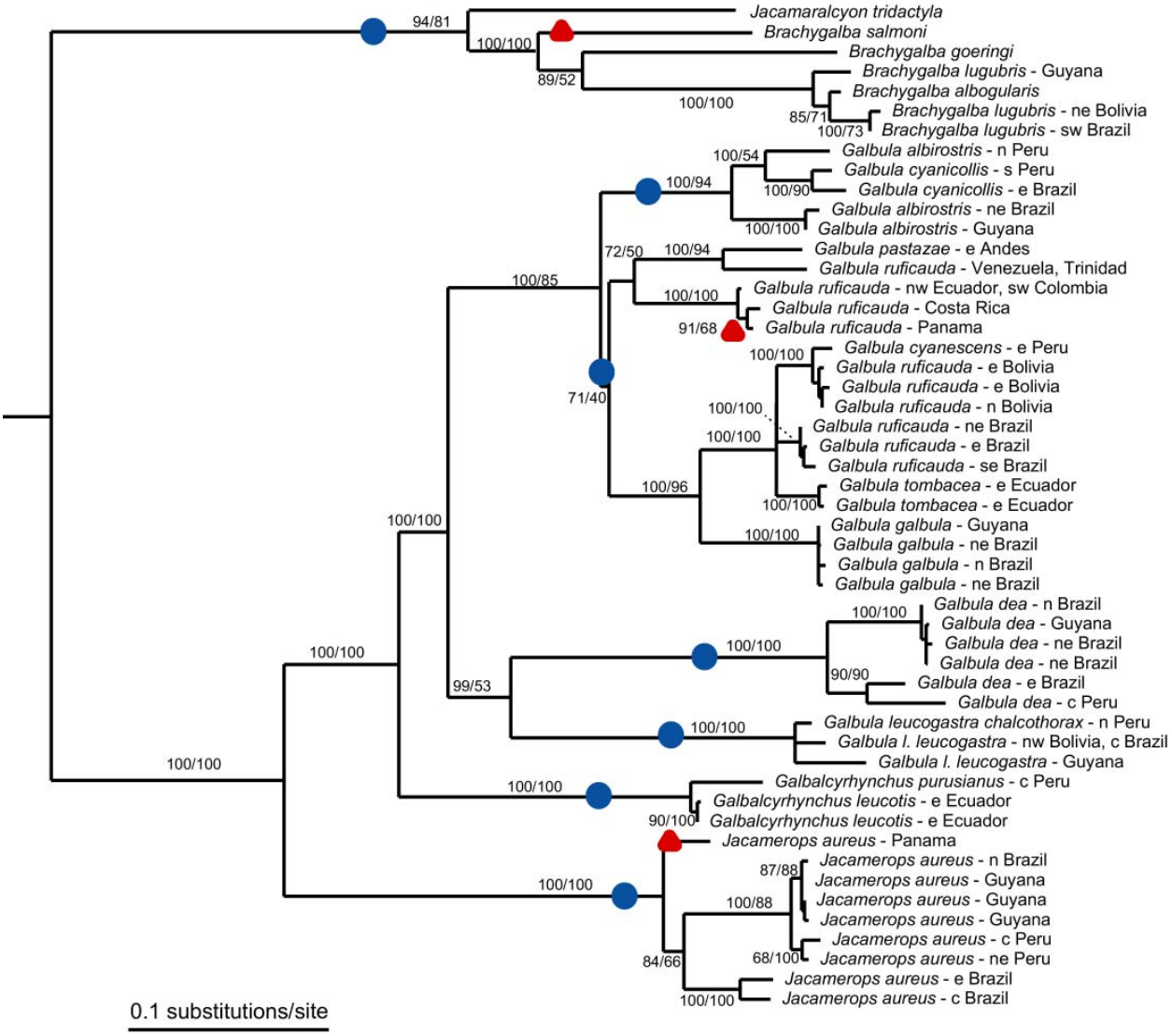

FIGURE 4.4. Phylogenetic hypothesis for the jacamars based on three mitochondrial genes. Branch lengths are proportional to the number of substitutions per site as inferred by maximum likelihood. Values at the nodes represent Bayesian posterior probability percentages (above the slash) and non-parametric bootstrap percentages for equally-weighted parsimony (below the slash). Red triangles represent inferred invasions of Central America. Blue circles denote superspecies groups, below which no taxa overlap in distribution by more than 10%.

FIGURE 4.5. Phylogenetic hypothesis for the motmots based on three mitochondrial genes. Branch lengths are proportional to the number of substitutions per site as inferred by maximum likelihood. Values at the nodes represent Bayesian posterior probability percentages (above the slash) and non-parametric bootstrap percentages for equally-weighted parsimony (below the slash). Red triangles represent inferred invasions of South America. Blue circles denote superspecies groups, below which no taxa overlap in distribution by more than 10%.

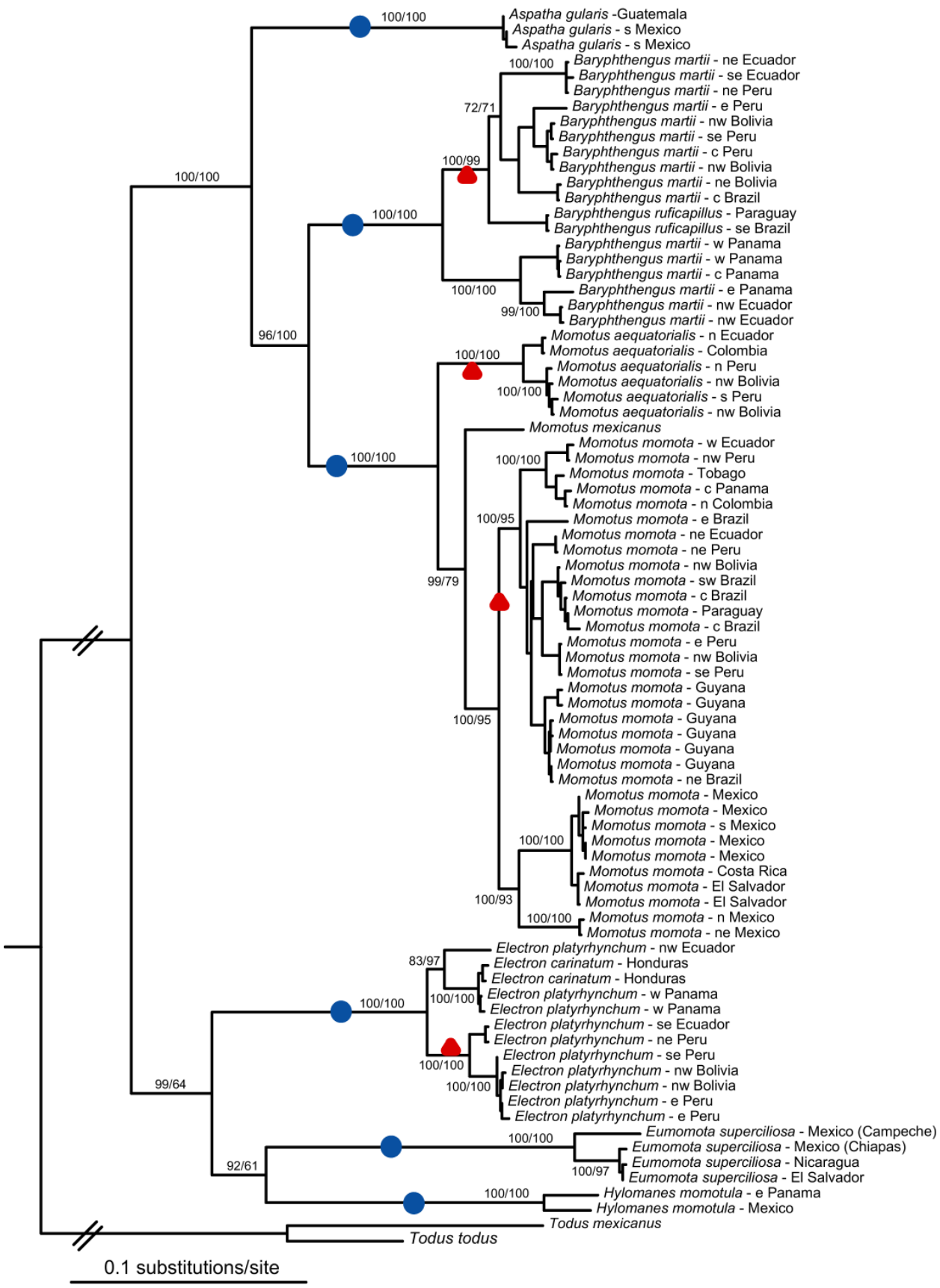
Aspatha gularis -Guatemala
Aspatha gularis - s Mexico
Aspatha gularis - s Mexico
Baryphthengus martii - ne Ecuador
Baryphthengus martii - se Ecuador
Baryphthengus martii - ne Peru
Baryphthengus martii - e Peru
Baryphthengus martii - nw Bolivia
Baryphthengus martii - se Peru
Baryphthengus martii - c Peru
Baryphthengus martii - nw Bolivia
Baryphthengus martii - ne Bolivia
Baryphthengus martii - c Brazil
Baryphthengus ruficapillus - Paraguay
Baryphthengus ruficapillus - se Brazil
Baryphthengus martii - w Panama
Baryphthengus martii - w Panama
Baryphthengus martii - c Panama
Baryphthengus martii - e Panama
Baryphthengus martii - nw Ecuador
Baryphthengus martii - nw Ecuador
Momotus aequatorialis - n Ecuador
Momotus aequatorialis - Colombia
Momotus aequatorialis - n Peru
Momotus aequatorialis - nw Bolivia
Momotus aequatorialis - s Peru
Momotus aequatorialis - nw Bolivia
Momotus mexicanus
Momotus momota - w Ecuador
Momotus momota - nw Peru
Momotus momota - Tobago
Momotus momota - c Panama
Momotus momota - n Colombia
Momotus momota - e Brazil
Momotus momota - ne Ecuador
Momotus momota - ne Peru
Momotus momota - nw Bolivia
Momotus momota - sw Brazil
Momotus momota - c Brazil
Momotus momota - Paraguay
Momotus momota - c Brazil
Momotus momota - e Peru
Momotus momota - nw Bolivia
Momotus momota - se Peru
Momotus momota - Guyana
Momotus momota - Guyana
Momotus momota - Guyana
Momotus momota - Guyana
Momotus momota - Guyana
Momotus momota - Guyana
Momotus momota - ne Brazil
Momotus momota - Mexico
Momotus momota - Mexico
Momotus momota - s Mexico
Momotus momota - Mexico
Momotus momota - Mexico
Momotus momota - Costa Rica
Momotus momota - El Salvador
Momotus momota - El Salvador
Momotus momota - n Mexico
Momotus momota - ne Mexico
Electron platyrhynchum - nw Ecuador
Electron carinatum - Honduras
Electron carinatum - Honduras
Electron platyrhynchum - w Panama
Electron platyrhynchum - w Panama
Electron platyrhynchum - se Ecuador
Electron platyrhynchum - ne Peru
Electron platyrhynchum - se Peru
Electron platyrhynchum - nw Bolivia
Electron platyrhynchum - nw Bolivia
Electron platyrhynchum - e Peru
Electron platyrhynchum - e Peru
Eumomota superciliosa - Mexico (Campeche)
Eumomota superciliosa - Mexico (Chiapas)
Eumomota superciliosa - Nicaragua
Eumomota superciliosa - El Salvador
Hylomanes momotula - e Panama
Hylomanes momotula - Mexico
Todus mexicanus
Todus todus
0.1 substitutions/site

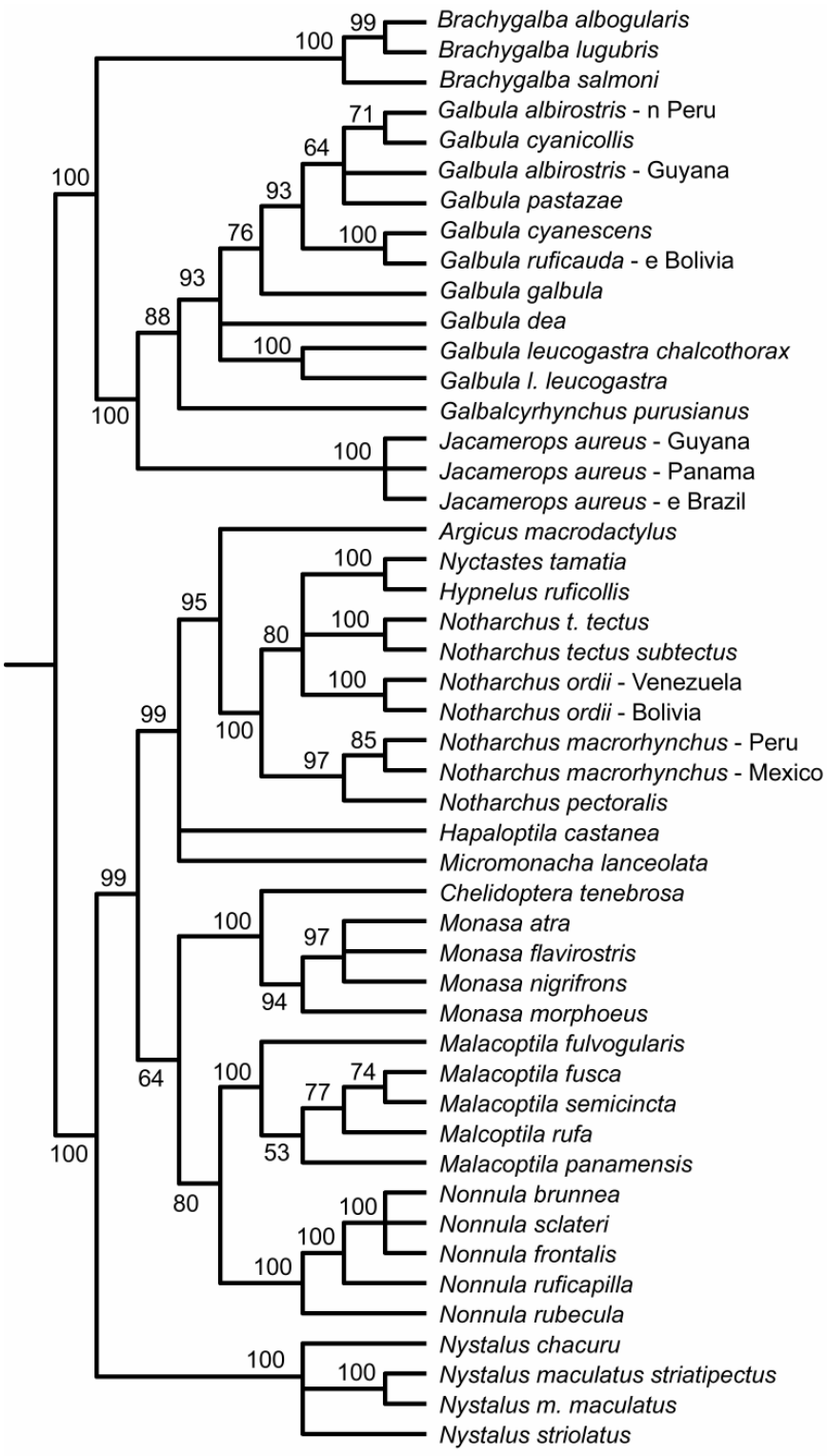

FIGURE 4.6. Phylogenetic hypothesis for the puffbirds and jacamars based on combined AK1 (604 bp) and BF7 (303 bp) alignments. Values at the nodes represent Bayesian posterior probability percentages.

TABLE 4.3. Shimodaira-Hasegawa test results comparing conflicting puffbird topologies for mitochondrial versus nuclear genes.

Data	Tree	-lnL	Difference	P
mtDNA	*Nonnula* basal	29257.818	–	–
combined	*Nystalus*+*Bucco* basal	29273.544	15.726	0.02*
AK1 and BF7	*Nystalus*+*Bucco* basal	4615.135	–	–
combined	*Nonnula* basal	4619.842	4.707	0.16

brown plumage. In contrast, the nuclear AK1 and BF7 intron sequences suggest that *Nonnula* is nested within the puffbirds and that a clade consisting of *Bucco* capensis and *Nystalus* is basal to the family. Shimodaira-Hasegawa (S-H) tests show that the latter topology is a significantly worse fit to the mitochondrial data. However, the topology with *Nonnula* basal is notsignificantly less likely given the nuclear intron data (Table 4.3). This was surprising given the high Bayesian posterior probability for a basal *Bucco*/*Nystalus* clade. Interestingly, *Nonnula* and *Bucco*/ *Nystalus* are the fastest evolving clades for the mitochondrial and nuclear datasets, respectively. The potential affects of this rate variation on generic level topology in puffbirds is worthy of future investigation.

Divergence Dates

Nearly all of the datasets appear to depart from the assumption of a molecular clock when likelihood scores are compared for trees that are optimized with or without the clock constraint (Table 4.4). The one exception was EEF2 for the motmots, which appeared to be evolving with a clocklike tempo; however, the potential utility of EEF2 (and the other nuclear introns) for dating divergence times is limited because there are very few variable sites among closely related allotaxa. All divergence date estimation was therefore performed using the combined mtDNA datasets.

TABLE 4.4. Likelihood ratio tests for clocklike molecular evolution.

Data	-lnL No Clock	-lnL Clock	Difference	P
Puffbird mtDNA combined	19260.391	19783.658	523.267	<0.0001
Jacamar mtDNA combined	10194.294	10378.166	183.872	<0.0001
Motmot mtDNA combined	13620.722	14736.239	1115.517	<0.0001
Puffbird/jacamar combined nucDNA	4627.834	4830.927	203.087	<0.0001
Motmot nuclear EEF2	3527.888	3533.875	5.998	>0.25

Penalized likelihood using biogeographic calibrations resulted in estimated rates of molecular evolution that were remarkably close to the two percent divergence per million years estimate that is frequently cited for birds and other vertebrates (Table 4.5). Maximum rates for each family, measured in substitutions per site per million years, occurred in *Nonnula*, the branch leading to *Galbula* dea, and *Eumomota*. The slowest rates were found for *Malacoptila*, *Galbalcyrhynchus*, and *Electron*.

The estimated dates and standard deviations for each node are reported for puffbirds (Fig. 4.7, Table 4.6), jacamars (Fig. 4.8, Table 4.7), and motmots (Fig. 4.9, Table 4.8). Standard deviations based on 100 bootstrap replicates of the penalized likelihood analysis averaged approximately 30 percent of the estimated node ages and were proportionately larger for nodes that were farther from the calibration point. It is important to note that these standard deviations do not account for error attributable to the calibration.

TABLE 4.5. Summary of rate variation as estimated under penalized likelihood, measured in substitutions per site per million years.

Data	Mean	SD	Minimum	Maximum	Max/min
Puffbird mtDNA combined	0.0093	0.0004	0.0089	0.0104	1.1685
Jacamar mtDNA combined	0.0112	0.0005	0.0099	0.0127	1.2828
Motmot mtDNA combined	0.0123	0.0005	0.0100	0.0135	1.3500

FIGURE 4.7. Chronogram showing the phylogeny of the puffbirds with branch lengths proportional to time as estimated by the penalized likelihood method. Node labels correspond to Table 4.6, numbers correspond to the estimated age of the node in millions of years.

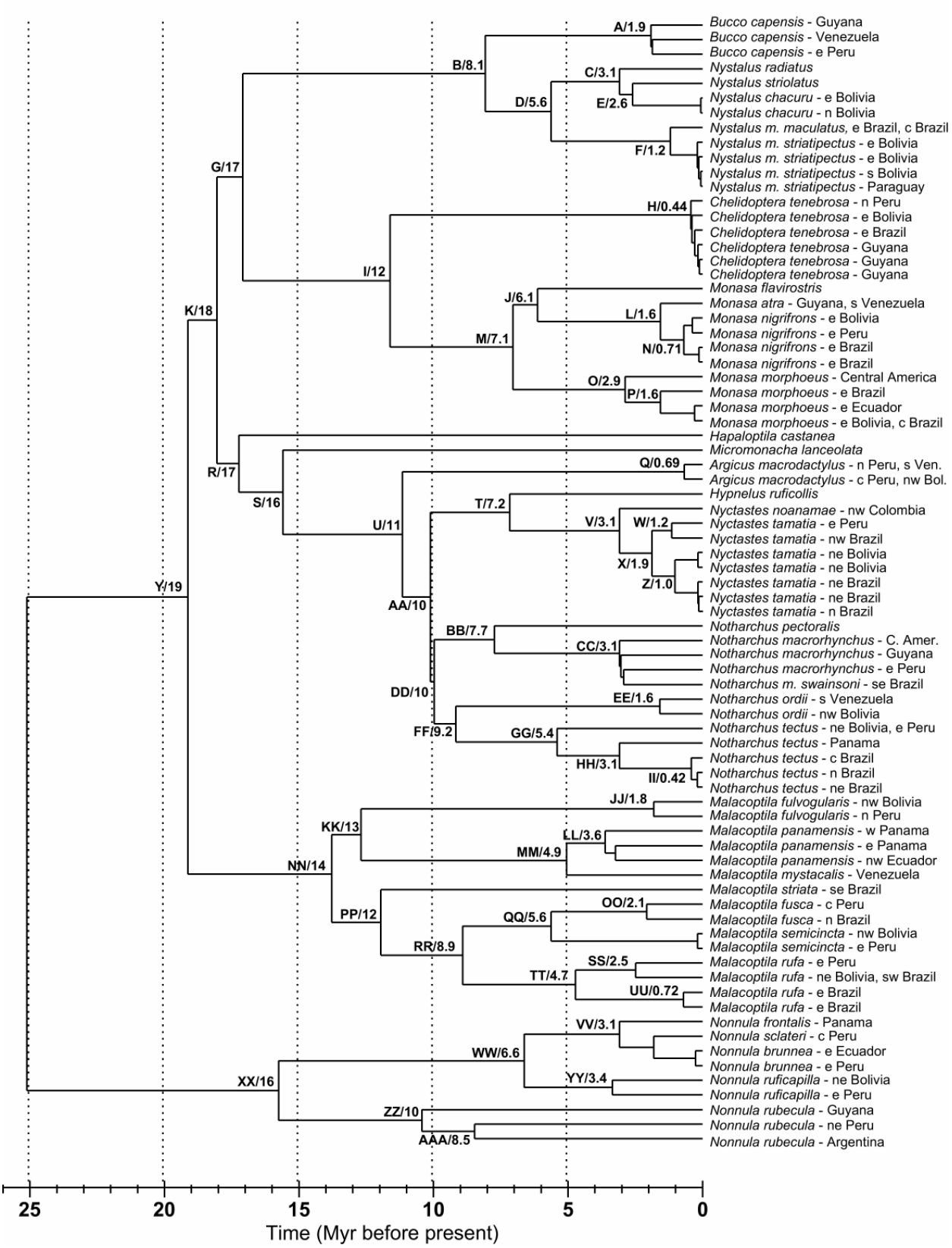
A/1.9
Bucco capensis - Guyana
Bucco capensis - Venezuela
Bucco capensis - e Peru
B/8.1
C/3.1
Nystalus radiatus
Nystalus striolatus
D/5.6
E/2.6
Nystalus chacuru - e Bolivia
Nystalus chacuru - n Bolivia
Nystalus m. maculatus, e Brazil, c Brazil
F/1.2
Nystalus m. striatipectus - e Bolivia
Nystalus m. striatipectus - e Bolivia
Nystalus m. striatipectus - s Bolivia
Nystalus m. striatipectus - Paraguay
G/17
H/0.44
Chelidoptera tenebrosa - n Peru
Chelidoptera tenebrosa - e Bolivia
Chelidoptera tenebrosa - e Brazil
Chelidoptera tenebrosa - Guyana
Chelidoptera tenebrosa - Guyana
Chelidoptera tenebrosa - Guyana
I/12
Monasa flavirostris
J/6.1
K/18
Monasa atra - Guyana, s Venezuela
L/1.6
Monasa nigrifrons - e Bolivia
Monasa nigrifrons - e Peru
M/7.1
N/0.71
Monasa nigrifrons - e Brazil
Monasa nigrifrons - e Brazil
O/2.9
Monasa morphoeus - Central America
P/1.6
Monasa morphoeus - e Brazil
Monasa morphoeus - e Ecuador
Monasa morphoeus - e Bolivia, c Brazil
Hapaloptila castanea
Micromonacha lanceolata
Q/0.69
R/17
Argicus macrodactylus - n Peru, s Ven.
Argicus macrodactylus - c Peru, nw Bol.
Hypnelus ruficollis
S/16
T/7.2
Nyctastes noanamae - nw Colombia
U/11
V/3.1
W/1.2
Nyctastes tamatia - e Peru
Nyctastes tamatia - nw Brazil
X/1.9
Nyctastes tamatia - ne Bolivia
Nyctastes tamatia - ne Bolivia
Z/1.0
Nyctastes tamatia - ne Brazil
Nyctastes tamatia - ne Brazil
Y/19
AA/10
Nyctastes tamatia - n Brazil
Notharchus pectoralis
BB/7.7
CC/3.1
Notharchus macrorhynchus - C. Amer.
Notharchus macrorhynchus - Guyana
Notharchus macrorhynchus - e Peru
DD/10
Notharchus m. swainsoni - se Brazil
EE/1.6
Notharchus ordii - s Venezuela
Notharchus ordii - nw Bolivia
FF/9.2
GG/5.4
Notharchus tectus - ne Bolivia, e Peru
Notharchus tectus - Panama
HH/3.1
Notharchus tectus - c Brazil
II/0.42
Notharchus tectus - n Brazil
Notharchus tectus - ne Brazil
JJ/1.8
Malacoptila fulvogularis - nw Bolivia
Malacoptila fulvogularis - n Peru
KK/13
LL/3.6
Malacoptila panamensis - w Panama
MM/4.9
Malacoptila panamensis - e Panama
Malacoptila panamensis - nw Ecuador
NN/14
Malacoptila mystacalis - Venezuela
Malacoptila striata - se Brazil
OO/2.1
PP/12
Malacoptila fusca - c Peru
QQ/5.6
Malacoptila fusca - n Brazil
Malacoptila semicincta - nw Bolivia
RR/8.9
Malacoptila semicincta - e Peru
SS/2.5
Malacoptila rufa - e Peru
TT/4.7
Malacoptila rufa - ne Bolivia, sw Brazil
UU/0.72
Malacoptila rufa - e Brazil
Malacoptila rufa - e Brazil
VV/3.1
Nonnula frontalis - Panama
Nonnula sclateri - c Peru
WW/6.6
Nonnula brunnea - e Ecuador
Nonnula brunnea - e Peru
XX/16
YY/3.4
Nonnula ruficapilla - ne Bolivia
Nonnula ruficapilla - e Peru
ZZ/10
Nonnula rubecula - Guyana
Nonnula rubecula - ne Peru
AAA/8.5
Nonnula rubecula - Argentina
25
20
15
10
5
0
Time (Myr before present)

TABLE 4.6. Node ages and standard deviations for the puffbirds, corresponding to the node labels in Fig. 4.7. Standard deviations derived from 100 bootstrap replicates.

Node	Age (Myr)	SD	Node	Age (Myr)	SD
A	1.9	0.82	BB	7.7	1.23
B	8.1	2.38	CC	3.1	constrained
C	3.1	Fixed	DD	9.9	2.11
D	5.6	1.10	EE	1.6	0.55
E	2.6	0.33	FF	9.2	1.79
F	1.2	0.49	GG	5.4	0.92
G	17.1	3.58	HH	3.1	constrained
H	0.44	0.49	II	0.42	0.35
I	12.4	4.14	JJ	1.8	0.59
J	6.1	2.05	KK	13	2.15
K	17.9	3.90	LL	3.6	0.74
L	1.6	1.16	MM	4.9	0.97
M	7.1	2.94	NN	14	2.79
N	0.71	0.73	OO	2.1	0.53
O	2.9	constrained	PP	12.0	2.08
P	1.6	0.50	QQ	5.6	1.10
Q	0.69	0.53	RR	8.9	1.49
R	17.2	3.94	SS	2.5	0.46
S	15.5	3.37	TT	4.7	0.96
T	7.2	2.10	UU	0.72	0.50
U	11	3.11	VV	3.1	constrained
V	3.1	constrained	WW	6.6	1.02
W	1.2	0.31	XX	15.7	2.18
X	1.9	0.35	YY	3.4	0.44
Y	19.1	3.98	ZZ	10.4	1.93
Z	1.0	0.29	AAA	8.5	1.68
AA	10.1	1.36			

FIGURE 4.8. Chronogram showing the phylogeny of the jacamars with branch lengths proportional to time as estimated by the penalized likelihood method. Node labels correspond to Table 4.7, numbers correspond to the estimated age of the node in millions of years.

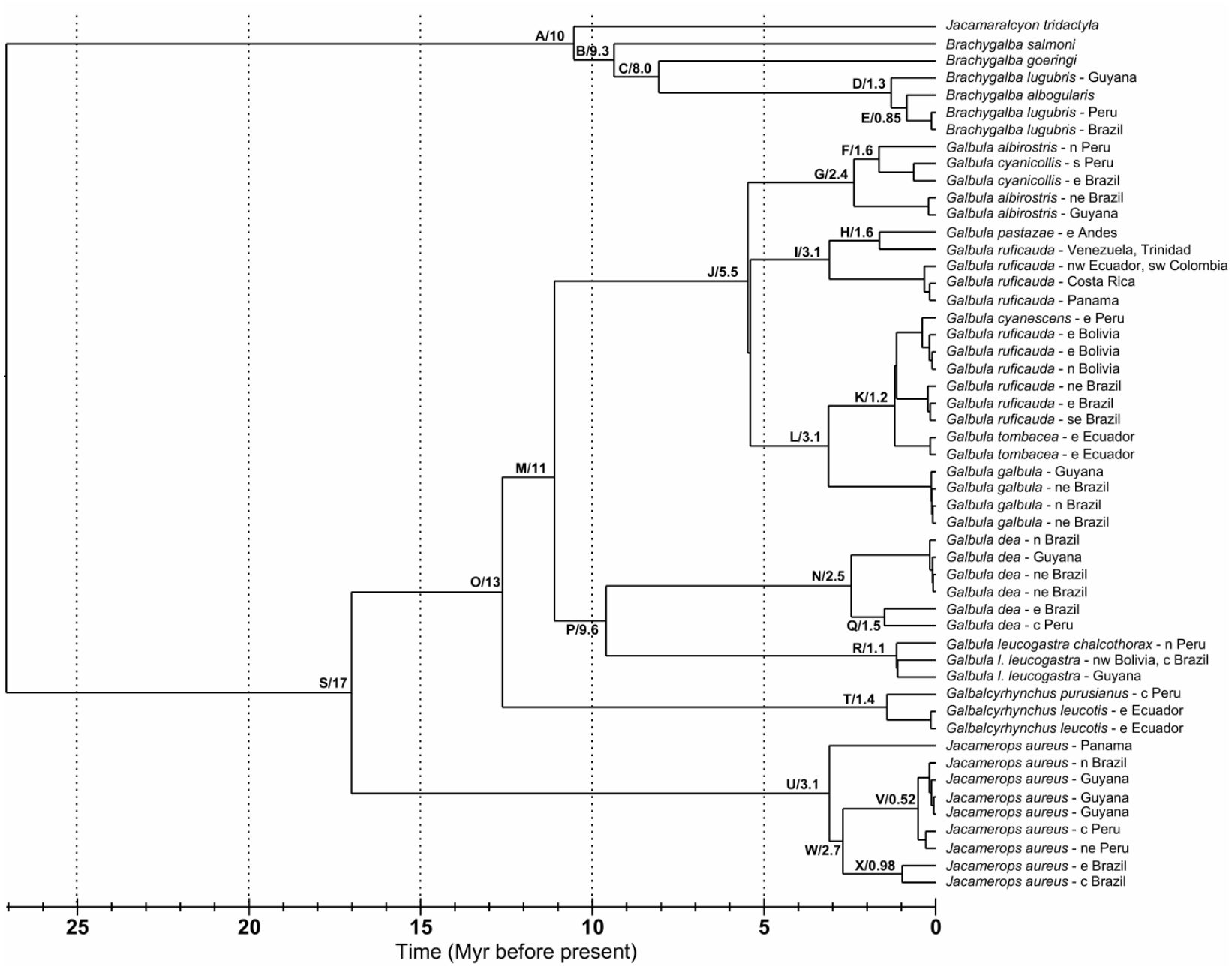
A/10
B/9.3
C/8.0
D/1.3
E/0.85
F/1.6
G/2.4
H/1.6
I/3.1
J/5.5
K/1.2
L/3.1
M/11
N/2.5
O/13
P/9.6
Q/1.5
R/1.1
S/17
T/1.4
U/3.1
V/0.52
W/2.7
X/0.98
Jacamaralcyon tridactyla
Brachygalba salmoni
Brachygalba goeringi
Brachygalba lugubris - Guyana
Brachygalba albogularis
Brachygalba lugubris - Peru
Brachygalba lugubris - Brazil
Galbula albirostris - n Peru
Galbula cyanicollis - s Peru
Galbula cyanicollis - e Brazil
Galbula albirostris - ne Brazil
Galbula albirostris - Guyana
Galbula pastazae - e Andes
Galbula ruficauda - Venezuela, Trinidad
Galbula ruficauda - nw Ecuador, sw Colombia
Galbula ruficauda - Costa Rica
Galbula ruficauda - Panama
Galbula cyanescens - e Peru
Galbula ruficauda - e Bolivia
Galbula ruficauda - e Bolivia
Galbula ruficauda - n Bolivia
Galbula ruficauda - ne Brazil
Galbula ruficauda - e Brazil
Galbula ruficauda - se Brazil
Galbula tombacea - e Ecuador
Galbula tombacea - e Ecuador
Galbula galbula - Guyana
Galbula galbula - ne Brazil
Galbula galbula - n Brazil
Galbula galbula - ne Brazil
Galbula dea - n Brazil
Galbula dea - Guyana
Galbula dea - ne Brazil
Galbula dea - ne Brazil
Galbula dea - e Brazil
Galbula dea - c Peru
Galbula leucogastra chalcothorax - n Peru
Galbula l. leucogastra - nw Bolivia, c Brazil
Galbula l. leucogastra - Guyana
Galbalcyrhynchus purusianus - c Peru
Galbalcyrhynchus leucotis - e Ecuador
Galbalcyrhynchus leucotis - e Ecuador
Jacamerops aureus - Panama
Jacamerops aureus - n Brazil
Jacamerops aureus - Guyana
Jacamerops aureus - Guyana
Jacamerops aureus - Guyana
Jacamerops aureus - c Peru
Jacamerops aureus - ne Peru
Jacamerops aureus - e Brazil
Jacamerops aureus - c Brazil
25
20
15
10
5
0
Time (Myr before present)

TABLE 4.7. Node ages and standard deviations for the jacamars, corresponding to the node labels in Fig. 4.8.

Node	Age (Myr)	SD	Node	Age (Myr)	SD
A	10	2.02	M	11	4.09
B	9.3	1.64	N	2.5	0.41
C	8.0	1.37	O	13	3.86
D	1.3	0.60	P	9.6	2.63
E	0.85	0.44	Q	1.5	0.72
F	1.6	0.42	R	1.1	0.35
G	2.4	0.82	S	17	4.78
H	1.6	0.50	T	1.4	0.96
I	3.1	fixed	U	3.1	constrained
J	5.5	1.04	V	0.52	0.29
K	1.2	0.25	W	2.7	0.31
L	3.1	0.61	X	0.98	0.60

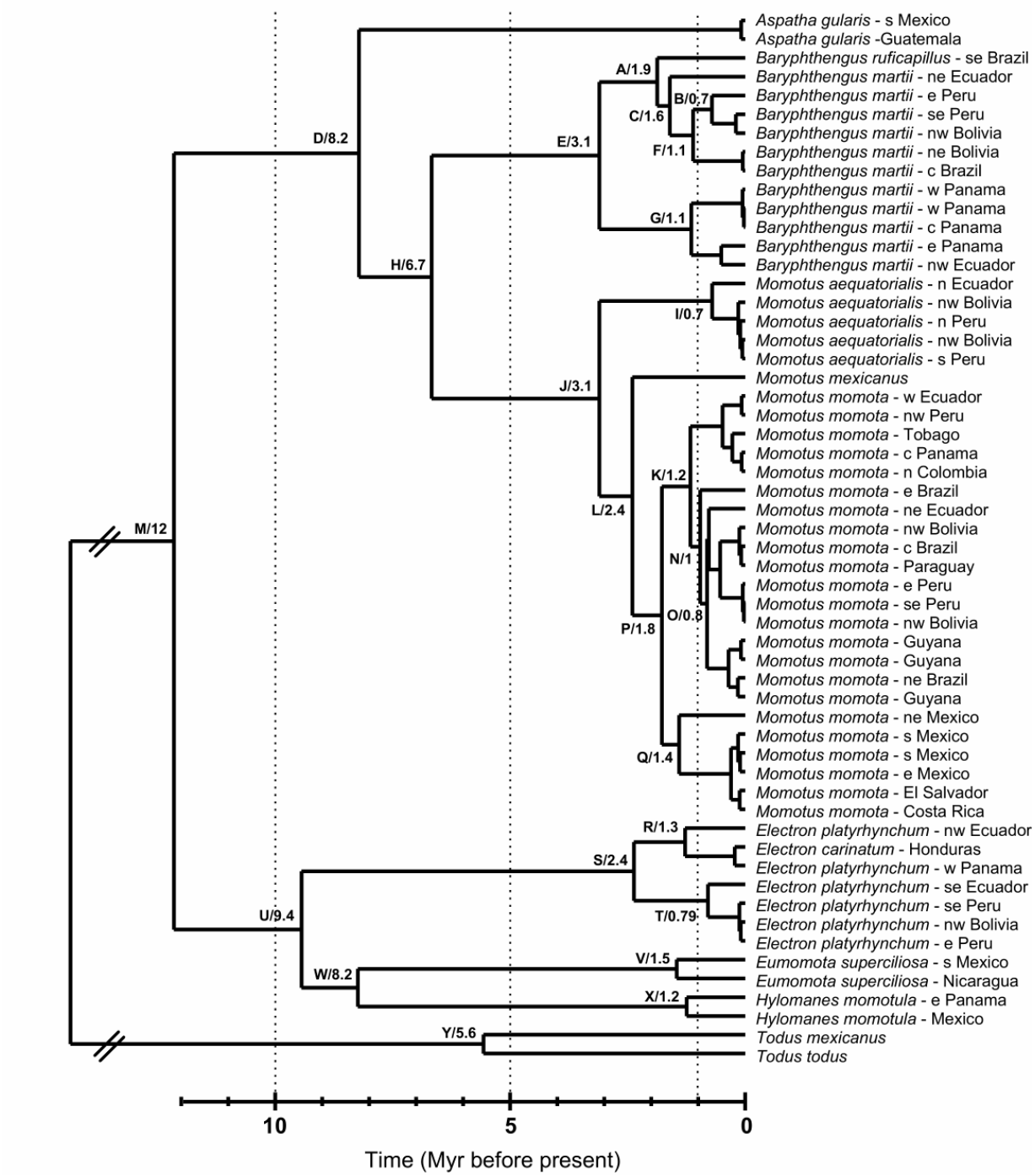

FIGURE 4.9. Chronogram showing the phylogeny of the motmots with branch lengths proportional to time as estimated by the penalized likelihood method. Node labels correspond to Table 4.8, numbers correspond to the estimated age of the node in millions of years.

TABLE 4.8. Node ages and standard deviations for the motmots, corresponding to the node labels in Fig. 4.9.

Node	Age (Myr)	SD	Node	Age (Myr)	SD
A	1.87	0.26	N	0.96	0.34
B	0.70	0.48	O	0.81	0.23
C	1.60	0.20	P	1.77	0.23
D	8.22	0.22	Q	1.42	0.32
E	3.10	fixed	R	1.28	0.27
F	1.11	0.41	S	2.42	0.42
G	1.15	0.38	T	0.79	0.34
H	6.67	0.15	U	9.44	0.25
I	0.70	0.56	V	1.46	0.25
J	3.10	fixed	W	8.24	0.22
K	1.16	0.21	X	1.24	0.23
L	2.40	0.20	Y	5.57	0.31
M	12.16	0.26			

Timing of Diversification

Absolute timing of diversification for each the three families at four hierarchical levels of sampling is compared in Figure 4.10. The most recent common ancestors of the jacamars and puffbirds were estimated to have occurred at approximately 27 and 25 Ma, respectively. The crown group of the motmots is much younger, having originated at approximately 12 to 13 Ma. Rates of diversification are generally similar for each family. Puffbird species and phylogroups appear to have undergone a steady rate of diversification throughout the history of the clade.

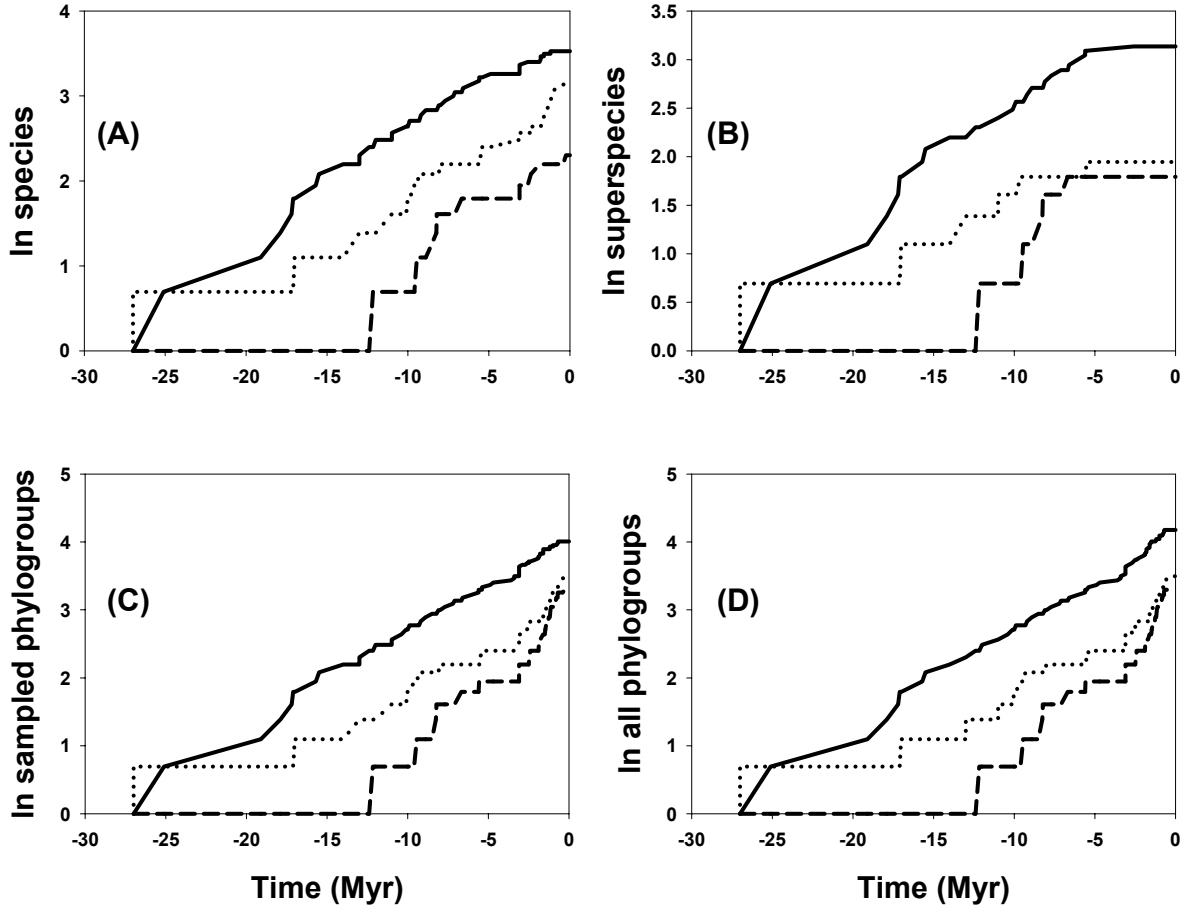

FIGURE 4.10. Cumulative number of lineages (log transformed) through real time for puffbirds (solid line), jacamars (dotted line), and motmots (dashed line) at different levels of sampling: (A) species, (B) superspecies, (C) all sampled phylogroups older than 0.5 Myr; and (D) phylogroups adjusted for unsampled taxa. Node ages estimated by penalized likelihood (see text).

Jacamar and motmot phylogroups appear to have undergone a recent sharp increase in diversity in the last 3 million years. This pattern could represent a real surge of diversification in these families, or it could be the signature of a constant background rate of extinction that has yet to affect recently formed taxa (Nee *et al.* 1994). Missing taxa had very little effect on the overall pattern of diversification (Fig. 4.10 D). All three families show an abrupt plateau in the number of superspecies at approximately 6 Ma.

Cumulative distribution frequencies of the number of lineages over time were compared between each pair of families with time scaled from the most recent common ancestor of each clade to the present (Fig. 4.11). The tempo of diversification across the entire histories of each clade was relatively similar (Table 4.9). In jacamars, diversification at the species level occurred later than in motmots, and diversification at the phylogroup level occurred later than in puffbirds, but these differences were only significant at the level of $p < 0.1$.

The effects of intercontinental dispersal on diversification following the formation of the Central American Landbridge are depicted in Figure 4.12, which compares the proportion of phylogroups in ancestral and descendant areas through time. Diversification of motmot phylogroups into South America is far more pronounced than diversification of puffbird and jacamar phylogroups into Central America. A higher proportion of motmot species have expanded into South America, and diversification following expansion has had a more profound impact on motmot than on puffbird or jacamar diversity.

Area Relationships

No sister taxa at the species or subspecies level overlap in distribution. This suggests that speciation has been primarily if not entirely allopatric. In order to compare area relationships among superspecies, sampling localities were assigned to one of the eight endemic areas as

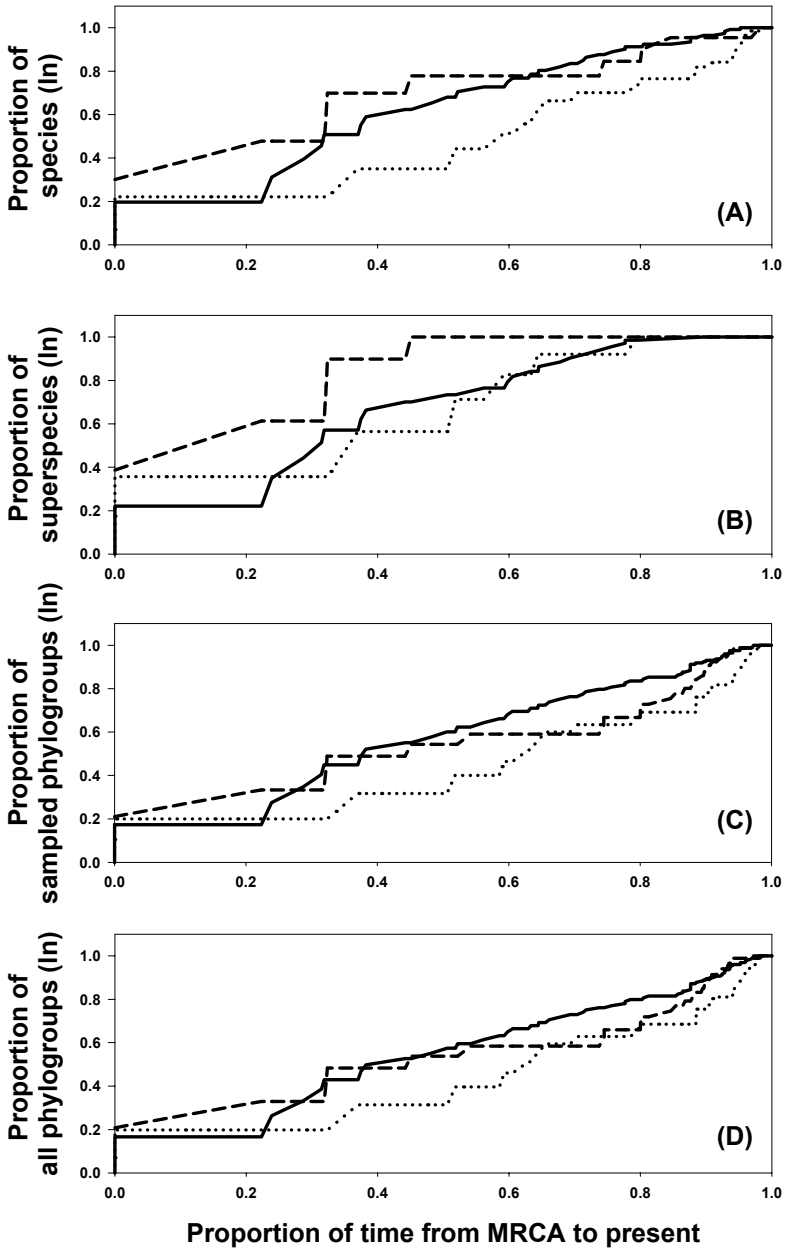

FIGURE 4.11. Cumulative frequency distributions of the number of lineages through time for the puffbirds, jacamars, and motmots, with time scaled from the most recent common ancestor of each group (0.0) to the present (1.0). (A) Species, defined by recent taxonomic treatments; (B) superspecies comprised of clades of allotaxa with non-overlapping distributions; (C) phylogroups, defined as all sampled named taxa plus additional clades or lineages that are estimated to have diverged at least 0.5 Ma ; and (D) phylogroups plus unsampled taxa whose positions on the tree were systematically estimated (see Methods). The timing of diversification for each level of sampling was compared using Kolmogorov-Smirnov tests, as reported in Table 4.9.

defined in Fig. 4.13. The phylogeographic relationships among allotaxa are illustrated for a subset of puffbird, jacamar, and motmot superspecies in Figures 4.14 to 4.26. Area relationships and estimated times of divergence for all superspecies that were sampled in more than one endemic area are illustrated in Figure 4.27, and the frequency and timing of specific phylogeographic patterns are listed in Table 4.10. Trans-Andean populations represented the basal clade in 10 of 11 superspecies. Guyanan shield populations were basal to all other cis-Andean populations in seven of 13 superspecies. Chocó and Central American populations were sister taxa relative cis-Andean populations in five of six superspecies, the only exception being the abberant Blue-crowned Motmot (*Momotus momota*, Fig. 4.25). Rondonia and Imerí populations were found at the tips of the superspecies trees in 12 of 12 and two of two cases, respectively. The Imerí populations were sister to Napo populations in both cases, whereas Rondonia populations were sister to Inambari, Pará, or Guyana populations. No consistent patterns emerged in the phylogenetic relationships of the Napo, Inambari, or Pará representatives. Southeast Brazil was represented by three very old (8.5 – 12 Ma) and four recent (0 – 3 Ma) lineages.

TABLE 4.9. Kolmogorov-Smirnov tests for differences in the timing of diversification among puffbirds, jacamars, and motmots, based on the cumulative distribution frequencies depicted in Fig. 4.11.

	Puffbirds vs. Motmots		Puffbirds vs. Jacamars		Jacamars vs. Motmots	
	D	P	D	P	D	P
Species	0.2806	n.s.	0.3296	n.s.	0.4779	<0.1
Superspecies	0.3921	n.s.	0.2152	n.s.	0.5420	n.s.
Sampled phylogroups	0.2063	n.s.	0.2841	<0.1	0.2883	n.s.
All phylogroups	0.1774	n.s.	0.2602	n.s.	0.2848	n.s.

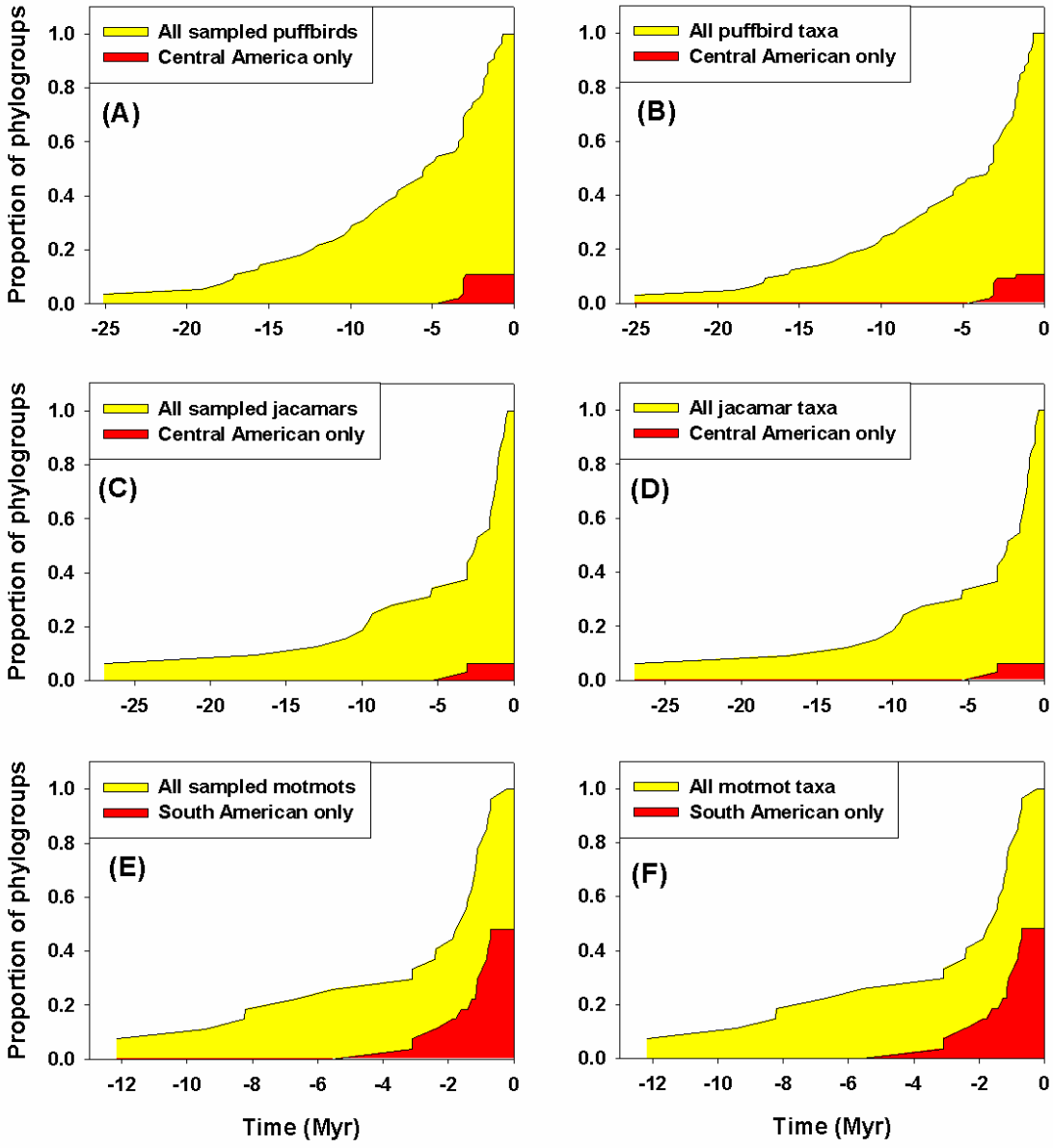

FIGURE 4.12. Cumulative frequency distributions of the number of lineages through time for the puffbirds (A, B), jacamars (C, D), and motmots (E, F), for all sampled phylogroups (A, C, E) and adjusted for missing taxa (B, D, F). The shaded areas under the curves represent the proportion of phylogroups occupying the original ancestral area (yellow) and the continent invaded following the formation of the Central American Landbridge (red).

FIGURE 4.13. Endemic areas for Neotropical lowland humid forest birds, adopted from Cracraft (1985).

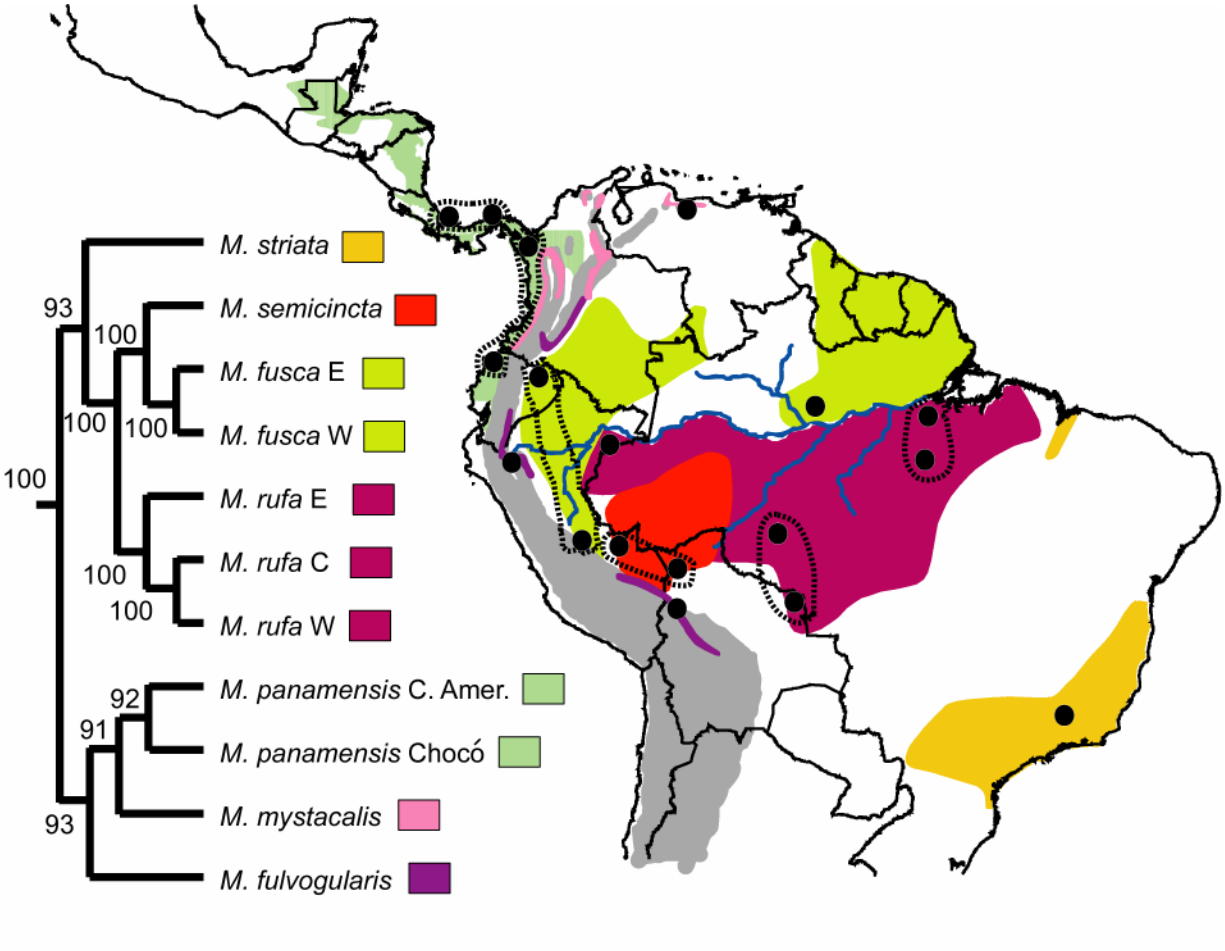

FIGURE 4.14. Phylogeny of geographical replacement species and populations in the puffbird genus *Malacoptila*. Numbers at nodes represent posterior probability percentages for Bayesian phylogenetic analysis of the combined mtDNA dataset. Black circles mark sampling localities. The 1000 m elevational contour of the Andes is shaded in gray. Dotted lines encircle identical or near identical haplotypes from different localities. *M. rufa* overlaps extensively with *M. semicincta*, but the area of overlap is not shown.

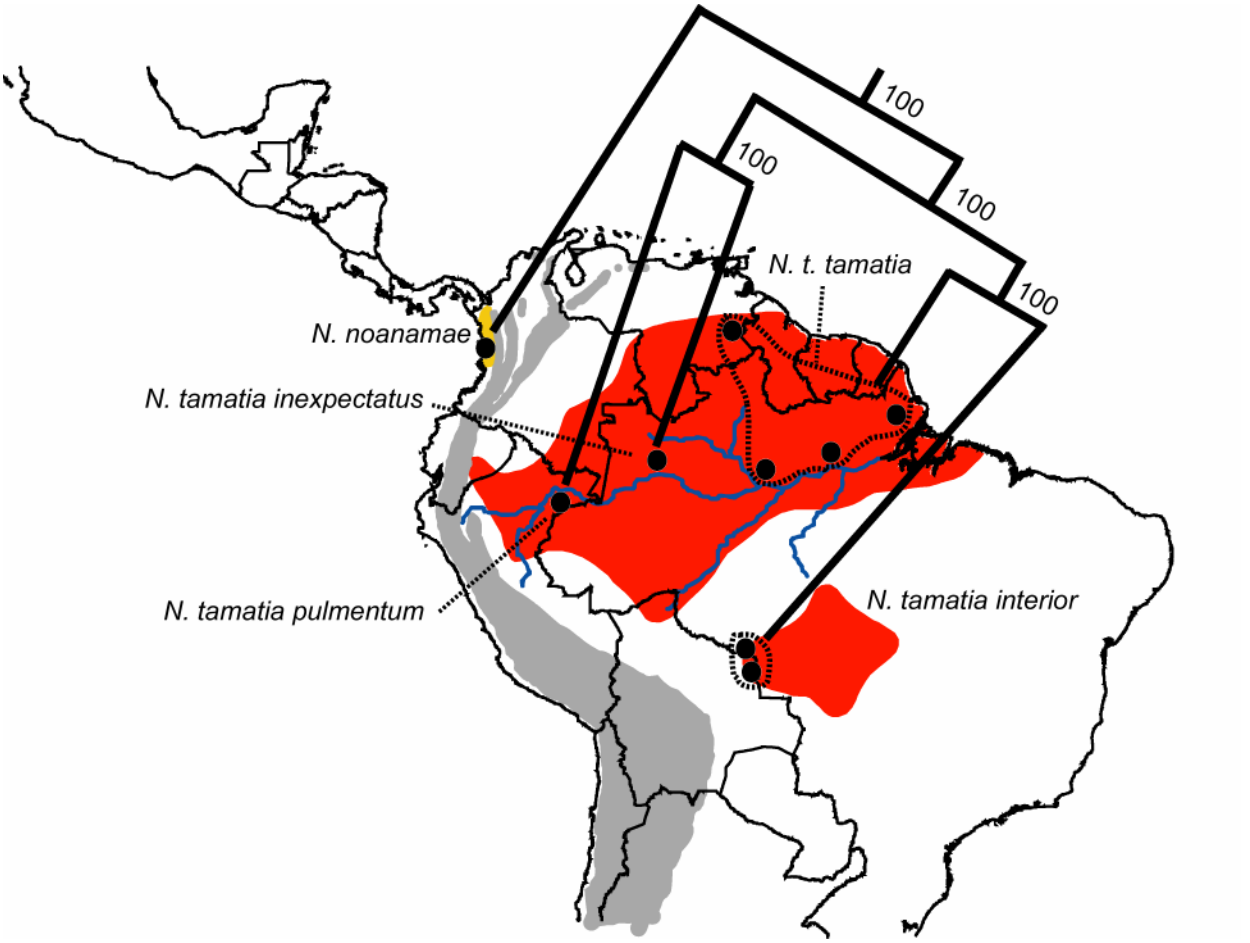

FIGURE 4.15. Phylogeny of geographical replacement populations in the puffbird genus *Nyctastes*. Numbers at nodes represent posterior probability percentages for Bayesian phylogenetic analysis of the combined mtDNA dataset. Black circles mark sampling localities. The 1000 m elevational contour of the Andes is shaded in gray. Dotted lines encircle identical or near identical haplotypes from different localities.

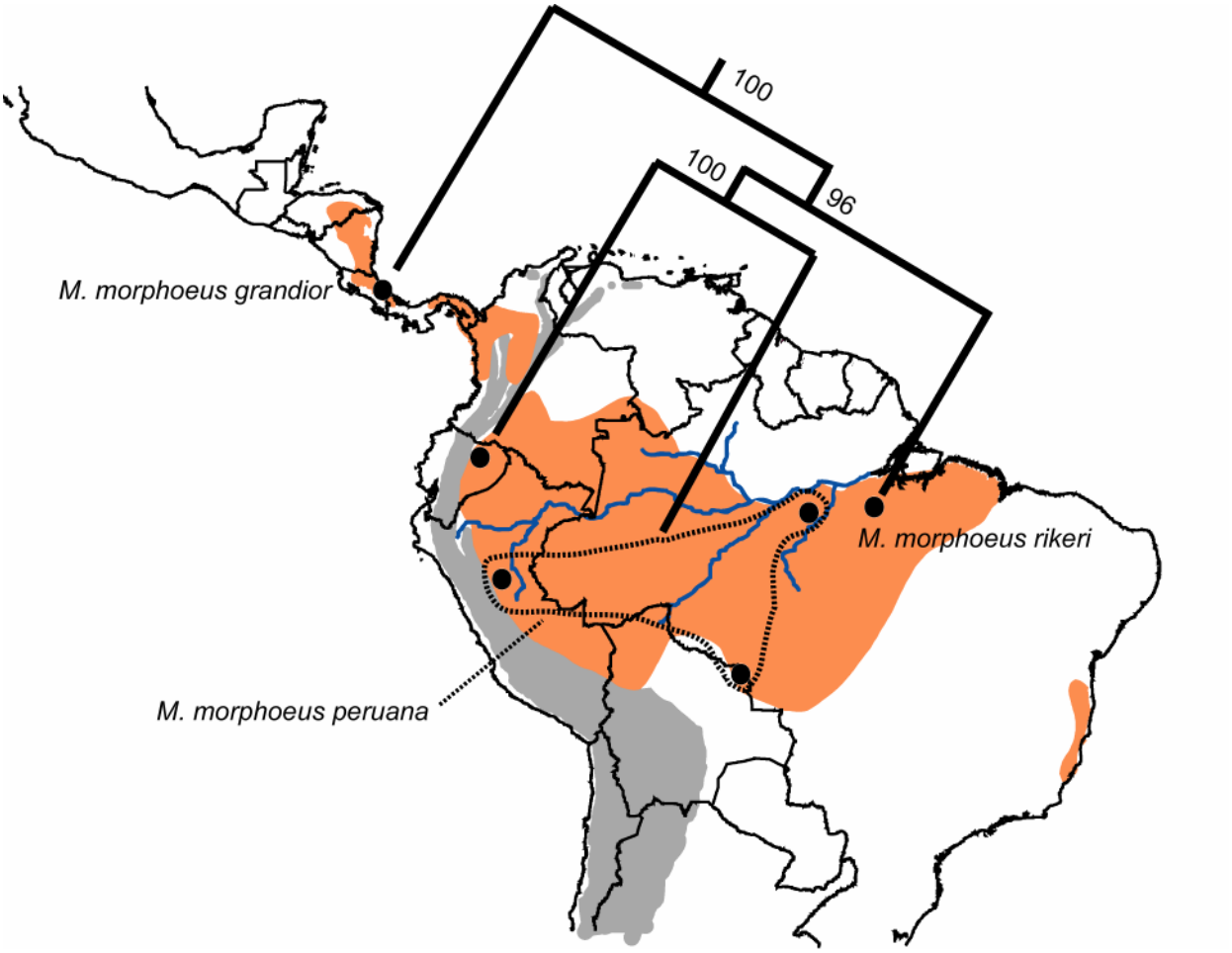

FIGURE 4.16. Phylogeny of geographical replacement populations in the puffbird superspecies *Monasa morphoeus*. Numbers at nodes represent posterior probability percentages for Bayesian phylogenetic analysis of the combined mtDNA dataset. Black circles mark sampling localities. The 1000 m elevational contour of the Andes is shaded in gray. Dotted lines encircle identical or near identical haplotypes from different localities.

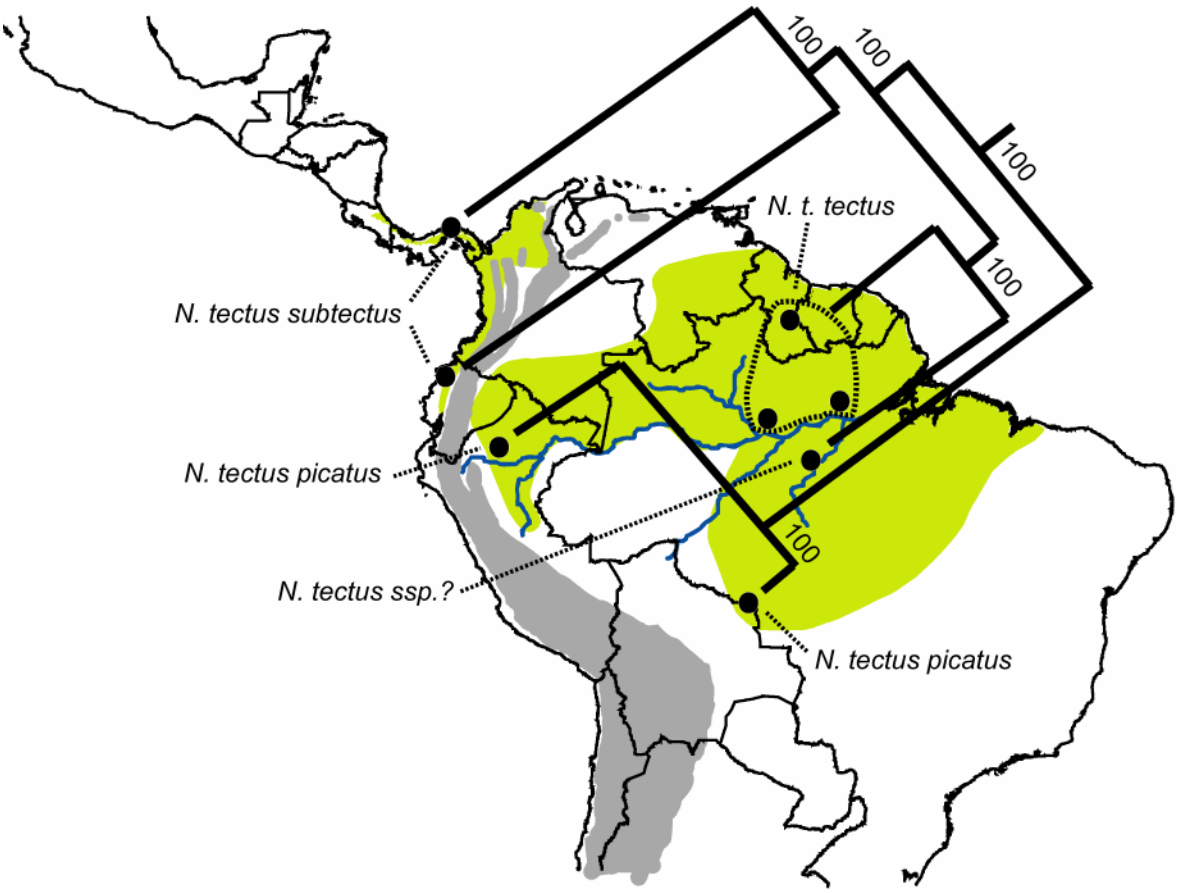

FIGURE 4.17. Phylogeny of geographical replacement populations in the puffbird superspecies *Notharchus tecuts*. Numbers at nodes represent posterior probability percentages for Bayesian phylogenetic analysis of the combined mtDNA dataset. Black circles mark sampling localities. The 1000 m elevational contour of the Andes is shaded in gray. Dotted lines encircle identical or near identical haplotypes from different localities.

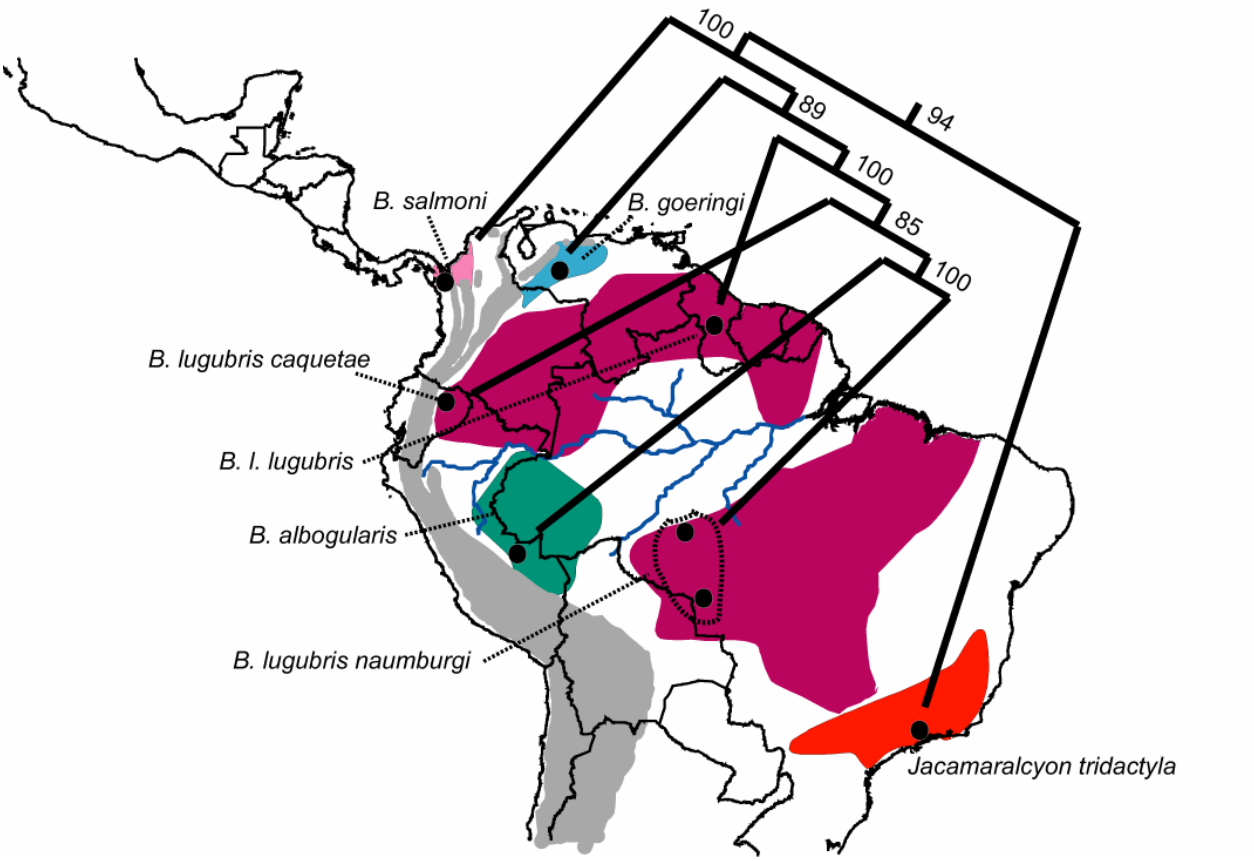

FIGURE 4.18. Phylogeny of geographical replacement species and populations in the jacamar superspecies comprised by *Brachygalba* and *Jacamaralcyon*. Numbers at nodes represent posterior probability percentages for Bayesian phylogenetic analysis of the combined mtDNA dataset. Black circles mark sampling localities. The 1000 m elevational contour of the Andes is shaded in gray. Dotted lines encircle identical or near identical haplotypes from different localities.

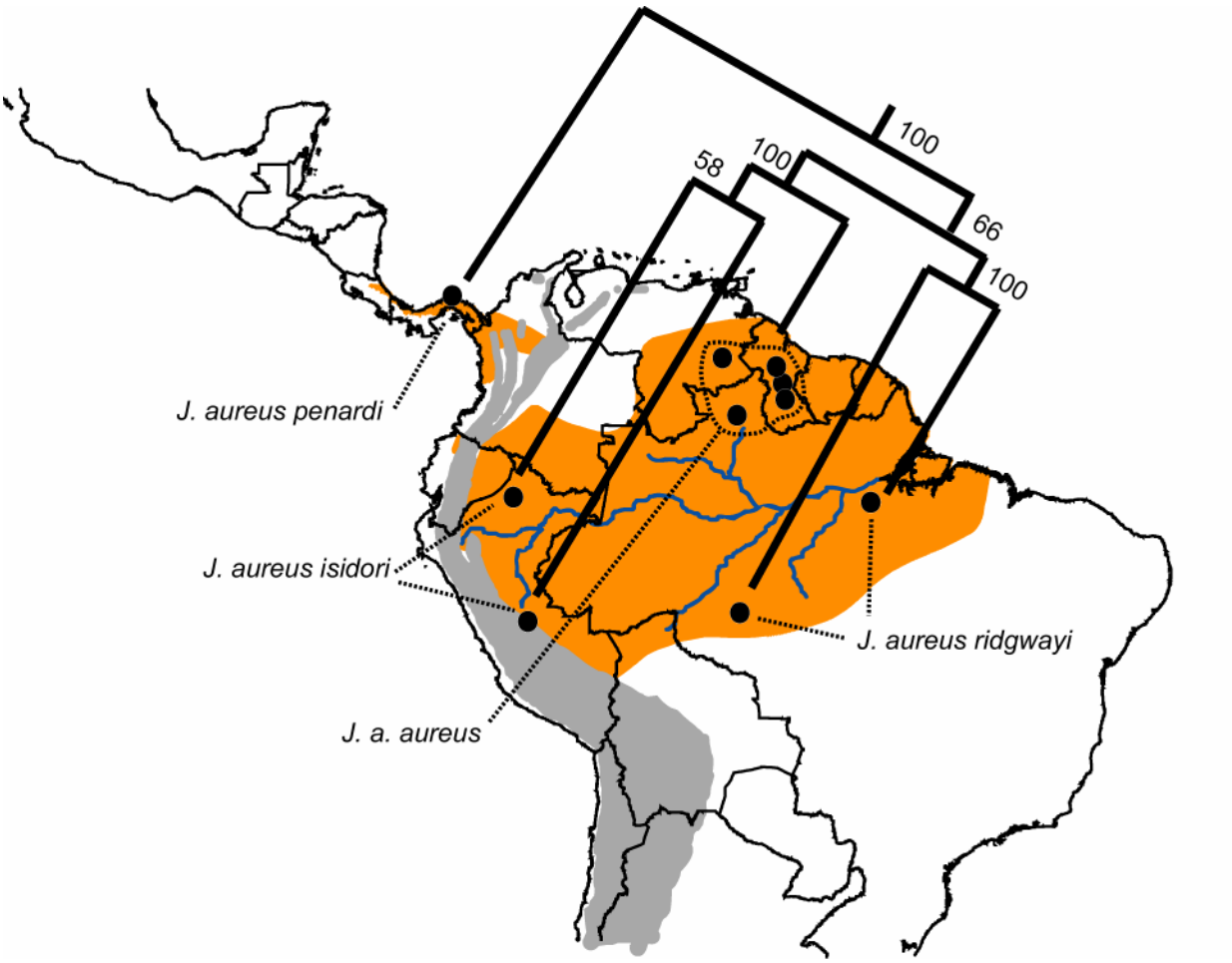

FIGURE 4.19. Phylogeny of geographical replacement populations in the jacamar genus *Jacamerops*. Numbers at nodes represent posterior probability percentages for Bayesian phylogenetic analysis of the combined mtDNA dataset. Black circles mark sampling localities. The 1000 m elevational contour of the Andes is shaded in gray. Dotted lines encircle identical or near identical haplotypes from different localities.

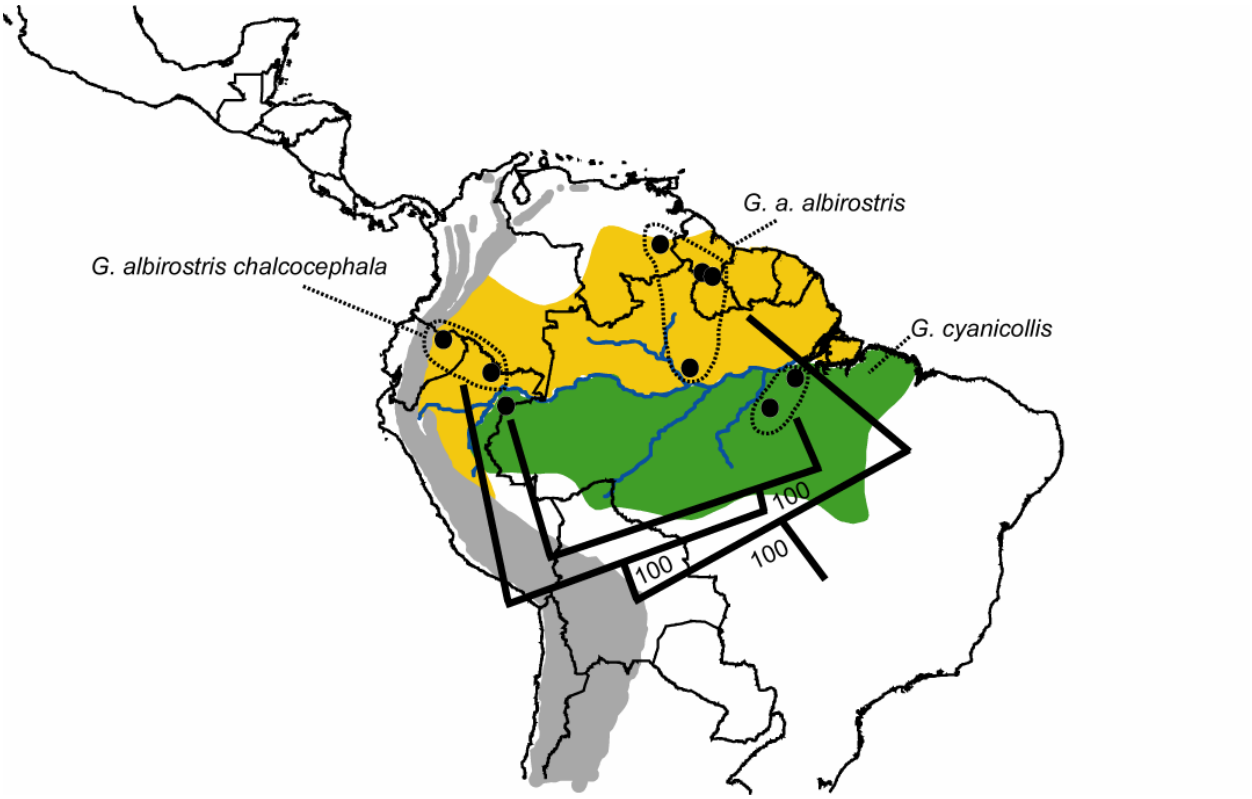

FIGURE 4.20. Phylogeny of geographical replacement populations in the jacamar superspecies comprised by *Galbula albirostris* and *G. cyanicollis*. Numbers at nodes represent posterior probability percentages for Bayesian phylogenetic analysis of the combined mtDNA dataset. Black circles mark sampling localities. The 1000 m elevational contour of the Andes is shaded in gray. Dotted lines encircle identical or near identical haplotypes from different localities.

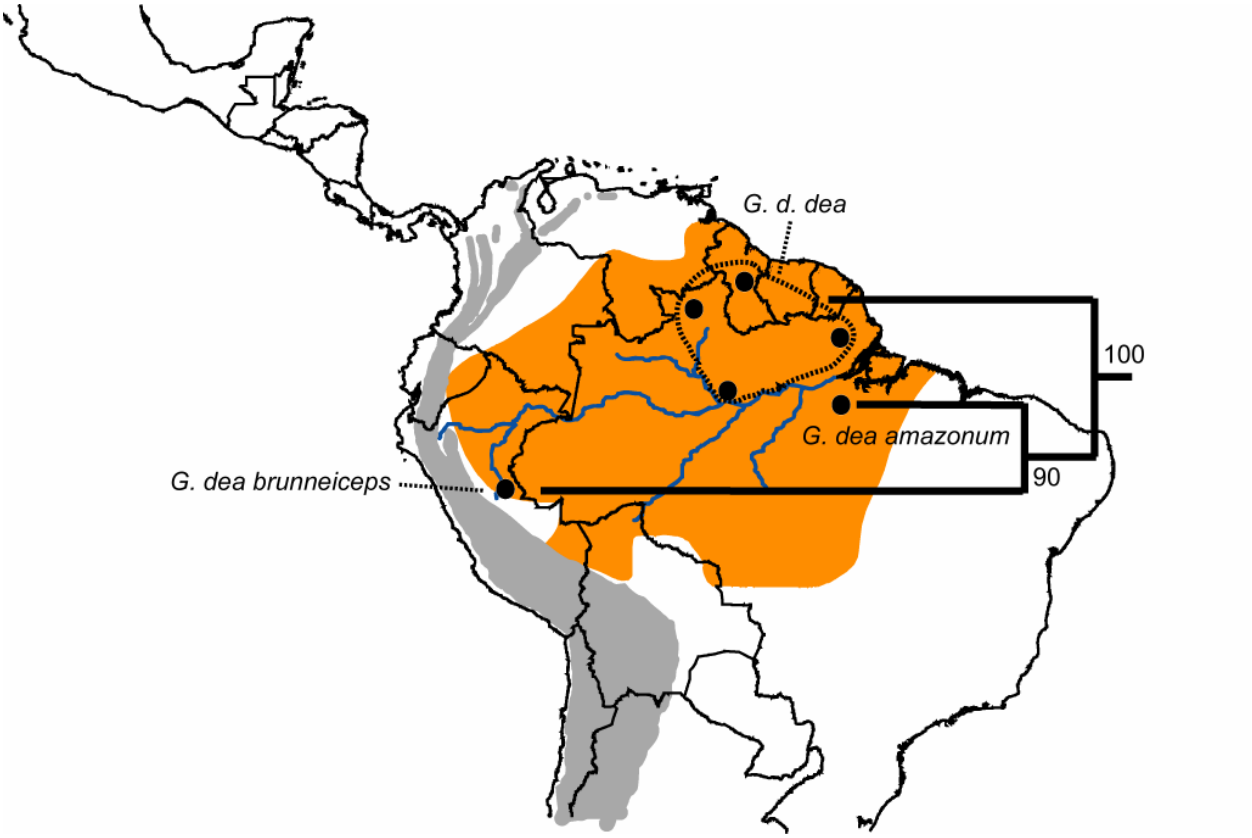

FIGURE 4.21. Phylogeny of geographical replacement populations in the jacamar species *Galbula dea*. Numbers at nodes represent posterior probability percentages for Bayesian phylogenetic analysis of the combined mtDNA dataset. Black circles mark sampling localities. The 1000 m elevational contour of the Andes is shaded in gray. Dotted lines encircle identical or near identical haplotypes from different localities.

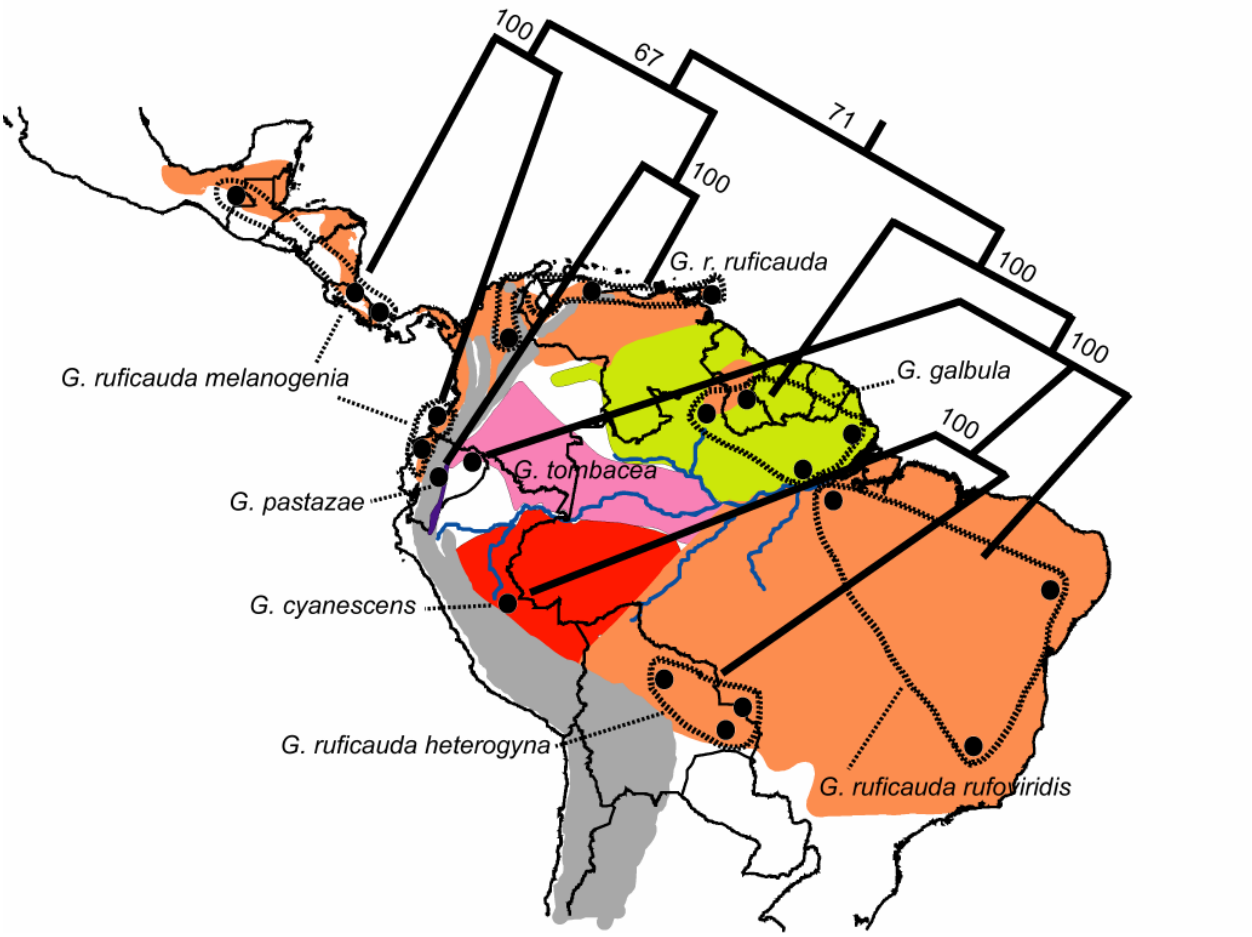

FIGURE 4.22. Phylogeny of geographical replacement populations in the jacamar superspecies comprised by *Galbula galbula*, *G. cyanescens*, *G. ruficauda*, *G. tombacea*, and *G. pastazae*. Numbers at nodes represent posterior probability percentages for Bayesian phylogenetic analysis of the combined mtDNA dataset. Black circles mark sampling localities. The 1000 m elevational contour of the Andes is shaded in gray. Dotted lines encircle identical or near identical haplotypes from different localities.

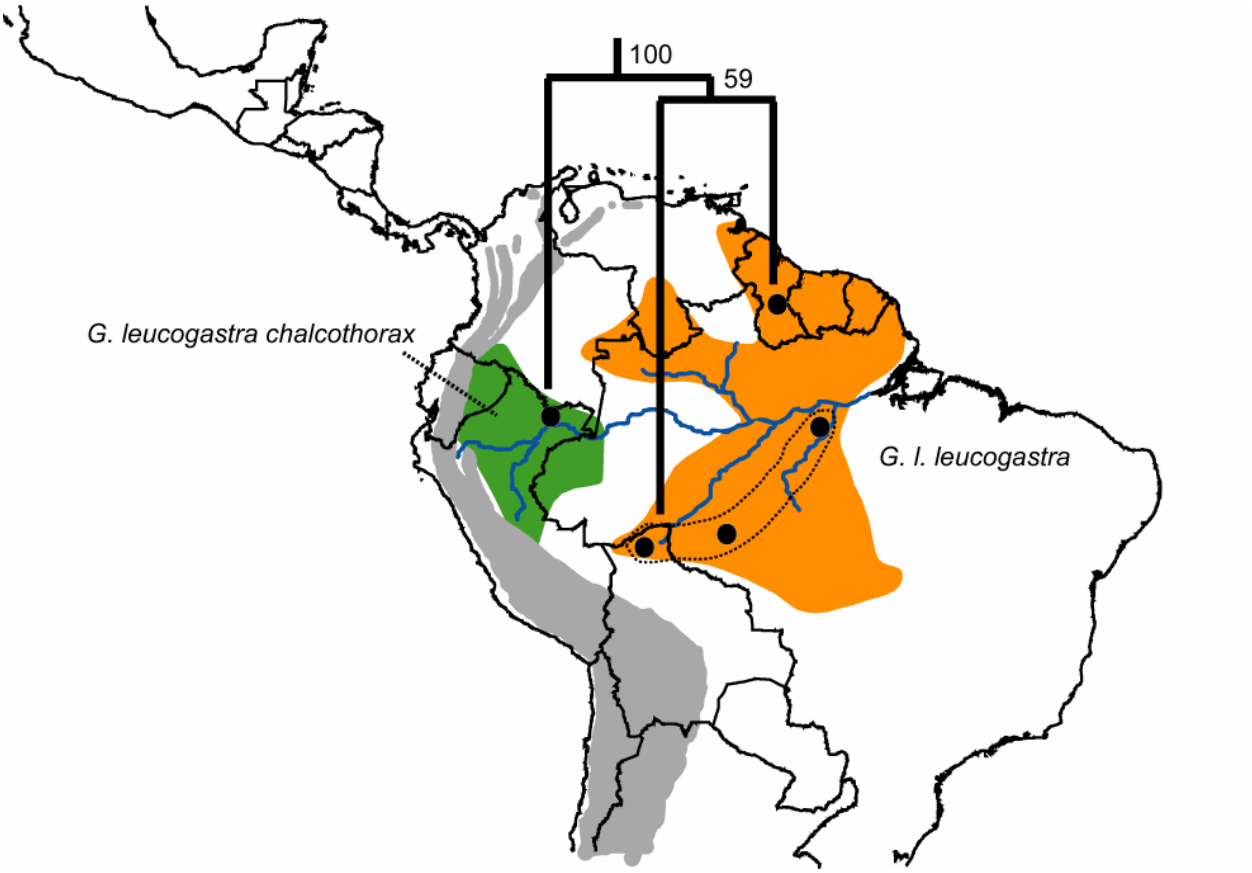

FIGURE 4.23. Phylogeny of geographical replacement populations in the jacamar superspecies comprised by *Galbula leucogastra* and *G. chalcothorax*. Numbers at nodes represent posterior probability percentages for Bayesian phylogenetic analysis of the combined mtDNA dataset. Black circles mark sampling localities. The 1000 m elevational contour of the Andes is shaded in gray. Dotted lines encircle identical or near identical haplotypes from different localities.

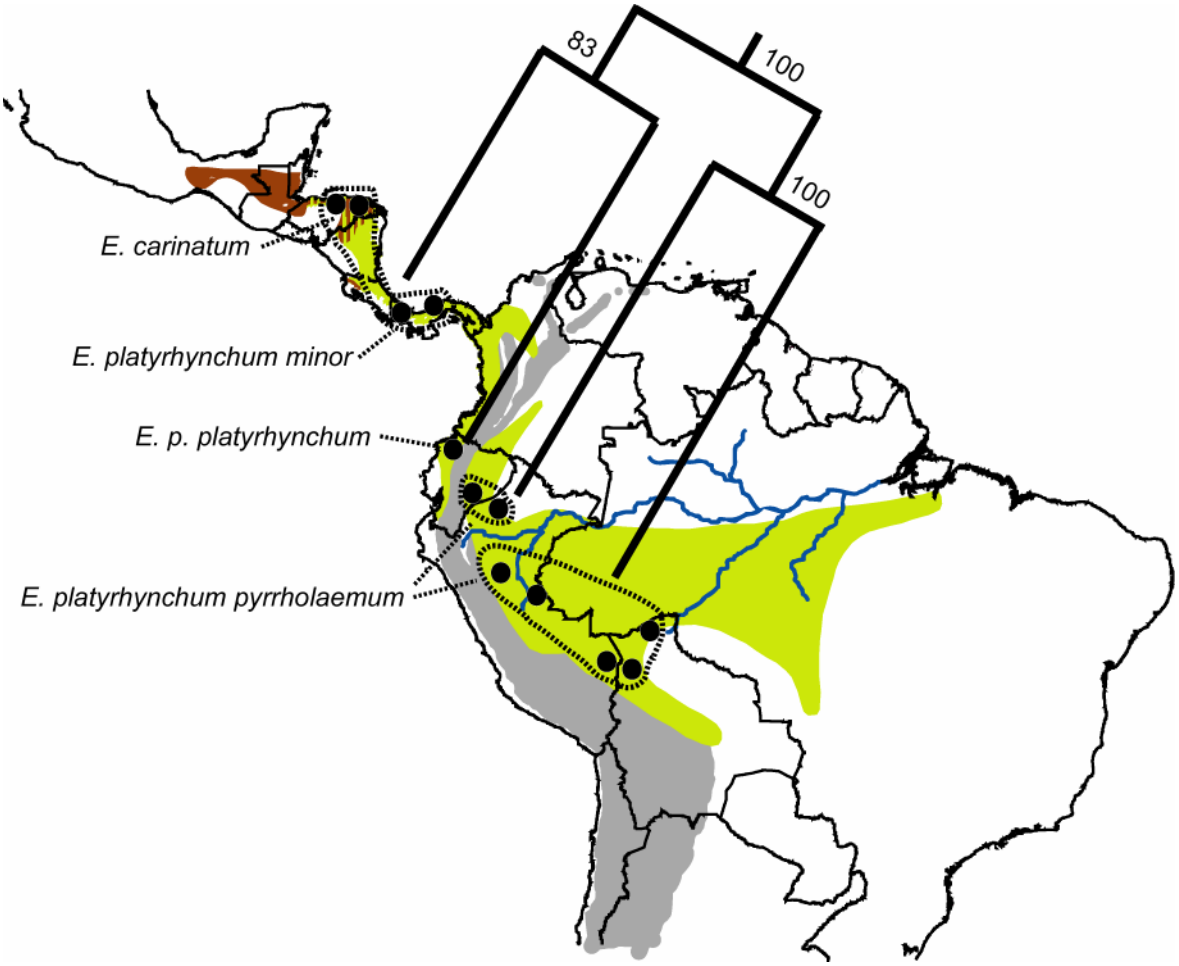

FIGURE 4.24. Phylogeny of geographical replacement populations in the motmot genus *Electron*. Numbers at nodes represent posterior probability percentages for Bayesian phylogenetic analysis of the combined mtDNA dataset. Black circles mark sampling localities. The 1000 m elevational contour of the Andes is shaded in gray. Dotted lines encircle identical or near identical haplotypes from different localities.

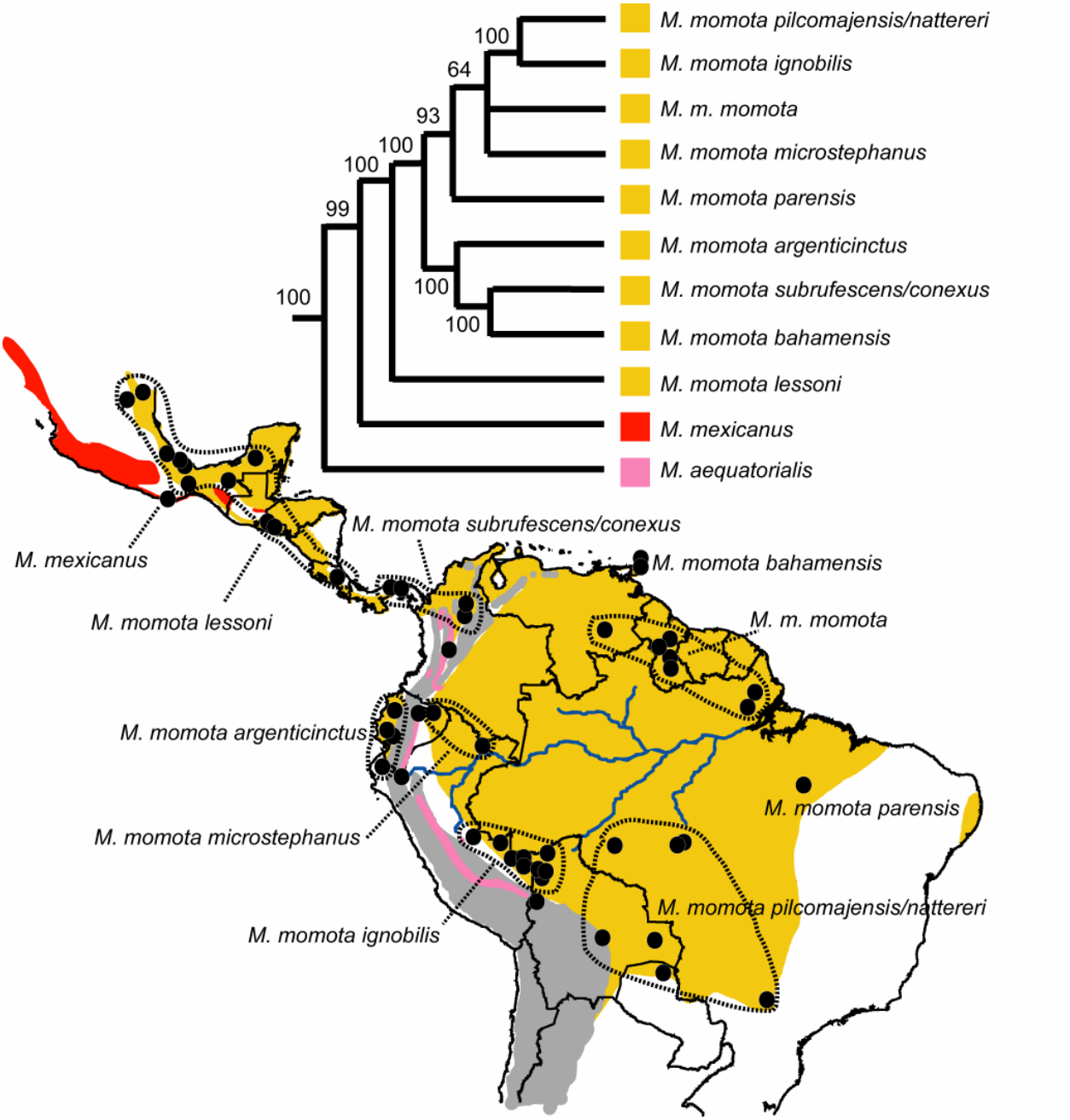

FIGURE 4.25. Phylogeny of geographical replacement populations in the motmot genus *Momotus*. Numbers at nodes represent posterior probability percentages for Bayesian phylogenetic analysis of the combined mtDNA dataset. Black circles mark sampling localities. The 1000 m elevational contour of the Andes is shaded in gray. Dotted lines encircle identical or near identical haplotypes from different localities.

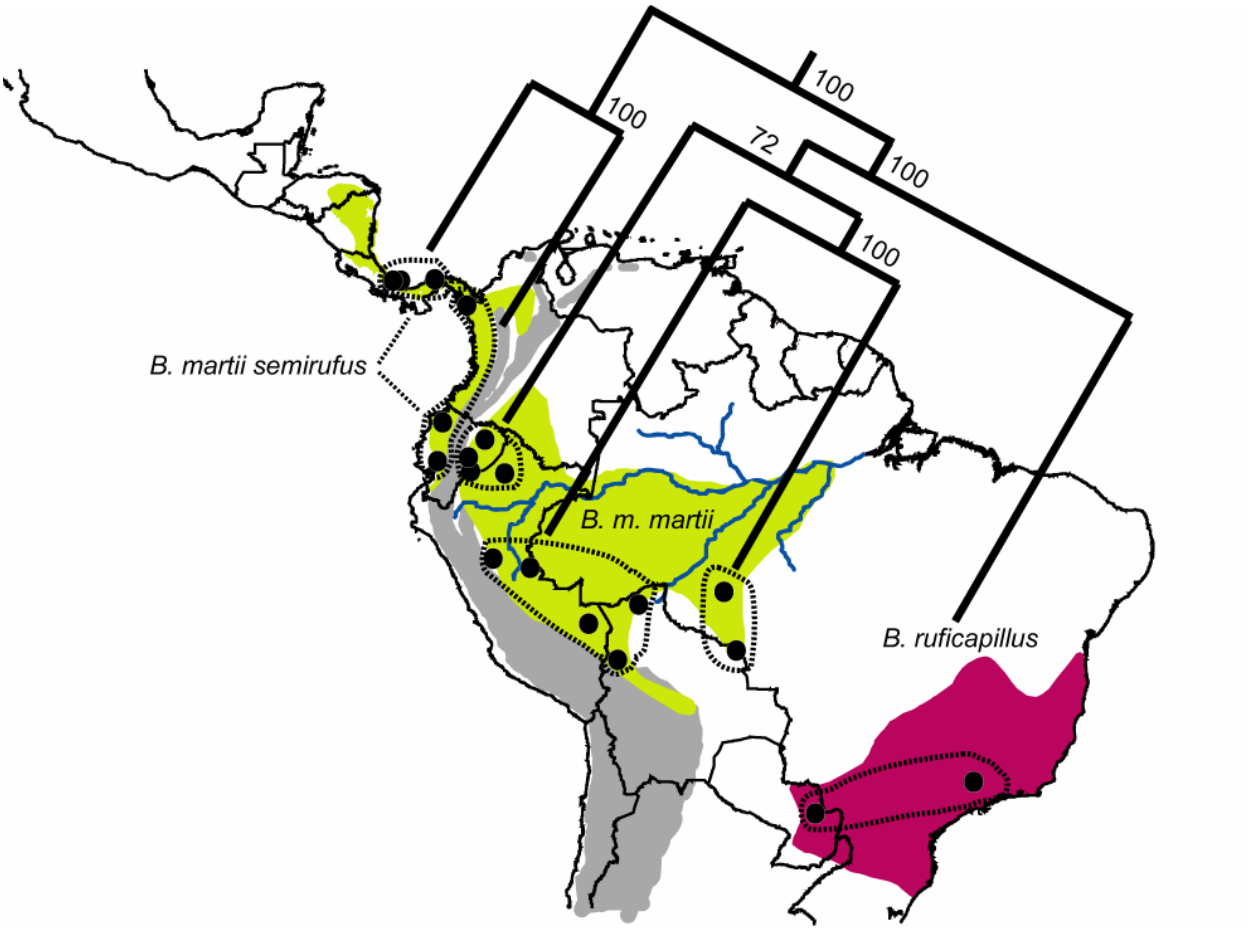

FIGURE 4.26. Phylogeny of geographical replacement populations in the motmot genus *Baryphthengus*. Numbers at nodes represent posterior probability percentages for Bayesian phylogenetic analysis of the combined mtDNA dataset. Black circles mark sampling localities. The 1000 m elevational contour of the Andes is shaded in gray. Dotted lines encircle identical or near identical haplotypes from different localities.

FIGURE 4.27. Area relationships for 19 superspecies groups, with node ages estimated in millions of years. Unlabeled nodes are presumed less than 0.5 Ma.

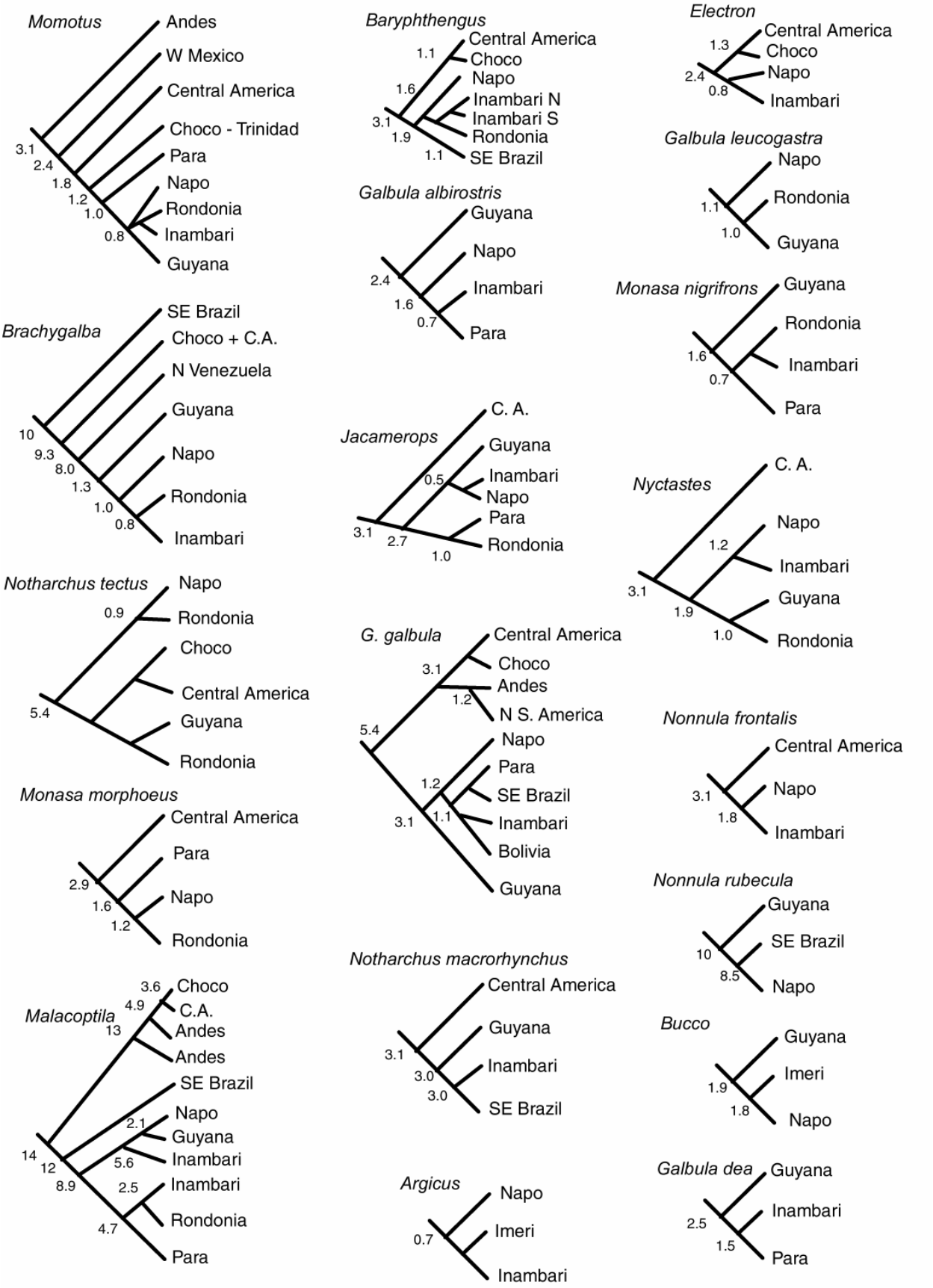
Momotus
Andes
W Mexico
Central America
Choco - Trinidad
Para
Napo
Rondonia
Inambari
Guyana
3.1
2.4
1.8
1.2
1.0
0.8
Brachygalba
SE Brazil
Choco + C.A.
N Venezuela
Guyana
Napo
Rondonia
Inambari
10
9.3
8.0
1.3
1.0
0.8
Notharchus tectus
Napo
Rondonia
Choco
Central America
Guyana
Rondonia
0.9
5.4
Monasa morphoeus
Central America
Para
Napo
Rondonia
2.9
1.6
1.2
Malacoptila
Choco
C.A.
Andes
Andes
SE Brazil
Napo
Guyana
Inambari
Inambari
Rondonia
Para
3.6
4.9
13
2.1
5.6
14
12
8.9
2.5
4.7
Baryphthengus
Central America
Choco
Napo
Inambari N
Inambari S
Rondonia
SE Brazil
1.1
1.6
3.1
1.9
1.1
Galbula albirostris
Guyana
Napo
Inambari
Para
2.4
1.6
0.7
Jacamerops
C. A.
Guyana
Inambari
Napo
Para
Rondonia
0.5
3.1
2.7
1.0
G. galbula
Central America
Choco
Andes
N S. America
Napo
Para
SE Brazil
Inambari
Bolivia
Guyana
3.1
1.2
5.4
1.2
1.1
3.1
Notharchus macrorhynchus
Central America
Guyana
Inambari
SE Brazil
3.1
3.0
3.0
Argicus
Napo
Imeri
Inambari
0.7
Electron
Central America
Choco
Napo
Inambari
1.3
2.4
0.8
Galbula leucogastra
Napo
Rondonia
Guyana
1.1
1.0
Monasa nigrifrons
Guyana
Rondonia
Inambari
Para
1.6
0.7
Nyctastes
C. A.
Napo
Inambari
Guyana
Rondonia
1.2
3.1
1.9
1.0
Nonnula frontalis
Central America
Napo
Inambari
3.1
1.8
Nonnula rubecula
Guyana
SE Brazil
Napo
10
8.5
Bucco
Guyana
Imeri
Napo
1.9
1.8
Galbula dea
Guyana
Inambari
Para
2.5
1.5

TABLE 4.10. Compatibility of area cladograms with previous hypotheses: (A) Central America sister to Chocó; (B) trans-Andes sister to cis-Andes; (C) Guyana sister to Inambari+Napo+Imerí; (D) Guyana sister to rest of cis-Andes; (E) Inambari sister to Napo; (F)Imerí derived; (G) Rondonia derived. Numbers indicate estimated node ages (Ma) for compatible nodes. A dash indicates no information. An asterisk indicates a fixed or constrained node age. "No" indicates that the area cladogram is incompatible with the hypothesis.

Superspecies	A	B	C	D	E	F	G
Argicus	–	–	–	–	no	<0.5	–
Bucco	–	–	1.9	1.9	–	1.8	–
Malacoptila	3.6	14	no	no	no	–	2.5
Monasa morphoeus	–	2.9	–	–	–	–	1.2
Monasa nigrifrons	–	–	no	1.6	–	–	<0.5
Nonnula frontalis	–	3.1*	–	–	1.8	–	–
Nonnula rubecula	–	–	no	10	–	–	–
Notharchus macrorhynchus	–	3.1*	no	3.0	–	–	–
Notharchus tectus	<0.5	no	no	no	–	–	0.9
Nyctastes	–	3.1*	no	no	1.2	–	1.0
Brachygalba	–	9.3	no	1.3	no	–	0.8
Galbula albirostris	–	–	no	2.4	no	–	–
Galbula dea	–	–	no	2.5	–	–	–
Galbula galbula	<0.5	3.1*	no	3.1	no	–	–
Galbula leucogastra	–	–	no	no	–	–	1.0
Jacamerops	–	3.1*	0.5	no	<0.5	–	1.0
Baryphthengus	1.1	3.1*	–	–	no	–	1.1
Electron	1.3	2.4	–	–	0.8	–	–
Momotus	no	1.2	0.8	no	no	–	<0.5

DISCUSSION

Phylogeny and Taxonomy

The phylogeny of the puffbirds highlights a problem with the traditional generic classification in which the genera *Nyctastes* and *Argicus* are included within the genus *Bucco*. *Bucco* capensis is sister to the genus *Nystalus*, well removed from *Nyctastes* and *Argicus*. *Argicus* is sister to the clade containing *Notharchus*, *Nyctastes*, and *Hypnelus*. *Nyctastes* and *Hypnelus* are sister taxa and are sister to or nested within the genus *Notharchus*. The monophyly of the genus *Notharchus* is weakly supported by this analysis. The generic classification in the Handbook of the Birds of

the World is appropriate, which is not surprising given that the authors had knowledge of the preliminary results of this study (Rasmussen and Collar 2002).

The current generic classifications of jacamars and motmots are supported by this study. In motmots, the pattern of serrations on the bill is an accurate indicator of relationship. The three genera with coarse serrations (*Aspatha*, Baryphthengus, and *Momotus*) form a clade, and the two genera with fine serrations (*Eumomota* and *Electron*) form a clade along with *Hylomanes*, whose bill is not serrated. The juvenile-like plumage, small size, and small, unserrated bill of *Hylomanes* suggest neoteny. The motmot topology strongly suggests that the most recent common ancestor of extant motmots possessed a serrated bill and prominent tail raquets, despite that the latter character has been repeatedly lost in subsequent lineages.

The jacamar species *Galbula ruficauda* is comprised of at least two separate species. The northern subspecies *G. r. melanogenia* and *G. r. ruficauda* are widely divergent from the southern *G. r. rufoviridis* and *G. r. heterogyna*. There is a possibility that more species may be involved, considering that the northern and southern G. *ruficauda* would be paraphyletic taxa with respect to *G. pastazae* and *G. cyanescens*, respectively. In the *G. galbula* superspecies, multiple transitions have occurred between white-throated and green throated forms, and a 'leapfrog' pattern of plumage variation has resulted in distantly related northern and southern white-throated forms being lumped into *G. ruficauda*.

The motmot taxon, *Momotus aequatorialis*, is of uncertain taxonomic status, but the results reported herein strongly support its status as a full species. It is basal to a clade containing *Momotus mexicanus* and all other *Momotus* taxa. It represents an early invasion of South America from Central America following the formation of the Central American Landbridge, and its restriction to montane habitats underscores its ecological distinctness.

Many of the cis-Andean and trans-Andean geminate pairs of subspecies should possibly be considered full species, including representatives of *Baryphthengus*, *Electron*, *Notharchus tectus*, *Monasa morphoeus*, and *Jacamerops aureus*. These pairs have probably been isolated for more than two million years and have undergone divergence in plumage and size. In the cases of *Baryphthengus* and *Electron*, apparent speciation within the cis-Andean and trans-Andean regions has occurred subsequent to the termination of dispersal across the Andes.

Rates of Evolution and Timing of Diversification

The degree of concordance between average rates of evolution calibrated using the biogeographic calibration and previous, independent rate estimates was rather remarkable. For puffbirds, the average rate was just under 1.9% divergence per million years. For jacamars and motmots, the average rates were 2.2% and 2.4%, respectively. This compares to rates estimated at 2.1% for geese (Paxinos *et al.* 2002), 1.6 – 1.9% for Hawaiian honeycreepers (Fleischer *et al.* 1998), 0.6 – 4.1% for cranes (Krajewski and King 1996) Use of the fossil calibration for the estimated mid-Oligocene split between todies and motmots did not have a strong effect on the average rate estimate for motmots and was probably too old to be useful for mitochondrial DNA. When the tody versus motmot divergence was left unconstrained its timing was estimated at 21 Ma under the biogeographic calibration alone. The discrepancy is probably a result of saturation. The standard devations generated using bootstrap resampling account for error from the DNA sequences, and provide a measure of the strength and consistency of signal in the data. They do not account for error caused by the calibration point or by violations of the models used to estimate branch lengths and rate transformation across the tree. The calibration point of 3.1 Myr is almost certainly not perfectly accurate. Furthermore, it is impossible to know the degree of genetic subdivision that was already present within populations at the time of the connection

between the continents. For example, in geminate pairs of marine invertebrates separated by the closure of the seaway, many were found to have undergone considerable divergence before 3.1 Ma (Knowlton and Weigt 1998). It is possible that differences in estimated rates between puffbirds, motmots, and jacamars could be entirely attributable to calibration error. Fortunately, the general findings of this study do not depend on precise divergence date estimates.

Neotropical birds of southern and northern origin have experienced a similar overall tempo of diversification. However, the link between the continents and subsequent expansion had a much more profound effect on the motmots which spread extensively and diversified within South America. The abrupt plateau in number of superspecies at 6 million years suggests either that six million years is the typical minimum duration between speciation and ecological coexistence, or, alternatively that ecological communities in Neotropical forests reached saturation at that time.

Area Relationships

The most recent common ancestors of modern superspecies vary in age tremendously, from 14 Ma (*Malacoptila*) to 0.7 m (*Argicus*). Nonetheless, some common patterns emerge that are concordant with previous studies. Most prominent is a sister relationship between Chocó and Central America, a pattern that was documented in detail by Brumfield and Capparella (1996). Rare exceptions to this pattern have been found, and are likely attributable to dispersal around the northern end of the Andes along the Caribbean coast or through the Tachirá gap in Venezuela. The Wedge-billed Woodcreeper (*Glyphorhynchus spirurus*) provides an example in which samples from the Imerí region are nested within a larger Central American clade, indicating a recent dispersal event from the trans-Andean to cis-Andean region that rendered the Chocó and Central American taxa paraphyletic (Marks *et al.* 2002). In the present study, only the

genus *Momotus* did not share the usual Chocó-Central America relationship. In *Momotus*, the Chocó taxon appears to be the result of a second expansion into South America from Central America approximately 1.8 Ma and resulted in two sister clades. One clade is distributed from northwestern Peru, throughout Chocó, eastern Panama, northern Colombia, and around the Caribbean rim to Trinidad and Tobago; the other is the widespread lowland clade found east of the Andes throughout Amazonia, and in the Guyanas, south-central South America, and eastern Brazil. The abberant phylogeographic pattern in *Momotus* is likely a result of it's broader habitat tolerance and its late arrival from Central America that likely followed the final closure of a humid lowland forest corridor between the trans-Andean and cis-Andean regions.

The trans-Andean populations tended to be the basal members of each superspecies complex. The only exception to this pattern was in *Notharchus tectus*, in which a deep split occurred at approximately 5.4 Ma, separating southern and western Amazonia from northeastern Amazonia. The trans-Andean clade is sister to the Guyanan clade, which includes one individual from northern Rondonia, south of the Amazon.

A third pattern confirmed by a plurality of puffbird and jacamar superspecies was the basal relationship of Guyana to other cis-Andean areas. This pattern was proposed by Cracraft and Prum (1988) and Prum (1988) based on cladistic analyses of plumage characters in several lineages of toucans, parrots, manakins, cotingas, and woodpeckers. It has also been found in butterflies (Hall and Harvey 2002). However, the pattern was not confirmed in analyses of area relationships based on cladistic analyses of distribution data for birds (Bates *et al.* 1998) or primates (Silva and Oren 1996), nor was it uncovered in *Glyphorhynchus* (Marks *et al.* 2002). Southeastern Brazil was found to have multiple histories, also in agreement with the findings of Prum (1988).

Another consistent pattern confirmed in this study was the derived position of Rondonia and Imerí areas within Amazonia. Bates (2002) predicted under the 'basal trichotomy' hypothesis that Rondonia and Imerí would have been inundated by a sea-level rise that would have isolated Guyana, the eastern Brazilian Shield, and western Amazonian populations. As a result, Rondonia and Imerí would be occupied with taxa that colonized from an adjacent Amazonian area, and therefore would be of derived phylogenetic position. However, the other predictions of the basal trichotomy hypothesis were not borne out by this study. These include a predicted sister relationship between Napo and Inambari relative to Guyana and Pará, and temporal concordance among divergence levels between Guyana, Pará, and western Amazonian populations. The lack of a consistent close relationship between Napo and Inambari, and the wide variation in temporal scale of divergence between Guyana, Pará, and western Amazonia casts doubt on the importance of a potential 'basal trichotomy', unless perhaps these three regions were isolated in repeated cycles of sea-level change over long periods. Precise geological evidence for the timing and frequency of Amazonian inundation is not yet available (Rasänen 1995; Nores 1999, 2004). The phylogenetic positions of the Napo, Inambari, and Pará regions showed no consistent patterns. The close relationship between the Napo and Inambari that has been found in other studies (Cracraft and Prum 1988, Prum 1988, Bates *et al.* 1998) was contradicted in *Momotus*, *Baryphthengus*, *Malacoptila*, *Argicus*, *Brachygalba*, *Galbula albirostris*, and *Galbula galbula*.

Overall, 19 superspecies showed some phylogenetic concordance with previous studies of Neotropical birds, despite extensive variation in the apparent timing of diversification among areas of endemism. Given the degree of temporal variation, it seems unlikely that any area of endemism has a single history for Neotropical birds. Prum (1988) argued that differences in

topology between superspecies across areas of endemism could be accounted for by differences in dispersal ability. The findings of this study suggest a different role for dispersal. If similar topologies occur at a range of temporal scales, it suggests a role for common patterns of dispersal between adjacent areas, rather than common vicariant events as the mechanism that has generated concordant biogeographic patterns among co-distributed Neotropical birds.

CHAPTER 5: CONCLUSIONS

Understanding the causes of molecular evolutionary rate variation among lineages has proven difficult. Undetectable evolutionary phenomena such as extinction, saturation, and high trait lability can create spurious, misleading patterns that obscure the true causes and consequences of rate variation. Fortunately, refined comparative methods and ever-increasing volumes of empirical data will constantly improve our potential resolving power. In my dissertation, I have demonstrated the importance of using appropriate data and carefully justified methods to identify patterns.

Concepts of evolutionary tempo and, specifically, variation in rates of morphological change are heavily influenced by the theory of punctuated equilibrium (Eldredge and Gould 1972). This theory holds that most evolutionary change accompanies the speciation process and, by extension, that speciation itself drives accelerated change. Recent findings that rate of molecular evolution is linked to rate of speciation (Mindell *et al.* 1989, 1990; Webster *et al.* 2003) suggest a solution to the long standing problem of explaining molecular rate variation among lineages. Furthermore, the enticing possibility exists that rate of molecular change is somehow linked to rate of morphological change (Omland 1997). However, I have demonstrated through phylogenetic simulations that previous findings of a strong link between speciation and molecular evolution reflected an artifact of phylogenetic methods. In future studies, I anticipate developing unbiased tests of molecular punctuated equilibrium by examining closely related species triads and using pairwise distances.

The notion that body size is inversely correlated with evolutionary rate in mtDNA pervades the literature, and the metabolic rate hypothesis provides an explanation for this purported pattern. It posits that fast evolutionary rates occur in organisms that have high mass-

specific metabolic rates and are therefore relatively small in size. However, animals with such large size as elephants and giant tortoises display relatively rapid rates of mtDNA evolution. Thus, an apparent anomaly exists. Chapter 3 demonstrates that there is no such anomaly. A large-scale comparative analysis of mtDNA evolution in birds refutes the widely held idea that metabolic rate drives evolutionary rate. In fact, it demonstrates that a link between large body size and rapid rate of nonsynonymous DNA substitutions may be a general feature of mtDNA evolution. Although this finding is opposite the predictions of the metabolic rate hypothesis, it fits well with existing (but less widely held) theories regarding population size effects and functional constraints, and it may help to explain why some exceptionally large-bodied animals evolve rapidly. The study illuminates the causes of variation in the overall tempo of evolution. It demonstrates that a widely cited hypothesis, and one that has literally become a 'textbook example,' is flawed. Furthermore, it suggests an alternative and theoretically plausible general pattern of mtDNA evolution.

The use of molecular data to date divergence times has been hampered by systematic error as a result of rate variation among lineages. In recent years, a family of methods has been developed that allow rates to vary to a limited degree across adjacent branches of a phylogenetic tree, as would any trait that expresses continuous variation. These include non-parametric rate-smoothing (Sanderson 1997), penalized likelihood (Sanderson 2002), and various other methods (Thorne *et al.* 1998, Huelsenbeck *et al.* 2000). These methods are based on the assumption that closely related lineages are expected to have similar rates of evolution. The degree of lability of molecular evolutionary rate through time and between closely related lineages is difficult to know with certainty because, unlike morphological or behavioral traits, inferred rates represent averages rather than instantaneous character states. However, evidence for 'local' molecular

clocks supports the assumption that rates might evolve gradually between adjacent branches in a tree. These methods seek to overcome rate variation to solve problems of divergence date estimation, but they make no assumptions about the underlying causes of rate variation.

In Chapter 4 of my dissertation, I applied the penalized likelihood method to three molecular datasets for co-distributed clades of Neotropical birds. The result was the establishment of a timescale of diversification for three characteristic components of the Neotropical avifauna. General patterns of biogeography in Neotropical birds have been established using cladistic analysis of distributions and morphological variation, without a robust temporal framework. This study reveals that widespread species complexes have diversified at different timescales, suggesting that exceptional beta diversity in Neotropical birds is a result of multiple cycles of vicariance and dispersal. Previous findings of concordant area relationships among Neotropical birds must be re-evaluated in light of this new evidence of temporal discordance. These findings suggest a reduced role for vicariance relative to dispersal in biogeographic reconstruction.

Better understanding of the causes of variation in rates of molecular evolution will continue to improve methods of divergence date estimation and our understanding of evolutionary forces across geographical space and geological time.

REFERENCES

Adachi, J., Y. Cao, and M. Hasegawa. 1993. Tempo and mode of mitochondrial DNA evolution in vertebrates at the amino acid sequence level: rapid evolution in warm-blooded vertebrates. J. Mol. Evol. 36:270–281.

Arbogast, B. S., S. V. Edwards, J. Wakeley, P. Beerli and J. B. Slowinski. 2002. Estimating divergence times from molecular data on phylogenetic and population genetic timescales. Ann. Rev. Ecol. Syst. 33:707–740.

Avise, J. C. 1977. Is evolution gradual or rectangular? Evidence from living fishes. Proc. Natl. Acad. Sci. USA 74:5083–5087.

Avise, J. C., and F. J. Ayala. 1975. Genetic change and rates of cladogenesis. Genetics 81:757–773.

Avise, J. C., and F. J. Ayala. 1976. Genetic differentiation in speciose versus depauperate phylads: Evidence from the California minnows. Evolution 30:46–58.

Avise, J. C., B. W. Bowen, T. Lamb, A. B. Meylan, and E. Bermingham. 1992. Mitochondrial DNA evolution at a turtle's pace: evidence for low genetic variability and reduced microevolutionary rate in Testudines. Mol. Biol. Evol. 9:457–473.

Barker, F. K., G. F. Barrowclough, and J. G. Groth. 2001. A phylogenetic hypothesis for passerine birds: taxonomic and biogeographic implications of an analysis of nuclear DNA sequence data. Proc. R. Soc. Lond. B 269:295–308.

Barraclough, T. G. and A. P. Vogler. 2000. Detecting the geographical pattern of speciation from species-level phylogenies. Am. Nat. 155:419–434.

Barraclough, T. G. and V. Savolainen. 2001. Evolutionary rates and species diversity in flowering plants. Evolution 55:677–683.

Barraclough, T. G., P. H. Harvey, and S. Nee. 1996. Rate of rbcL gene sequence evolution and species diversification in flowering plants (angiosperms). Proc. R. Soc. Lond. B 263:589–591.

Bates, J. M. 2000. Allozymic genetic structure and natural habitat fragmentation: data for five species of Amazonian forest birds. Condor 102: 770–783.

Bates, J. M. 2002. Avian diversification in Amazonia: evidence for historical complexity and a vicariance model for a basic diversification pattern. Bol. Mus. Para. Emílio Goeldi, Ser. Zoologia.

Bates, J.M., S.J. Hackett, and J. Cracraft. 1998. Area-relationships in the Neotropical lowlands: a hypothesis based on raw distributions of Passerine birds. J. Biogeog. 25:783–793.

Bates, J.M., S.J. Hackett, and J.M. Goerck. 1999. High levels of mitochondrial DNA differentiation in two lineages of Antbirds. (*Drymophila* and *Hypocnemis*). Auk 116:1039–1106.

Beven, S., E. F. Conner, and K. Beven. 1984. Avian biogeography in the Amazon basin and the biological model of diversification. J. Biogeogr. 11: 383–399.

Bolger, P.F. and T.G. Russell. 1983. Late Tertiary marine transgression in the Brisbane Ranges, Victoria (Australia). Proc. Roy. Soc. Vict. 951:25–32.

Bromham, L. 2002. Molecular clocks in reptiles: life history influences rate of molecular evolution. Mol. Biol. Evol. 19:302–309.

Bromham, L., M. Woolfit, M. S. Y. Lee, and A. Rambaut. 2003. Testing the relationship between morphological and molecular rates of change along phylogenies. Evolution 56:1921–1930.

Bromham, L., A. Rambaut, and P. H. Harvey. 1996. Determinants of rate variation in mammalian DNA sequence evolution. J. Mol. Evol. 43:610–621.

Brower, A. V. Z. 2004. Comment on "Molecular phylogenies link rates of evolution and speciation" (II). Science 303:173c.

Brumfield, R.T. and A.P. Capparella. 1996. Historical diversification of birds in northwestern South America: a molecular perspective on the role of vicariant events. Evolution 50:1607–1624.

Burns, K. J., and S. J. Hackett. 2002. Phylogenetic relationships and morphological diversity in Darwin's finches and their relatives. Evolution 56:1240–1252.

Caccone A., G. Gentile, J. P. Gibbs, T. H. Fritts, H. L. Snell, J. Betts, and J. R. Powell. 2002. Phylogeography and history of giant Galápagos tortoises. Evolution 56:2052–2066.

Calder, W. A., III. 1984. Size, Function, and Life History. Harvard Univ. Press, Cambridge, MA.

Cantatore, P. *et al.* 1994. Evolutionary analysis of cytochrome b sequences in some Perciformes: Evidence for a slower rate of evolution than in mammals, J. Mol. Evol. 39:589–597.

Capparella, A. P. 1988. Genetic variation in Neotropical birds: implications for the speciation process. In: H. Quellet (Ed.), Acta XIX Congressus Internationalis Ornithologici. XIX Internat. Ornithol. Congress, Ottawa, pp.2562–2572.

Capparella. A.P. 1988. Genetic variation in tropical birds: implications for the speciation process. Acta XIX Congr. Int. Ornithol. 19:1658–1673.

Cavers, S., C. Navarro, and A. J. Lowe. Chloroplast DNA phylogeography reveals colonization history of a Neotropical tree, *Cedrela odorata*, L., in Mesoamerica. Mol. Ecol. 12:1451–1460.

Chesser, R. T. 1999. Molecular systematics of the rhinocryptid genus Pteroptochos. Condor 101: 439-446.

Chiba, S. 1999. Accelerated evolution of land snails Mandarina in the oceanic Bonin Islands: evidence from mitochondrial DNA sequences. Evolution 53:460–471.

Coates, A. G., And J. A. Obando. 1996. The geologic evolution of the Central American isthmus. Pp. 21–56 in J. B. C. Jackson, A. F. Budd, and A. G. Coates, eds. Evolution and environment in tropical America. Univ. Chicago Press, Chicago.

Cooper A., *et al.* 2001. Complete mitochondrial genome sequences of two extinct moas clarify ratite evolution. Nature 409:704–707.

Cortés-Ortíz, L, E. Bermingham, C. Rico, E. Rodríguez-Luna, I. Sampaio and M. Ruiz-García. 2003. Molecular systematics and biogeography of the Neotropical monkey genus *Alouatta*. Mol. Phylogenet. Evol. 26:64–81.

Cracraft, J. 1985. Historical biogeography and patterns of differentiation within the South American areas of endemism. Ornithol. Monogr. 36: 49–84.

Cracraft, J. and R.O. Prum. 1988. Patterns and processes of diversification: speciation and historical congruence in some Neotropical birds. Evolution 42(3):603–620.

Cubo, J. 2003. Evidence for speciational change in the evolution of ratites (Aves: Paleognathae). Biol. J. Linn. Soc. 80:99–106.

del Hoyo, J., *et al.*, Eds. 1992. The Handbook of the Birds of the World. Lynx Edicions, Barcelona.

Dick, C. W., K. Abdul-Salim, and E. Bermingham. 2003. Molecular systematic analysis reveals cryptic Tertiary diversification of a widespread tropical rain forest tree. Am. Nat. 162:691–703.

Dickinson, E. C. 2003. The Howard and Moore Complete Checklist of the Birds of the World, 3rd Edition. Princeton Univ. Press, Princeton, NJ.

Donoghue, M. J., and B. R. Moore. 2003. Toward an integrative historical biogeography. Integr. Comp. Biol. 43:261–270.

Dunning, J. B. 1993. CRC Handbook of Avian Body Masses CRC, Boca Raton, FL.

Eldredge, N., and S. J. Gould. 1972. Punctuated equilibria: An alternative to phyletic gradualism. Pages 82–155 in Models in paleobiology (T. J. M. Shopf, ed.). Freeman Cooper and Co., San Francisco.

Fay, J. C., and Wu, C.-I. 2000. Hitchhiking Under Positive Darwinian Selection. Genetics 155:1405–1413.

Felsenstein, J. 1978. Cases in which parsimony or compatibility methods will be positively misleading. Syst. Zool. 27:401–410.

Fitch, W. M., and J. J. Beintema. 1990. Correcting parsimonious trees for unseen nucleotide substitutions: the effect of dense branching as exemplified by ribonuclease. Mol. Biol. Evol. 7:438–443.

Fitch, W. M., and M. Bruschi. 1987. The evolution of prokaryotic ferredoxins—with a general method correcting for unobserved substitutions in less branched lineages. Mol. Biol. Evol. 4:381–394.

Fleischer, R.C., C.E. McIntosh, and C.L. Tarr. 1998. Evolution on a volcanic conveyor belt: using phylogeographic reconstructions and K-Ar based ages of the Hawaiian Islands to estimate molecular evolutionary rates. Mol. Ecol. 7:533–545.

Furness, R. W. 1987. The Skuas. Poyser, Calton, U.K.

Gascon, C., J.R. Malcom, J.L. Patton, M.N.F. da Silva, J.P. Bogart, S.C. Lougheed, C.A. Peres, S. Neckel, and P.T. Boag. 2000. Riverine barriers and the geographic distribution of Amazonian species. Proc. Natl. Acad. Sci. USA 97:13672–13677.

Gaut, B. S., B. R. Morton, B. C. McCaig, and M. T. Clegg. 1996. Substitution rate comparisons between grasses and palms: synonymous rate differences at the nuclear gene Adh parallel rate differences at the plastid gene rbcL. Proc. Natl. Acad. Sci U.S.A. 93:10274–10279.

Gissi, C., A. Reyes, G. Pesole, and C. Saccone. 2000. Lineage-specific evolutionary rate in mammalian mtDNA. Mol. Biol. Evol. 17:1022–1031.

Goodman, M., G. W. Moore, J. Barnabas, and G. Matsuda. 1974. The phylogeny of human hemoglobin genes investigated by the maximum parsimony method. J. Mol. Evol. 3:1–48.

Gould, S. J. 2002. The Structure of Evolutionary Theory. Harvard University Press, Cambridge, MA.

Gould, S. J., and N. Eldredge. 1977. Punctuated equilibria: The tempo and mode of evolution reconsidered. Paleobiology 3:115–151.

Gould, S. J., and N. Eldredge. 1993. Punctuated equilibrium comes of age. Nature 366:223–227.

Graybeal A. 1998. Is it better to add taxa or characters to a difficult phylogenetic problem? Systematic Biology 47:9–17.

Groth, J. G., and G. F. Barrowclough. 1999. Basal divergences in birds and the phylogenetic utility of the nuclear RAG-1 gene. Mol. Phylogenet. Evol. 12:115–123.

Hackett, S.J. 1996. Molecular phylogenetics and biogeography of tanagers in the genus *Ramphocelus* (Aves). Mol. Phylo. Evol. 5:368–382.

Haffer, J. 1969. Speciation in Amazonian forest birds. Science 165:131–137.

Haffer, J. 1974. Avian Speciation in Tropical South America. Nuttall Ornithological Club, Cambridge.

Haffer, J. 1997. Alternative models of vertebrate speciation in Amazonia: an overview. Biodiversity and Conservation. 6:451–476.

Hafner, M. S., *et al.* 1994. Disparate rates of molecular evolution in cospeciating hosts and parasites. Science 265:1087–1090.

Hall, J. P. W., and D. J. Harvey. 2002. The phylogeography of Amazonia revisited: new evidence from riodinid butterflies. Evolution 56:1489–1497.

Haq, B., Hardenbol, J., and P. R. Vail. 1987. Chronology of fluctuating sea levels since the Triassic. Science 235: 1156–1167.

Haq, B., J. Hardenbol, and P. R. Vail. 1987. Chronology of fluctuating sea levels since the Triassic. Science 235: 1156–1167.

Harrison, R. G. 1991. Molecular changes at speciation. Annu. Rev. Ecol. Syst. 22:281–308.

Hauf, J., P. J. Waddell, N. Chalwatzis, U. Joger, and F. K. Zimmermann. 1999. The complete mitochondrial genome sequence of the African elephant (*Loxodonta africana*), phylogenetic relationships of Proboscidea to other mammals, and D-loop heteroplasmy. Zoology 102:184–195.

Helmens, K. F. and T. van der Hammen. 1994. The Pliocene and Quaternary of the high plain of Bogotá (Colombia): A history of tectonic uplift, basin development and climatic change. Quaternary Int. 21:41–61.

Hillis, D. M., D. D. Pollock, J. A. McGuire, and D. J. Zwickl. 2003. Is sparse taxon sampling a problem for phylogenetic inference? Syst. Biol. 52:124–126.

Hoffman, F. G., and R. J. Baker. 2003. Comparative phylgeography of short-tailed bats (*Carollia*: Phyllostomidae). Mol. Ecol. 12: 3403–3414.

Hoorn, C. 1996. Technical comments: Miocene deposits in the Amazonian foreland basin. Science 273: 122.

Huelsenbeck and Ronquist 2001. MRBAYES: Baysian inference of phylogeny. Bioinformatics 17:754–755.

Huelsenbeck J. P., B. Larget, D. Swofford, 2000. A compound Poisson process for relaxing the molecular clock Genetics 154:1879–1892.

Huelsenbeck, J. P., and K. A. Crandall. 1997. Phylogeny estimation and hypothesis testing using maximum likelihood. Annu. Rev. Ecol. Syst. 28: 437–466.

Irestedt, M., U. S. Johansson, T. J. Parsons, and P. G. P. Ericson. 2001. Phylogeny of major lineages of suboscines (Passeriformes) analysed by nuclear DNA sequence data. J. Avian Biol. 32:15–25.

Jennings, W. B., E. R. Pianka, and S. Donnellan. 2003. Systematics of the lizard family Pygopodidae with implications for the diversification of Australian temperate biotas. Systematic Biology 52:757–780.

Jobson, R. W., and V. A. Albert. 2002. Molecular rates parallel diversification contrasts between carnivorous plant sister lineages. Cladistics 18:127–136.

Johansson, U. S. and Ericson, P. G. P. 2003. Molecular support for a sister group relationship between Pici and Galbulae (Piciformes *sensu* Wetmore 1960). J. Avian Biol. 34: 185–197.

Johnson, K. P. and J. Seger. 2001. Elevated rates of nonsynonymous substitution in island birds. Mol. Biol. Evol. 18:874–881.

Keigwin, L. D. 1982. Isotopic paleooceanography of the Caribbean and east Pacific: role of Panama uplift in late Neogene time. Science 217:350–352.

Kimura, M. 1983. The Neutral Theory of Molecular Evolution. Cambridge Univ. Press, Cambridge, U.K.

Knowlton, N., and L. A. Weigt. 1998. New dates and new rates for divergence across the Isthmus of Panama. Proc. R. Soc. Lond. Ser. B. Biol. Sci. 265:2257–2263.

Kocher, T.D., W.K. Wilson, A. Meyer, S.V. Edwards, S. Pääbo, F.X. Villablanca and A.K. Wilson. 1989. Dynamics of mitochondrial DNA evolution in animals: amplification and sequencing with conserved primers. Proc. Natl. Acad. Sci. USA 86:6196–6200.

Krabbe, N., *et al.* 1999. A new species of antpitta Formicariidae: *Grallaria* from the southern Ecuadorian Andes. Auk 116:882–890.

Krajewski, C., and D. G. King. 1996. Molecular divergence and phylogeny: Rates and patterns of cytochrome *b* evolution in cranes. Mol. Biol. Evol. 13:21–30.

Kubo, T., and Y. Iwasa. 1995. Inferring the rates of branching and extinction from molecular phylogenies. Evolution 49:694–704.

Kumar, S., K. Tamura, I. B. Jakobsen, and M. Nei. 2001. MEGA2: molecular evolutionary genetics analysis software. Bioinformatics 17:1244–1245.

Legendre, S., J. Clobert, and A. P. Møller. 1999. Demographic stochasticity and social mating system in the process of extinction of small populations: the case of passerines introduced to New Zealand. American Naturalist 153:449–463.

Levinton, J. S. 2001. Genetics, Paleontology, and Macroevolution. 2nd ed. Cambridge University Press, NY.

Lovejoy, N.; Bermingham, R.E. & Martin, A.P. 1998. Marine incursions into South America. Nature 396: 421–422.

Lovette, I. 2004. Mitochondrial dating and mixed support for the "2% rule" in birds. Auk 121:1–6.

Marko, P. B. 2002. Fossil calibration of molecular clocks and the divergence times of geminate species pairs separated by the Isthmus of Panama. Mol. Biol Evol. 19:2005–2021.

Marks, B.D., S.J. Hackett, and A.P. Capparella. 2002. Historical relationships among Neotropical lowland forest areas of endemism as inferred from mitochondrial DNA sequence variation within the Wedge-billed Woodcreeper (Aves: Dendrocolaptidae: *Glyphorhynchus spirurus*. Mol. Phylo. Evol. 24:155–167.

Marshall, L.G., and J. G. Lundberg. 1996. Technical comments: Miocene deposits in the Amazonian foreland basin. Science 273: 123–124.

Martin, A. P. 1995. Metabolic rate and directional nucleotide substitution in animal mitochondrial DNA. Mol. Biol. Evol. 12:1124–1131.

Martin, A. P. 1999. Substitution rates of organelle and nuclear genes in sharks: implicating metabolic rate (again). Mol. Biol. Evol. 16:996–1002.

Martin, A. P. and S. R. Palumbi. 1993. Body size, metabolic rate, generation time and the molecular clock. Proc. Natl. Acad. Sci. U.S.A. 90:4087–4091.

Martin, A. P., G. J. P. Naylor, and S. R. Palumbi. 1992. Rate of mitochondrial DNA evolution is slow in sharks compared to mammals. Nature 357:153–155.

Martins, E. P. 1994. Estimating the rate of phenotypic evolution from comparative data. Am. Nat. 144:193–209.

Mayden, R. L. 1986. Speciose and depauperate phylads and tests of punctuated and gradual evolution: fact or artifact? Syst. Zool. 35:591–602.

Mayr, E. 1954. Changes of genetic environment and evolution. In "Evolution as a Process" (J. Huxley, A. C. Hardy, and E. B. Ford, Eds.), pp. 157–180. Allen and Unwin, London.

Mayr, E. 1963. Animal Species and Evolution. Harvard Univ. Press, Cambridge, MA.

Mindell, D. P., A. Knight, C. Baer, and C. J. Huddleston. 1996. Slow rates of molecular evolution in birds and the metabolic rate and body temperature hypotheses. Mol. Biol. Evol. 13:422–426.

Mindell, D. P., J. W. Sites, and D. Graur. 1989. Speciational evolution: A phylogenetic test with allozymes in Sceloporus (Reptilia). Cladistics 5:49–61.

Mindell, D. P., J. W. Sites, and D. Graur. 1990. Mode of allozyme evolution: increased genetic distance associated with speciation events. J. Evol. Biol. 3:125–131.

Mindell, D. P., J. W. Sites, and D. Graur. 1991. Assessing the relationship between speciation and evolutionary change. Cladistics 6:393–398.

Mooers, A. Ø., and P. H. Harvey. 1994. Metabolic rate, generation time, and the rate of molecular evolution in birds. Mol. Phylogenet. Evol. 3:344–350.

Moore, G. W. 1977. Proof of the populous path algorithm for missing mutations in parsimony trees. J. Theor. Biol. 66:95–106.

Moore, G. W., M. Goodman, C. Callahan, R. Holmquist, and H. Moise. 1976. Stochastic versus augmented maximum parsimony method for estimating superimposed mutations in the divergent evolution of protein sequences. J. Molec. Biol. 105:15–37.

Murphy, R. W., and N. R. Lovejoy. 1998. Punctuated equilibrium or gradualism in the lizard genus Sceloporus? Lost in plesiograms and a forest of trees. Cladistics 14:95–103.

Nee S., E. C. Holmes, R. M. May, and P. H. Harvey, 1994 Extinction rates can be estimated from molecular phylogenies Philos. Trans. R. Soc. Lond. B 344:77–82.

Nelson, G. and P. Y. Ladiges. 1996. Paralogy in cladistic biogeography and analysis of paralogy-free subtrees. Am. Mus. Novit. 3167:1–58.

Nores, M. 1999. An alternative hypothesis for the origin of Amazonian bird diversity. J. Biogeog. 26:475–485.

Nores, M. 2004. The implications of Tertiary and Quaternary sea level rise events for avian distribution patterns in the lowlands of northern South America. Glob. Ecol. Biogeog. 13:149–161.

Nunn, G. B., and S. E. Stanley. 1998. Body size effects and rates of cytochrome b evolution in tube-nosed seabirds. Mol. Biol. Evol. 15:1360–1371.

Ohta, T. 1992. The nearly neutral theory of molecular evolution. Annu. Rev. Ecol. Syst. 23:263–286.

Ohta, T. 1995. Synonymous and nonsynonymous substitutions in mammalian genes and the nearly neutral theory, J. Mol. Evol. 40, 56–63.

Omland, K. E. 1997. Correlated rates of molecular and morphological evolution. Evolution 51:1381–1393.

Omland, K.E., S.M. Lanyon, and S.J. Fritz. 1999. A molecular phylogeny of the New World orioles (*Icterus*): the importance of dense taxon sampling. Mol. Phylogenet. Evol. 12: 224–239.

Orr, H. A. 1995. The population genetics of speciation: the evolution of hybrid incompatibilities. Genetics 139:1805–1813.

Page, R. D. M., and E. C. Holmes. 1998. Molecular Evolution: A Phylogenetic Approach. Blackwell, Oxford, U. K.

Pagel, M. 1997. Inferring evolutionary processes from phylogenies. Zoologica Scripta 26:331–348.

Pagel, M. 1999. Inferring the historical patterns of biological evolution. Nature 401:877–884.

Paton, T., O. Haddrath, and A. J. Baker. 2002. Complete mitochondrial DNA genome sequences show that modern birds are not descended from transitional shorebirds. Proc. R. Soc. Lond. B 269:839–846.

Patton, J. L., and M. N. F. da Silva. 1998. Rivers, refuges, and ridges: the geography of speciation of Amazonian mammals. Pages 202–213 *in* Endless forms: species and speciation (D. J. Howard and S. H. Berlocher, Eds.). Oxford University Press, Oxford, England.

Patton, J. L., Silva, M. N. F., and J. R. Malcolm. 2000. Mammals of the Rio Juruá and the evolutionary and ecological diversification of Amazonia. Bull. Amer. Mus. Nat. Hist. 244: 1–306.

Paxinos, E. E., H. F. James, S. L. Olson, M. D. Sorenson, J. Jackson, and R. C. Fleischer. 2002. MtDNA from fossils reveals a radiation of Hawaiian geese recently derived from the Canada Goose (*Branta Canadensis*). Proc. Natl. Acad. Sci. U.S.A. 99:1399–1404.

Paxton, C.G.M.; Crampton, W.G.R. & Burgess, P. 1996. Technical comments: Miocene deposits in the Amazonian foreland basin. Science 273:123–124.

Pearson, P. N. 1999. Apomorphy distribution is an important aspect of cladogram symmetry. Syst. Biol. 48:399–406.

Pergams, O. R. W., and M. V. Ashley. 2001. Microevolution in island rodents. Genetica 112–113: 245–256.

Posada, D. & Crandall, K. A. 1998. MODELTEST: testing the model of DNA substitution. Bioinformatics 14:817–818.

Prance, G. T., ed. 1982. Biological diversification in the tropics. Columbia Univ. Press, New York.

Prum, R.O. 1988. Historical relationships among avian forest area of endemism in the Neotropics. Acta XIX Congr. Inter. Ornithol. 19:2562–2572.

Prychitko, T. M., and W. S. Moore. 1997. The utility of DNA sequences of an intron from the ß-fibrinogen gene in phylogenetic analysis of woodpeckers (Aves: Picidae). Mol. Phylogenet. Evol. 8:193-204.

Rambaut A., and N. C. Grassly. 1997. Seq-Gen: an application for the Monte Carlo simulation of DNA sequence evolution along phylogenetic trees. Comput. Appl. Biosci. 13:235–238.

Rambaut, A. 2002. Phyl-o-gen: Phylogenetic Tree Simulator Package. Version 1.1. Department of Zoology, University of Oxford.

Rambaut, A. and L. Bromham. 1998. Estimating divergence dates from molecular sequences. Mol. Biol. Evol. 15:442–448.

Rand, D. M. 1994. Thermal habit, metabolic rate and the evolution of mitochondrial DNA. TREE 9:125–131.

Rand, D. M. 2001. The units of selection on mitochondrial DNA. Annu. Rev. Ecol. Syst. 32: 415–448.

Räsänen, M. E., Linna, A. M., Santos, J. C. R., and F. R. Negri. 1995. Late Miocene tidal deposits in the Amazonian foreland basin. Science 269: 386–390. 120

Rasmussen, P. C. and N. J. Collar. 2002. Family Bucconidae (Puffbirds). Pp. 102–138 in del Hoyo, J., A. Elliot, and J. Sargatal, eds. Handbook of the Birds of the World. Vol. 7. Jacamars to Woodpeckers. Lynx Edicions, Barcelona.

Refinetti, R. 1999. Amplitude of the daily rhythm of body temperature in eleven mammalian species. J. Therm. Biol. 24:477–481.

Remsen, J. V., Jr., M. A. Hyde and A. Chapman. 1993. Diets of Neotropical trogons, motmots, barbets and toucans. Condor 95:178–192.

Ridgely, R.S., T.F. Allnutt, T. Brooks, D.K. McNicol, D.W. Mehlman, B.E. Young, and J.R. Zook. 2003. Digital Distribution Maps of the Birds of the Western Hemisphere, version 1.0. NatureServe, Arlington, Virginia, USA.

Ronquist, F. 1996. DIVA version 1.1. Computer program and manual available by anonymous FTP from Uppsala University (ftp.uu.se or ftp.systbot.uu.se).

Rowe, D. L., and R. L. Honeycutt. 2002. Phylogenetic relationships, ecological correlates, and molecular evolution within the Cavioidea (Mammalia, Rodentia). Mol. Biol. Evol. 19: 263–277.

Sanderson M. J., 1997 A nonparametric approach to estimating divergence times in the absence of rate constancy Mol. Biol. Evol 14:1218–1231.

Sanderson, M. J. 2002. Estimating absolute rates of molecular evolution and divergence times: a penalized likelihood approach. Mol. Biol. Evol. 19:101–109.

Sanderson. M. 1990. Estimating rates of speciation and evolution: a bias due to homoplasy. Cladistics 6:387–391.

Savolainen, V., and J. Goudet. 1998. Rate of gene sequence evolution and species diversification in flowering plants: a re-evaluation. Proc. R. Soc. Lond. B 265:603–607.

Shapiro, L. H., and J. P. Dumbacher. 2001. Adenylate kinase intron 5: A new nuclear locus for avian systematics. Auk 118:248-255.

Sheldon, F.H., C.E. Jones, and K.G. McCracken. 2000. Relative patterns and rates of evolution in heron nuclear and mitochondrial DNA. Mol. Biol. Evol. 17:437–450.

Shields, G. F. and A. C. Wilson. 1987. Calibration of mitochondrial DNA evolution in geese. J. Mol. Evol. 24:212–217.

Shigenaga, M. K., C. J. Gimeno, and B. N. Ames. 1989. Urinary 8 hydroxy-2'-deoxyguanosine as a biological marker of in-vivo oxydative DNA damage. Proc. Natl. Acad. Sci. U.S.A. 86: 9697–9701.

Sibley, C. G., and B. L. Monroe. 1990. Distribution and Taxonomy of Birds of the World. Yale Univ. Press, New Haven, CT.

Sibley, C. G., and J. A. Ahlquist. 1990. Phylogeny and Classification of Birds: A Study in Molecular Evolution. Yale Univ. Press, New Haven, CT.

Silva, J. M. C., and Oren, D. C. 1996. Application of the parsimony analysis of endemicity in Amazonian biogeography: an example with primates. Biol. J. Linn. Soc. 58: 427–437.

Silva, M. N., and J. L. Patton. 1998. Molecular phylogeography and the evolution and conservation of Amazonian mammals. Mol. Ecol. 7: 475–486.

Slowinski, J. B., and B. S. Arbogast. 1999. Is the rate of molecular evolution inversely related to body size? Syst. Biol. 48:396–399.

Sorenson, M. D., and R. B. Payne. 2001. A single ancient origin of brood parasitism in African finches: Implications for host-parasite coevolution. Evolution 55:2550–2567.

Stotz, D. F., J. W. Fitzpatrick, T. A. Parker III, and D. B. Moskovits. 1996. Neotropical birds: ecology and conservation. University of Chicago Press, Chicago.

Swofford D. L., 2001 PAUP*: phylogenetic analysis using parsimony (*and Other Methods) Sinauer Associates, Sunderland, Mass

Swofford, D. L. 2002. PAUP*. Phylogenetic analysis using with parsimony (* and other methods). Version 4.0b10. Sinauer, Sunderland, Massachusetts.

Swofford, D. L. PAUP*: 2000. Phylogenetic Analysis Using Parsimony (*and Other Methods). Sinauer, Sunderland, MA, version 4.

Swofford, D. L., G. J. Olsen, P. J. Waddell, and D. M. Hillis. 1996. Phylogenetic inference. In: D. M. Hillis, C. Moritz and B. K. Mable, (Eds.), Molecular Systematics. Sinauer Associates, Sunderland, MA, pp. 407–514.

Tarr, C. L. and R. C. Fleischer. 1993. Mitochondrial DNA variation and evolutionary relationships in the Amakihi complex. Auk 110:825–831.

Thorne J. L., H. Kishino, I. S. Painter, 1998 Estimating the rate of evolution of the rate of molecular evolution Mol. Biol. Evol 15:1647–1657.

Van der Hammen, T., and H. Hooghiemstra. 2000. Neogene and Quaternary history of vegetation, and plant diversity in Amazonia. Quaternary Sci. Rev. 19: 725–742.

Van der Hammen, T., and M. L. Absy. 1994. Amazonia during the last glacial. Paleogeogr. Paleoclimat. Paleoecol. 109: 247–261.

Van Tuinen, M., C. G. Sibley, and S. B. Hedges. 2000. The early history of modern birds inferred from DNA sequences of nuclear and mitochondrial ribosomal genes Mol. Biol. Evol. 17:451–457.

Van Tuinen, M., D. B. Butvill, J. A. W. Kirsch, and S. B. Hedges. 2001. Convergence and divergence in the evolution of aquatic birds. Proc. R. Soc. Lond. B 268:1345–1350.

Webb, S. D., and A. Rancy. 1996. Late Cenozoic evolution of the Neotropical mammal fauna. Pp. 335–358 *in* J. B. C. Jackson, A. F. Budd, and A. G. Coates, eds. Evolution and environment in tropical America. University of Chicago Press, Chicago.

Webb, S.D. 1995. Biological implications of the middle Miocene Amazon Seaway. Science 269: 361–362.

Webster, A. J., R. J. H. Payne, and M. Pagel. 2003. Molecular phylogenies link rates of evolution and speciation. Science 301:478.

Webster, A. J., R. J. H. Payne, and M. Pagel. 2004. Response to comments on "Molecular phylogenies link rates of evolution and speciation". Science 303:173d.

Winker, H., D. A. Christie, and D. Nurney. Woodpeckers: A Guide to the Woodpeckers of the World. Houghton Mifflin, New York, 1995.

Witt, C. C., and R. T. Brumfield. 2004. Comment on "Molecular phylogenies link rates of evolution and speciation" (I). Science 303:173b.

Wollenberg K., J. Arnold, and J. C. Avise, 1996 Recognizing the forest for the trees: testing temporal patterns of cladogenesis using a null model of stochastic diversification Mol. Biol. Evol 13:833–849.

Wright, S. D., R. D. Gray, and R. C. Gardner. 2003. Energy and the rate of evolution: inferences from plant rDNA substitution rates in western Pacific. Evolution 57:2893–2898.

Yang, Z. 1994. Maximum likelihood phylogenetic estimation from DNA sequences with variable rates over sites: Approximate methods. J. Mol. Evol. 39:306–314.

Yang, Z. 1996. Among-site rate variation and its impact on phylogenetic analyses. TREE 11:367-372.

Zamudio, K. R., and Greene, H. W. 1997. Phylogeography of the bushmaster (*Lachesis muta*: Viperidae): implications for neotropical biogeography, systematics, and conservation. Biol. J. Linn. Soc. 62:421–442.

Zharkikh, A. 1994. Estimation of evolutionary distances between nucleotide sequences. J. Mol. Evol. 39:315–329.

APPENDIX: SOURCES OF DNA SEQUENCES ANALYZED IN CHAPTER 3.

Taxon 1	Genbank accession number	Taxon 2	Genbank accession number
Casuarius bennetti	U76051	*Casuarius casuarius*	NC_002778
Apteryx owenii	U28699	*Apteryx haastii*	U28704
Crypturellus strigulosus	U76056	*Crypturellus tataupa*	AY016012
Crax alector	AF106507	*Crax globulosa*	AF106506
Megapodius eremita	AF082065	*Alectura lathami*	AF082058
Alectoris magna	Z48776	*Alectoris philbyi*	Z48774
Francolinus capensis	U90632	*Francolinus adspersus*	U90633
Francolinus gularis	U90649	*Francolinus pondicerianus*	U90648
Francolinus africanus	U90629	*Francolinus levaillantoides*	U90644
Tetrao mlokosiewiczi	AF230173	*Tetrao tetrix*	AF230174
Chrysolophus pictus	AF028793	*Catreus wallichi*	AF028792
Lophura nycthemera	L08380	*Lophura leucomelana*	AF314643
Lophura diardi	AF028797	*Lophura ignita*	AF314641
Polyplectron bicalcaratum	AF028799	*Polyplectron chalcurum*	AF330061
Pavo cristatus	L08379	*Pavo muticus*	AF013763
Dendragapus obscurus	AF230178	*Lagopus mutus*	AF230172
Anser albifrons	AY072598	*Anser erythropus*	AY072600
Cereopsis novaehollandiae	U46467	*Dendrocygna guttata*	AF173770
Malacorhynchus membranaceus	U46483	*Biziura lobata*	U46487
Chloephaga melanoptera	AF173763	*Neochen jubatus*	AF173762
Tachyeres pteneres	AF059112	*Speculanas specularis*	AF059090
Pteronetta hartlaubi	AF059110	*Cyanochen cyanopterus*	AF059101
Cairina moschata	L08385	*Aix galericulata*	U46484
Anas strepera	AF059109	*Anas falcata*	AF059106
Anas versicolor	AF059094	*Anas puna*	AF059085
Anas hottentota	AF059077	*Anas querquedula*	AF059086
Spheniscus mendiculus	AF338606	*Spheniscus humboldti*	AF338597
Pygoscelis antarctica	AF076089	*Pygoscelis papua*	AF076090
Gavia stellata	AF158250	*Gavia immer*	AF158249
Fulmarus glacialoides	AF076055	*Fulmarus glacialis*	U74348
Puffinus griseus	U74353	*Puffinus tenuirostris*	U74352
Garrodia nereis	AF076056	*Pelagodroma marina*	AF076072
Oceanodroma tethys	AF076066	*Halocyptena microsoma*	AF076058
Oceanodroma castro	AJ004204	*Oceanodroma tristrami*	AF076067
Hydrobates pelagicus	AF076059	*Oceanodroma furcata*	AF076063
Phalacrocorax brasilianus	U83163	*Phalocrocorax auritus*	U83165
Sula variegata	U90008	*Sula nebouxii*	U90006
Botaurus lentiginosus	AF193833	*Ixobrychus exilis*	AF193832
Egretta rufescens	U83153	*Egretta caerulea*	AF193825
Ardea herodias	AF193821	*Ardea alba*	AF193822
Ciconia ciconia	NC_002197	*Ciconia boyciana*	AB026193
Ciconia nigra	U72771	*Leptoptilos crumeniferus*	X86754
Ephippiorhynchus asiaticus	U72782	*Ephippiorhynchus senegalensis*	U72781
Cathartes burrovianus	AF494342	*Cathartes aura*	X86743
Coragyps atratus	U08946	*Gymnogyps californianus*	U08947
Sarcoramphus papa	X86760	*Vultur gryphus*	X86763
Haliaeetus leucoryphus	Z73469	*Haliaeetus pelagicus*	Z73470
Haliaeetus leucogaster	Z73468	*Haliaeetus sanfordi*	Z73471
Circus aeruginosus	AF172376	*Circus cyaneus*	AF115891
Accipiter striatus	U83305	*Accipiter gentilis*	X86738
Aquila pomarina	Z73466	*Aquila clanga*	Z73464

(APPENDIX, cont.)

Gypaetus barbatus	X86749	*Neophron percnopterus*	X86757
Herpetotheres cachinans	U83319	*Micrastur gilvicollis*	U83315
Polihierax semitorquatus	U83317	*Microhierax erythrogenys*	U83318
Falco sparverius	U83306	*Falco tinnunculus*	AF172378
Gallirallus sylvestris	U77176	*Gallirallus philippensis*	U77174
Porzana tabuensi	U77170	*Porzana pusilla*	U77171
Grus nigricollis	U27547	*Grus monacha*	U27548
Grus vipio	U11065	*Grus rubicunda*	U11062
Elseyornis melanops	U62690	*Thinornis rubricollis*	U62698
Oreopholus ruficollis	U62696	*Charadrius alexandrinus*	AF417931
Tringa glareola	AF417923	*Tringa totanus*	AF417932
Calidris alpina	U34686	*Calidris tenuirostris*	AF417924
Recurvirostra avosetta	AF417926	*Haematopus ostralegus*	AF440782
Jacana spinosa	AF146618	*Jacana jacana*	AF146617
Irediparra gallinacea	AF146622	*Microparra capensis*	AF146621
Catharacta skua	U76807	*Stercorarius pomarinus*	U76814
Stercorarius parasiticus	U76826	*Stercorarius longicaudus*	U76820
Larus michahelli	AF268493	*Larus marinus*	AF268496
Larus heermanni	AF268506	*Larus occidentalis*	AF268502
Larus philadelphia	AF268517	*Larus genei*	AF268513
Larus serranus	AF268512	*Larus novae-hollandiae*	U37301
Larus modestus	AF268507	*Larus pipixcan*	AF268508
Larus ichthyaetus	AF268511	*Larus melanocephalus*	AF268510
Pagophila eburnea	AF268521	*Xema sabini*	AF268520
Sterna sandvicensis	AF268525	*Sterna maxima*	AF268526
Synthliboramphus hypoleucus	U37305	*Synthliboramphus craveri*	U37304
Aethia cristatella	U37087	*Aethia pygmaea*	U37286
Fratercula cirrhata	U37298	*Fratercula arctica*	U37297
Columba plumbea	AF182691	*Columba subvinacea*	AF182692
Streptopelia senegalensis	AF279710	*Streptopelia chinensis*	AF182695
Oena capensis	AF182707	*Ducula bicolor*	AF182705
Phaps chalcoptera	AF182713	*Geopelia cuneata*	AF182711
Zenaida asiatica	AF251534	*Zenaida meloda*	AF182699
Zenaida graysoni	AF182702	*Zenaida macroura*	AF251530
Ptilinopus leclancheri	AF182708	*Ptilinopus occipitalis*	AF279713
Aegotheles albertisi	X95764	*Aegotheles cristatus*	X95775
Podargus papuensis	X95772	*Podargus ocellatus*	X95771
Nyctibius maculosus	X95769	*Nyctibius leucopterus*	X95768
Chaetura pelagica	AF168105	*Chaetura vauxi*	U50029
Aerodramus elaphrus	U49988	*Aerodramus francicus*	U49991
Cypsiurus balasiensis	U50032	*Apus nipalensis*	U50001
Lafresnaya lafresnaya	U90104	*Agleactis cupripennis*	U90102
Sephanoides fernandensis	AH005242	*Sephanoides sephanoides*	AH005241
Eriocnemis nigrivestis	U90096	*Chlorostilbon aureoventris*	U89181
Heliangelus viola	AF022675	*Metallura tyrianthina*	AF022667
Todus multicolor	AF441617	*Todus angustirostris*	AF441626
Momotus momota	U89188	*Momotus mexicanus*	U89187
Ceryle torquata	AF441633	*Chloroceryle americana*	U89183
Bucco tamatia	this study	*Hypnelus bicinctus*	this study
Notharchus macrorhynchos	this study	*Notharchus ordii*	this study
Malacoptila fulvogularis	this study	*Malacoptila panamensis*	this study
Monasa nigrifrons	this study	*Monasa flavirostris*	this study
Galbula dea	this study	*Galbula albirostris*	this study

(APPENDIX, cont.)

Galbula leucogastra	this study	*Galbula chalcothorax*	this study
Lybius bidentatus	AF123527	*Pogoniulus bilineatus*	AF123528
Semnornis ramphastinus	AF123510	*Semnornis frantzii*	AF123511
Picoides major	AF389317	*Picoides leucotos*	AF389313
Picoides maculatus	AF389315	*Picoides canicapillus*	AF389309
Veniliornis callonotus	U83298	*Veniliornis nigriceps*	AF389337
Piculus rubiginosus	U83292	*Colaptes rupicola*	U83301
Dendropicos fuscescens	AF389334	*Dendropicos griseocephalus*	AF389335
Tyrannus melancholicus	AF135051	*Sublegatus modestus*	AF447623
Laniisoma elegans	AF123641	*Piprites chloris*	AF123644
Xipholena punicea	AF123624	*Carpodectes hopkei*	AF123623
Haematoderus militaris	AF123636	*Querula purpurata*	AF123635
Lipaugus unirufus	AF123626	*Lipaugus fuscocinereus*	AF123627
Gymnoderus foetidus	AF123625	*Conioptilon mcilhennyi*	AF123622
Pipreola chlorolepidota	AF123618	*Pipreola arcuata*	AF123617
Pipra pipra	AF118154	*Pipra fasciicauda*	AF453817
Rupicola peruviana	AF123614	*Rupicola rupicola*	AF082055
Tityra cayana	AF453814	*Tityra inquisitor*	AF123643
Lepidocolaptes souleyetii	AF045743	*Lepidocolaptes lacrymiger*	AF045744
Xiphorhynchus obsoletus	AY089823	*Lepidocolaptes fuscus*	AY089819
Grallaria ridgelyi	AF127196	*Grallaria nuchalis*	AF127197
Corvus corax	AY005951	*Corvus cryptoleucus*	AY005978
Menura novaehollandiae	U76509	*Pitohui dichrous*	AF308767
Manorina melanocephala	AF197859	*Meliphaga lewini*	AF197857
Pyrrhocorax pyrrhocorax	U86044	*Pyrrhocorax graculus*	U86043
Smicrornis brevirostris	AF129213	*Acanthiza ewingii*	AF129224
Orthonyx spaldingii	AY148035	*Orthonyx temminkii*	AY148036
Pomatostomus isidori	X60938	*Pomatostomus superciliosus*	X54909
Lanius ludovicianus	AY030105	*Lanius excubitor*	AY030106
Cyanocitta cristata	X74258	*Cyanocitta stelleri*	AY030113
Cissa chinensis	U86037	*Urocissa erythrorhyncha*	U86038
Manucodia keraudrenii	X74252	*Manucodia comrii*	U15207
Epimachus fastuosus	X74253	*Epimachus meyeri*	U15206
Hypothymis helenae	AF096468	*Terpsiphone viridis*	AF094616
Myiagra cyanoleuca	AF096464	*Myiagra caledonica*	AF096463
Vireo latimeri	AF383108	*Vireo bellii bellii*	U12304
Bombycilla cedrorum	AF285786	*Bombycilla garrulus*	AF285796
Myadestes obscurus	AF295080	*Myadestes genibarbis*	AF295083
Cinclus cinclus	AF151393	*Cyornis banyumas*	AF151408
Toxostoma longirostre	AF130235	*Toxostoma guttatum*	AF130236
Parus ater	U63396	*Parus major*	AF394577
Baeolophus inornatus	X60944	*Baeolophus bicolor*	AF347957
Tachycineta bicolor	AF074585	*Progne chalybea*	AF074583
Neochelidon tibialis	AF074590	*Atticora fasciata*	AF074584
Riparia riparia	AF074578	*Riparia cincta*	AF074580
Hirundo rustica	AF074577	*Notiochelidon cyanoleuca*	AF074586
Hippolais icterina	AJ004796	*Hippolais polyglotta*	AJ004797
Hippolais olivetorum	AJ004795	*Hippolais languida*	AJ004794
Phylloscopus bonelli	Z73486	*Phylloscopus sibilatrix*	Z73491
Phylloscopus schwarzi	Y10728	*Phylloscopus affinis*	Y10730
Phylloscopus pulcher	Y10732	*Phylloscopus maculipennis*	Y10731
Sylvia melanocephala	L77121	*Sylvia atricapilla*	AF074596
Anthus campestris	U46771	*Anthus berthelotii*	U46769

(APPENDIX, cont.)

Vidua paradisaea	U18865	*Vidua chalybeata*	NC_000880
Serinus canaria	L76296	*Serinus mozambicus*	L76265
Carduelis magellanica	AF310066	*Carduelis pinus*	AF290142
Haematospiza sipahi	AF342875	*Carpodacus erythrinus*	AF342883
Mycerobas carniceps	AF342880	*Mycerobas affinis*	AF342879
Pseudonestor xanthophrys	AF015762	*Loxops coccineus*	AF015757
Euphonia musica	AF310067	*Euphonia laniirostris*	AF006232
Emberiza rustica	AF284082	*Emberiza pusilla*	AF284083
Oreomanes fraseri	AF006244	*Lamprospiza melanoleuca*	AF006238
Delothraupis castaneoventris	AF006228	*Dubusia taeniata*	AF006230
Tangara gyrola	AF006254	*Thraupis episcopis*	AF089065
Hemithraupis flavicollis	AF006235	*Heterospingus xanthopygius*	AF006236
Creurgops dentata	AF006224	*Schistochlamys melanopsis*	AF006250
Saltator striatipectus	AF383107	*Saltator coerulescens*	AF290154
Poospiza torquata	AY005215	*Poospiza alticola*	AY005199
Loxigilla noctis	AF310041	*Tiaris bicolor*	AF310044
Geospiza difficilis	AF108787	*Geospiza scandens*	AF108783
Sporophila castaneiventris	AF310056	*Oryzoborus angolensis*	AF310055
Cyanocompsa parellina	AF301460	*Cyanocompsa brissonii*	AF301461
Spiza americana	AF290147	*Cyanocompsa cyanoides*	AF301462
Pheucticus aureoventris	AF310057	*Pheucticus ludovicianus*	AF310058
Passerina caerulea	AF301449	*Passerina amoena*	AF301451
Passerina leclancherii	AF301455	*Passerina rositae*	AF301453
Passerina ciris	AF301459	*Passerina versicolor*	AF301457
Piranga ludoviciana	AY124545	*Piranga bidentata*	AF011760
Piranga leucoptera	AF011771	*Piranga rubriceps*	AF011781
Pipilo aberti	U26189	*Pipilo crissalis*	AF092880
Geothlypis aequinoctialis	AY030121	*Geothlypis trichas*	AF383003
Cacicus uropygialis	AY117711	*Cacicus cela*	AY117703
Agelaius ruficapillus	AF089009	*Molothrus badius*	AF089042
Agelaius flavus	AF089066	*Pseudoleistes virescens*	AF089052
Gnorimopsar chopi	AF089025	*Agelaius thilius*	AF089010
Scaphidura oryzivora	AF089060	*Molothrus aeneus*	AF089040
Dolichonyx oryzivorus	AF447367	*Xanthocephalus xanthocephalus*	AF089067

VITA

Christopher C. Witt was born in 1974, in Philadelphia, Pennsylvania, to Loretta Cooper Witt and Thomas Powell Witt. He attended high school in Philadelphia at Germantown Friends School. Birdwatching has been a major part of his life since age 10, and his weekends and vacations during middle school and high school were often devoted to bird-finding expeditions with his friends Matt Sharp and George and Harry Armistead, to New Jersey, Delaware, Maryland, and Virginia. In high school, he worked part time and summers in the Ornithology Department at the Academy of Natural Sciences of Philadelphia, where he was mentored by professional ornithologists including Frank Gill, Doug Wechsler, Mark Robbins, and Fred Sheldon. He took time off after high school during which he worked seasonal jobs in environmental education, bird collecting, and bird banding. In 1997, he earned his bachelor's degree in Human Ecology at College of the Atlantic, Bar Harbor, Maine. After college, he decided to pursue a career studying bird systematics and evolution, and he began a doctoral program under Drs. Van Remsen and Fred Sheldon at the Louisiana State University Museum of Natural Science.